THE KINETICS OF THE REACTION OF FORMIC ACID AND NITROGEN DIOXIDE

BILLY K. T. SIE
B.SC. IN CHEM. ENG.

THE KINETICS OF THE REACTION OF FORMIC ACID AND NITROGEN DIOXIDE

by

© Billy K.T. Sie
B.Sc. in Chem. Eng.
(National Taiwan University)

A THESIS

Submitted to

Memorial University of Newfoundland

in partial fulfillment of the requirements
for the degree of

MASTER OF SCIENCE

Department of Chemistry

1970

TO

my mother and brothers and sisters

ADVISORY COMMITTEE

_____

_____

_____

THESIS EXAMINERS

_____

_____

Approved by the Faculty of
Graduate Studies

Date: _____

_____
Chairman of Examining Board

ACKNOWLEDGEMENTS

The author would like to express his sincere appreciation to Dr. D. Barton for his invaluable advice, guidance and encouragement throughout this work. His enthusiasm and dedication were a constant source of inspiration.

The contribution of other members of the Faculty and of fellow graduate students is also gratefully recognized. In particular, the author wishes to thank Dr. J.F. Ogilvie for helping with the Programma 101.

The help of Mr. D.H. Seymour in the construction of the recording spoon gauge and of Mrs. S. Banfield in the tracing of the graphs is also gratefully acknowledged.

The author is pleased to acknowledge generous financial support from the National Research Council of Canada and from the Memorial University of Newfoundland for the period September, 1967 to December, 1969.

ABSTRACT

The kinetics of the gas phase reaction between formic acid and nitrogen dioxide has been studied at 182° and 214°C. The results confirm that the rate expression contains the term k_1 [FA] [NO_2], as suggested in earlier papers (1), (3). The results also confirm the autocatalytic nature of the reaction and the existence of induction periods as suggested by D. Barton and Peter E. Yankwich (3). The autocatalytic term is however much more complex than was suggested. The results were fitted to the rate expression

$$-\frac{d[FA]}{dt} = k_1[FA][NO_2] + \frac{k'_a\,[FA][NO_2]^{2/5}[NO]}{k'_b + k'_c\,[NO]/[FA]^{1/2}}$$

with the exclusion of an induction period when NO was added initially. Although a mechanism has not yet been found which gives this rate expression, reasonable interpretations of the role of NO_2 and NO in the autocatalytic reaction have been discussed.

TABLE OF CONTENTS

LIST OF TABLES

LIST OF FIGURES

INTRODUCTION

In spite of work extended over decades, satisfactory interpretations of the kinetics of oxidation of organic compounds by nitrogen dioxide are still scarce. For example, the kinetics of the reaction between formic acid and nitrogen dioxide has not been thoroughly investigated. Pollard and Holbrook (1) have studied this reaction in packed and unpacked Pyrex vessels. They found the major products to be carbon dioxide, water and nitric oxide, and that the rate was increased by packing the vessel, roughly in proportion to the increase in the surface to volume ratio. The effect of nitric oxide on the reaction rate was unusual. It had been known for over twenty-five years that nitric oxide plays the role of inhibitor in organic pyrolysis reactions (2). Pollard and Holbrook discovered that nitric oxide behaves as a catalyst in the reaction between formic acid and nitrogen dioxide. They attempted to fit their results to the rate expression given below:

$$[1] \quad -\frac{d\,[HCOOH]}{dt} = k_1\,[HCOOH]\,[NO_2] + k'\,[HCOOH]\,[NO_2]\,[NO]$$

Their proposed mechanism[1] is:

$$[2] \quad HCOOH + NO_2 \rightarrow (HCO_2H.NO_2) \rightarrow COOH + HNO_2$$

$$[3] \quad COOH + NO_2 \rightarrow CO_2 + HNO_2$$

$$[4] \quad 2HNO_2 \rightarrow H_2O + NO + NO_2$$

---

[1] k' defined by Pollard is equal to k_5k_7/k_6.

[5.] $NO + NO_2 \rightarrow N_2O_3$

[6] $N_2O_3 \rightarrow NO + NO_2$

[7.] $HCOOH + N_2O_3 \rightarrow COOH + NO + HNO_2$

It is doubtful, however, if their rate expression actually fits their observations. It can be seen from their Table 4 that the value of k' obtained from plot 1 (their Figure 3) is 3.40×10^{-7} mm $Hg^{-2}sec^{-1}$ and from plot 3 is 7.87×10^{-7} mm $Hg^{-2}sec^{-1}$. In fact k' is not a constant.

The results of further work were published by D. Barton and Peter E. Yankwich (3), who measured the rate of reaction of HCOOH, HCOOD, DCOOH and DCOOD with nitrogen dioxide in a Vycor glass vessel at 191.3°C. The simple stoichiometry and the non-autocatalytic term of the rate expression were confirmed, but the rate could not be fitted to eq. (1). Particularly, it is noticeable in the peculiar shape of some of the pressure-time curves which remained linear up to 75% of the reaction. The order with respect to nitric oxide was found to be approximately 2/3. The magnitudes of the kinetic isotope effects were difficult to interpret clearly as either primary or secondary in origin. However, they suggested that hydrogen abstraction from both carbon and oxygen were kinetically important in both non-autocatalytic and autocatalytic reactions.

Since they did not obtain sufficient kinetic data to find the complete rate expression, it became apparent that

considerably more work would be necessary before the mechanism of such a complex reaction could be clarified.

The work to be reported was undertaken in order to determine the autocatalytic term of the rate expression.

EXPERIMENTAL DETAILS

(A) MATERIALS

Formic Acid

The formic acid, Baker and Adamson C.P. Grade, was reported to contain 98-100% HCOOH. It was treated as follows (4): the sample was cooled to 0°C, at which temperature both solid and liquid phases were present. It was then pumped until 1/4 of it had evaporated, without allowing the rest to melt. The sample was then distilled twice from a trap at room temperature to a trap at 0°C. Each time the remaining liquid in the trap at room temperature was pumped away. The sample in the trap at 0°C was in the form of white crystals. After this procedure, the sample was checked by mass spectrometry up to m/e 100. Small amounts of the possible impurities, CH_3OH, HCHO, or H_2O would be difficult to detect because of overlapping peaks of formic acid. A small peak, 1/200 of the height of that at m/e 46, appeared at m/e = 60 which could be acetic acid or the dimer of HCHO. The NMR spectrum (See appendix) of the sample (liquid) was then taken using a Varian A60 NMR spectrometer. The spectrum contained two peaks (singlet, τ = -0.07 O-H and τ = 2.2 C-H. The average height of the integrated O-H peak was about 6.5% larger than than of the C-H peak. This indicated that no impurities other than water were detected. In addition, the infrared spectrum (Appendix 1) of this sample was taken using a grating infrared spectrometer. This was done by evaporating the sample at room

temperature. The pressure in the gas cell, with CaF_2 windows, was about 40 mm Hg. The spectrum obtained was compared with a reportedly reliable spectrum of formic acid (5) in the range 1300 cm^{-1} to 4000 cm^{-1}. The spectra were identical. By titration with 0.0985 N NaOH (standardized with 0.1193 N potassium hydrogen phthalate), using a pH meter, the water content was found to be 1.5 mole %. The sample was stored at -78°C and degassed at -78°C before use in kinetic runs.

Nitrogen Dioxide

Liquid nitrogen tetroxide, supplied by Matheson Company, was distilled from the cylinder to a trap at -196°C. Subsequently, it was distilled from 0°C to -196°C through a drying column, packed with glass beads and powdered phosphorus pentoxide. After the trap was warmed to 0°C, dry air was added, to convert nitric oxide to nitrogen dioxide. The nitrogen dioxide was condensed as a white solid in the storage bulb at -196°C and excess dry air was removed by pumping. The spectrum (Appendix 1) obtained by infrared spectrometry was found to be similar to that given in references (5) and (6). No other oxide of nitrogen or other impurity was detected. NO_2 was stored at -196°C.

Nitric Oxide

Nitric oxide was purified by the technique described

by Ernest E. Hughes (7). The gas from the cylinder (Matheson Company) was passed slowly through silica gel (BDH, for chromatographic adsorption) in a trap at -78°C, directly to the storage bulb. The silica gel had been dried at 250°C. This procedure is said to remove all impurities except nitrogen. The gas was frozen in a side arm of the storage bulb at -196°C and the nitrogen was pumped away. After such treatment, the sample was checked on a Consolidated Model 21-614 mass spectrometer. A very small peak at m/e = 46 appeared. It could have been due to nitrogen dioxide resulting from oxidation of nitric oxide by air during the transfer process. The infrared spectrum was taken. Two bands were observed, at 2.7 and 5.2μ as reported in references (5) and (6). No other bands were observed.

(B) APPARATUS

1. Vacuum System

The design of this system was conventional. It consisted of a fore-pump (Welch Duo-Seal Serial No. 8698-3), traps, pyrex tubing, high vacuum stopcocks, diffusion pump (VEECO Model No. EP25W), thermocouple gauge (C.V.C. GTC-100), McLeod gauge and a toepler pump (See Figure 1).

2. Reaction Vessel

A spherical reaction vessel (Figure 2) was fabricated from pyrex glass; its volume was 527.9 cm^3 and its surface to volume ratio was 0.6 cm^{-1}. Before connecting to the vacuum line

it was cleaned with detergent and subsequently rinsed many times with deionized water. The reaction vessel was joined to the sample introduction and the vacuum-system by a short length of 2 mm capillary tubing joined the neck of the reaction vessel to the spoon gauge via a 2 mm two-way stopcock. The volume of this portion, the so called dead space of the reaction vessel, was estimated to be 6 cm^3, approximately 1% of the total reactor volume. The vessel also contained a thermocouple well, 70 mm long and 4 mm inside diameter.

3. Furnace

The furnace used for heating the reaction vessel was constructed by Paul Ke and used by him and Ted Huang. It consisted of an aluminum cylinder wound with asbestos and several heaters made of 20 gauge chromel-A wire. The furnace was kept in a 25 gallon steel drum. The bottom of the steel drum was insulated by asbestos. The space between the cylinder and the steel drum was insulated with vermiculite. The capillary between the air furnace and the reaction vessel was wrapped with asbestos tape.

4. Recording Spoon Gauge

The design was slightly modified from that of

---

[2]A V-shaped groove was ground at both ends of the bore of the plug.

J.G. Hooley (8). The main difference was that the transformer (Linear Variable Differential Transformer, LVDT, 1000 LS, serial No. 6489 Schaevitz Engineering) was contained in the envelope, where the core (length 3.3 cm, O.d. 0.64 cm and weight 4 grams) was screwed firmly to a 1.5 cm long teflon screw. It was suspended by means of a thin pyrex glass rod from the tip of the spoon gauge arm to reach the center of the transformer. The transformer was covered by a teflon adapter attached to an antimagnetic steel rod. The rod was supported by the tip of the plug of an Ace O-ring stopcock. An antimagnetic spring above the transformer pressed it downward. Tungsten wires were sealed into the glass for electrical connections with the "Carrier" (Schaevitz Engineering Model CAS 25000) from which the amplified signal was fed to the millivolt recorder (Model YEW LER-12A). The height of the transformer was adjusted by turning the plug of the inverted teflon stopcock, so that the output voltage could easily be set to zero with both sides of the spoon gauge at the same pressure. In order to measure the pressure the side arm of the envelope was connected to a two-way stopcock; one arm was connected to a vacuum pump and the other end to a manometer and a ground stopcock. The stopcock served as a leak to the atmosphere. For details see Figures 3 and 4.

5. Thermocouples and Potentiometer

A Type K-3 L & N Universal Guarded Potentiometer was

used in conjunction with chromel-alumel thermocouples (TC #2, TC #3, TC #4, and TC #6). The thermocouples, which were placed at various points on the reaction vessel, were calibrated by a procedure similar to that recommended by the National Bureau Standards (9), using NBS standard tin with a reported melting point of 231.88°C. TC #4 was located near the bottom of the reaction vessel; TC #3 and TC #6 were in the well; and TC #2 was near the connection between the 2 mm capillary tubing and the reaction vessel (see Figure 2). The results of a series of calibrations (Tables XII, XIII, XIV and XV) indicated that the average deviation between the measured and tabulated values (10) was ± 0.02°C. In fact, it was less than the deviation among various thermocouples around the reaction vessel. No correction was required under these circumstances. The temperature of the reference-junction was controlled by placing the thermocouples, protected by a 10 cm pyrex glass tube, in an ice bath. The bath consisted of crushed ice and water in a wide-mouthed Dewar flask. For standardizing, an Eppley Standard Cell (Cat. No. 100, Serial No. 814799) of 1.01934 volts was used.

(C) EXPERIMENTAL PROCEDURE

1. Temperature Control and Measurement

The temperature of the furnace was controlled by means of a platinum probe and electronic relay. The temperature of the air furnace was maintained at approximately 40.8°C by means of a metallic strip regulator and relay placed near the spoon gauge envelope.

As mentioned in the foregoing section, thermocouples (TC #2, TC #3, TC #4, and TC #6) were used for measuring the furnace temperature. Readings from two typical runs (93 and 13) are given below. The individual readings are averages of four readings taken before, after, and twice during a run.

Run # 93:	TC #2	TC #3	TC #4	TC #6
	8.6891	8.7027	8.7102	8.6944

Average = 8.6991 ± 0.0073 or 213.98 ± 0.18°C

Run # 13:	TC #2	TC #3	TC #4	TC #6
	7.4095	7.4231	7.4209	7.4108

Average = 7.4161 ± 0.006 or 182.15 ± 0.15°C

(In this temperature range 1.00°C is equivalent to 0.04 millivolts.)

2. Calibration of the Recording Spoon Gauge

The calibration of the recording spoon gauge was carried out by measuring the output voltage as a function of pressure differential. Before calibrating, both sides of the

gauge were evacuated below 10^{-4} mm HG with the diffusion pump. The air furnace temperature was regulated at 40.8 °C. The height of the LVDT core was then adjusted by turning the inverted teflon stopcock, so that the output voltage was about zero. This occurred when the recorder controls were set with the pen near one side of the chart. This reading was the null point, which was checked from time to time, and found to be very stable. A known pressure of air could be leaked to the gauge envelope by opening the stopcock. The displacement on the recorder was found to vary linearly with the pressure differential, as shown in Figure 5. The sensitivity was found to be 13.62 ± 0.24 mv per mm Hg. Actually the apparatus was calibrated at the beginning of each run, using the first gas to be introduced. The results from a great number of such calibrations gave the average sensitivity as 13.47 ± 0.31 mv per mm Hg.

3. Introduction of Reactants

The order of addition of reactants into the reaction vessel was, in most of the experiments, formic acid, nitric oxide (if needed) and nitrogen dioxide. In runs 128, 129, and 131, the order was nitrogen dioxide followed by formic acid.

The formic acid was degassed in trap ST_1 at -78°C at least once daily whenever kinetic runs were to be carried out. Pressures of formic acid above the vapor pressure at room temperature were obtained by distilling some of the acid from the

storage bulb ST_1 to a small finger tube near the reaction vessel inlet (Figure 1) where it was warmed up to 40.8 °C. After this procedure, a known pressure of air was leaked gradually through stopcock S_5 to the spoon gauge envelope. Subsequently formic acid was introduced to the reaction vessel by carefully opening stopcock S_1. The stopcock (S_1) was then closed. A similar procedure was followed for introduction of the other gases. Nitric oxide (if needed) was introduced directly from bulb B_3 to the reaction vessel. Nitrogen dioxide was introduced from the 500 cm^3 bulb B_2 in which it was stored as a gas for a few minutes preceeding each run.

For the measurement of pressure greater than 100 mm Hg (runs 123, 124, and 125), this procedure was carried out in at least two steps, to prevent the breakage of the spoon.

4. Recording of the pressure change

Due to the noise level at the 100 MV setting of the recorder, which was found to be about 4-5% of the full scale, most of the experiments were performed at a setting of 200 MV. The noise level at 200 MV was found to be less than 2% of full-scale. In runs before 15 the experiments were started with the recorder setting at about 200 MV. When the pressure change caused the pen to go off scale, it was returned by switching the recorder sensitivity to 500 MV. In run 15 and subsequent runs the pen was returned to zero by leaking air into the envelope. The recorder setting was retained at 200 MV throughout the course of the reaction.

5. Qualitative analysis of products volatile at -110°C

In three experiments (runs 114, 120 and 122) some of the products were collected after the reaction had proceeded to completion. The contents of the reaction vessel were condensed into a trap (T_1) at -196°C. The condensation was found to be complete since the recorder pen returned to the starting position. The trap was then warmed to -110 to -115°C using an ethanol slush bath. The toepler pump was started and the nitric oxide and carbon dioxide were collected. (Some of the nitric oxide is retained in the trap as N_2O_4 in an excess of NO_2.) A sample was removed from the line and examined qualitatively by means of a Consolidated 21-614 mass spectrometer.

RESULTS AND DISCUSSION

1. Characteristics of pressure-time curves

The maximum rate of many reactions is observed at or near zero time. The rate then decreases throughout the course of the reaction. However, in autocatalytic reactions, concentration-time curves are usually S-shaped, and the time at which the maximum rate occurs is dependent upon the rate expression. For example, in a reaction A → B in which B is a catalyst, it would appear at ≈ 30% reaction if the rate expression is

$$[8] \qquad -\frac{d[A]}{dt} = k[A]^2 [B_o + B]$$

where $[B_o]$ is the initial concentration of [B] (11).

The pressure-time curves obtained from the reaction of formic acid and nitrogen dioxide, observed by Pollard and Holbrook (1), are combinations of two types of pressure-time curves, autocatalytic and non-autocatalytic. Naturally, the pressure-time curves reported here, are of the same type.

The pressure-time curves were obtained for the following five arbitrary classifications of experiments:

Type	A_o mm Hg	B_o mm Hg	C_o mm Hg
A	30	various	0
B	various	30	0
C	32	23	various
D	32	various	33
E	various	23	33

where A_o, B_o and C_o are initial pressures of HCOOH, NO_2 and NO respectively.

Type A pressure-time curves are shown in Figure 6. In some cases, the pressure is rapidly changing initially; this can be seen in runs 80 and 86 with high initial pressures of nitrogen dioxide. These pressure-time curves are slightly convex toward the ΔP axis for approximately 200 seconds. No such behaviour is detectable in runs 118, 119,and 121 with low initial pressures of nitrogen dioxide. In attempting to learn the cause of this curvature, two experiments (129 and 131) were carried out in which the usual order of introduction of reactants was reversed; nitrogen dioxide was introduced first to the reaction vessel. The order of introduction slightly affected the initial portion of the pressure-time curves. Instead of being slightly convex

toward the ΔP axis, they were linear, i.e., the rate was constant; the difference can be seen in Figure 7 and Figure 8. Apparently the convex shape of the curves is not caused by an instrumental problem. Also it is not caused by small amounts of fast reacting impurities, such as formaldehyde (12); otherwise the order of introduction would not change the shape. It was found, in preparation for run 128, that the decomposition reaction of $NO_2 \rightleftharpoons NO + \frac{1}{2} O_2$ at 214°C is discernible.

A pressure change of 1.5% in pure NO_2 was observed after 4028 seconds. However, the rate is not great enough to be responsible for the convex shape of the curves. No satisfactory explanation for the phenomenon has so far been obtained.

After this portion, the pressure-time curves were linear, i.e. the rate was constant, up to 45% of the final pressure change, when a gradual fall-off in rate occurred. The reproducibility of this type of pressure-time curve is excellent, as shown in Figure 9.

The shape of the type A pressure-time curves, which were found at 182°C were similar to those found at 214°C.

Pressure-time curves from type B experiments can be seen in Figure 10. In runs 114, 122 and 117, with high initial pressures of formic acid, the rate was almost constant until 75% reaction, with an indistinct maximum at about 50%. This behaviour is similar to that found in Pollard's run 17 (their Figure 2) and run 25 of unpublished work of D. Barton and Peter E. Yankwich. It can be seen in Figure 11 that a high degree of reproducibility was achieved.

In addition, the shapes of pressure-time curves at 182°C were similar.

In type C, D, and E experiments, in which nitric oxide was added initially, the pressure-time curves (Figures 12, 13, 14 and 15) at both 182°C and 214°C were slightly sigmoidal. An induction period is present, varying from approximately one minute at 214°C to two minutes at 182°C. The presence of an induction period at 191.3°C had previously been suggested (3). The maximum rate occurs at less than 20% reaction. The reproducibility is excellent, as shown in Figure 16.

Some peculiar shapes of pressure-time curves were observed when the initial nitric oxide pressures were high, such as in runs 123, 124, and 125. After the maximum rate, at about 20% reaction, the rate decreases gradually with time until about 80% reaction, then the rate decreases sharply and reaction continues very slowly. Moreover, it can be seen in Figure 12 that the higher the initial pressure of nitric oxide, the lower is the percent reaction at which the sharp decrease in rate is observed.

Similarly, peculiar shapes of pressure-time curves (Figure 15) were observed when the initial formic acid pressures were high, such as in runs 73, 72, 74, and 75. After the maximum rate at about 20% reaction, the rate decreases slowly until 80% reaction is reached, then the rate decreases sharply and reaction continues very slowly. Apparently, there is no relationship between the time of appearance of the sharp decrease in rate and the initial pressure of formic acid.

2. Comments on the reaction between formic acid and nitric oxide

Blake and Hinshelwood (13) studied the decomposition reactions of gaseous formic acid in carbon coated silica vessels at 500°C. They observed a small increase in the rate of pressure change when nitric oxide was added. They said that the small increase in rate could be attributed to the reaction of NO with the carbon surface, thus exposing the silica surface. The rate of reaction in the uncoated vessel had been found to be faster than in the coated vessels. No product analysis was mentioned. This result was one of the results which were interpreted by Blake and Hinshelwood as making it very improbable that radical-chain processes contribute significantly to the reaction. However, Watson suggested that since the nitric oxide was added in only modest amounts, i.e. NO:HCOOH ratio was 2:1, the results probably indicate that only long chain processes are not involved in the reaction, and that short chain process may not be seriously affected by modest amounts of nitric oxide (14).

In this work at 214°C, a slow increase in pressure was observed when nitric oxide and formic acid were mixed in the reaction vessel. For example, in run 125, with an excess of nitric oxide, the observed pressure change was 1.20 mm Hg after 1200 seconds and in run 73 with an excess of formic acid, the observed pressure change was 0.52 mm Hg after 225 seconds. (These pressure changes were recorded before NO_2 was introduced.)

In order to confirm this observation in a qualitative way a few experiments, runs 76, 77, and 78, were carried out, in which HCOOH and NO were introduced into the reaction vessel. The

initial conditions and pressure changes are shown below.

Run	Initial Pressure of formic acid (mm Hg)	Initial Pressure of NO (mm Hg)	ΔP_{obs} (mm Hg)	t (sec)
76	72.27	32.39	3.34	7955
77	35.95	64.23	0.66	5645
78	21.46	20.93	0.29	10587[3]

Runs 76 and 77 were carried out with no mass spectrometric analysis. In run 78 HCOOH and NO were mixed and allowed to stand overnight in the reaction vessel. The contents were passed into a trap at -196°C and a fraction of the gas was collected by means of a toepler pump and examined by means of the mass spectrometer. The trap was then warmed to -78°C, and a second fraction was collected. The results are tabulated on the following page.

---

[3] Although run 78 was continued for 24 hours, the ΔP_{obs} was recorded after 10587 seconds.

Trap $T_1 \tilde{=} -196^{o}C$

1	2	3	4	5	6	7	8
m/e	Mixture (before subtracting BG)	BG	Mixture (after subtracting BG)	NO pattern	Δ1 (residual I)	CO pattern	Δ2 (residual
12	675	--	675	--	675.0	785.9	--
14	2950	6.6	2943.4	2210.6	733	222.5	510.3
15	1450	--	1450	1520.4	--	--	--
16	600	5.4	594.6	356.4	238.4	269.2	--
20	22.5	9	13.5	--	13.5	--	13.5
28	26000	105	25895	759.8	25135.2	26835.8	--
29	250	--	242.5	--	242.5	82.82	--
30	32800	--	32800	32800	--	--	--
31	118	--	118	121.3	--	--	--
32	135	48	87	99.5	--	--	--
40	102	3	99	--	99	--	99
44	55.5	9	46.5	26.9	19.6	--	19.6

Trap T $\cong$ -78°C

m/e	Output	BG	Mixture	Output % based on m/e = 30
12	28.5	6	22.5	0.08
14	3950	7.5	3942.5	13.4
15	2700	-	2700	9.2
16	630	-	630	2.1
22	15	-	15	0.06
28	990	117	873	3.1
30	29500	-	29500	100
31	225	-	225	0.7
32	240	49.5	190.5	0.6
44	214.5	12	202.5	0.7

The NO pattern, as shown in column 5 of the first table, was obtained from the height of m/e = 30 in the mixture and the pure NO pattern. The CO pattern in column 7 is a pure CO pattern. The values in column 6 were obtained by subtracting the values in column 5 from the values in column 4. The values for m/e = 12 and m/e = 28 in column 6 were compared with the values for the same m/e values in column 7. Definitely, a small amount of CO is produced. However, it should be noticed that the value for m/e = 14, as shown in column 6 is relatively large. This would indicate the presence of N_2.

Since the quantity of products and the observed pressure change are small, this reaction can be ignored when considering the reaction between formic acid and nitrogen dioxide.[b]

Although our work was carried out under different conditions than was the work reported by Blake and Hinshelwood (13), it is possible that the reaction observed here between NO and HCOOH could be the same as observed by them at a higher temperature. In any case, this reaction would be a good project for a detailed study.

3. Stoichiometry

The simple stoichiometry proposed by Pollard and Holbrook (1) is

$$HCOOH + NO_2 \rightarrow H_2O + CO_2 + NO$$

This simple equation was confirmed by D. Barton and Peter E. Yankwich (15). Their results at 191.3°C are tabulated below.

(a) complete reactions, excess NO_2; values are in moles x 10^4. ΔPf is final pressure change.

Run	Initial formic acid	CO_2 found
12	2.12	2.11
13	2.13	2.09
14	2.12	2.11
15	2.11	2.11

[b] See appendix II.

(b) Complete reactions, excess formic acid

Run	Initial NO_2	CO_2 cal. from ΔP_f	CO_2 found	NO found
18	1.35	1.37	1.33	1.33
26	2.13	2.12	2.13	2.09

(c) Incomplete reactions

Run	CO_2 cal. from ΔP_f	CO_2 found
16	2.03	2.05
17	2.02	2.07
20	0.64	0.63
22	0.61	0.64

The simple stoichiometry appears to hold for incomplete as well as complete reaction, at least within 6%. No doubt, one can assume that no large quantity of long lived intermediates are produced.

In the present work further evidence for the simple stoichiometry can be seen in experiments which were allowed to go to completion. The observed final pressure change is equal to the initial pressure for formic acid if NO_2 is in excess, and equal to the initial pressure of NO_2 if formic acid is in excess. The results are tabulated below.

Complete reactions, excess NO_2, T = 214°C. Moles x 10^4

Run	Initial formic acid	Formic acid reacted (calculated from ΔP_f)
127	2.62	2.52
80	5.40	5.43
86	5.13	5.00
87	5.27	5.07
108	5.53	5.52
135	5.56	5.40
136	5.59	5.53

Complete reactions, excess NO_2, T = 182°C. Moles x 10^4

Run	Initial formic acid	Formic acid reacted Calculated from ΔP_f
10	5.55	5.48
20	5.56	5.39
42 *	5.41	5.26
45 *	5.32	5.07

* indicates NO was added initially

Complete reactions, excess formic acid. T = 214°C. Moles x 10^4

Run	Initial NO_2	NO_2 reaction Calculated from ΔP_f
121	2.46	2.40
117	5.17	5.10
98 *	4.03	3.88
107 *	3.94	3.76
74 *	4.18	4.04
70 *	3.86	3.69

Complete reaction, excess formic acid. T = 182°C. Moles x 10^4

Run	Initial NO_2	NO_2 reacted Calculated from ΔP_f
33	5.47	5.37
31	5.38	5.04
30	5.47	5.25
26	5.64	5.64
25	5.58	5.58

* indicates NO was added initially

Since the simple stoichiometry has been well established, no detailed analysis of products was undertaken. However, in the three experiments 114, 120 and 122, which were allowed to go to completion, the products which were not condensable at ≃ -110°C were collected. They were examined qualitatively by mass spectrometry up to m/e = 100. The pattern indicated that NO and CO_2 were present, but small amounts of products such as N_2O, N_2 and CO would not have been detectable, due to overlapping of the peaks. In runs 114 and 122 with excess formic acid, it was observed that the total number of moles of gases collected was about 7% and about 9% less than twice the number of moles of the NO_2 introduced. It is not known whether or not these results are reliable and it was not possible to carry out further work on product analysis. In any event, further work is suggested in which a search for minor products is made. The discovery of these might assist in understanding the mechanism.

4. Determination of the rate expression

I. Non-autocatalytic term in the rate expression

The non-autocatalytic term in the rate expression was assumed to be of the following form:

$$[8] \quad \frac{dx}{dt} = k_1(A_o - x)^n \quad (B_o - x)^m$$

as was previously proposed (1), (3). A_o and B_o are the initial pressures of HCOOH and NO_2 respectively and x is the pressure change. The procedure for obtaining the initial rate[4] of the reaction was to use the least-squares treatment for determining the slope of the observed linear portion of the pressure-time curves. Some of the curves used are shown in Figures 6 and 10. The data are displayed in Tables I and II.

The double logarithmic plots of the initial rate of pressure change against initial pressure of the reactants are shown in Figures 17, 18, and 19. The slopes of these lines were obtained by the least-squares method.

The orders were found to be:

Temperature (C^o)	Order with respect to HCOOH (n)	Order with respect to NO_2 (m)
182	1.02 ± 0.12	1.03 ± 0.05
214	1.08 ± 0.07	0.99 ± 0.05

The orders are consistent with those previously reported (1).

The average value of the rate constant k_1 at each temperature was calculated from equation [8] using the initial rates and pressures. The results are:

[4] The initial rate was taken by omitting the initial convex shaped portion of the curve in the type A experiments.

$$k_1 = 0.402 \pm 0.024 \times 10^{-5} \text{ mm Hg}^{-1}\text{sec}^{-1} \text{ or}$$
$$0.114 \text{ ℓ mole}^{-1}\text{sec}^{-1} \text{ at } 182^{\circ}\text{C}$$

$$k_1 = 1.034 \pm 0.084 \times 10^{-5} \text{ mm Hg}^{-1}\text{sec}^{-1} \text{ or}$$
$$0.314 \text{ ℓ mole}^{-1}\text{sec}^{-1} \text{ at } 214^{\circ}\text{C}$$

The values of k_1 at 182°C and 214°C were also calculated by using the Arrhenius equation for k_1 as obtained by Pollard and Holbrook, which is:

$$k_1 = 10^{6.73 \pm 0.25} e^{\frac{-16270 \pm 559}{RT}} \text{ ℓ mole}^{-1}\text{sec}^{-1}$$

The results are:

$$k_1 = 0.085 \text{ ℓ mole}^{-1}\text{sec}^{-1} \text{ at } 182^{\circ}\text{C}$$
$$k_1 = 0.295 \text{ ℓ mole}^{-1}\text{sec}^{-1} \text{ at } 214^{\circ}\text{C}$$

As mentioned in the introductory section, Pollard and Holbrook found that the rate increase caused by packing the vessel is roughly proportional to the increase in surface to volume ratio. The S/V ratio of their unpacked pyrex vessel was equal to 1 cm^{-1}, while ours was 0.6 cm^{-1}. Apparently our value of the rate constant k_1 should decrease by a factor of nearly two below theirs. As shown above, however, the values of k_1 are very close. Consequently, it seems that the non-autocatalytic term is not affected by the surface to volume ratio. In order to further clarify this aspect of the problem the spherical pyrex vessel (S/V = 0.6 cm^{-1}) was replaced by the

cylindrical pyrex vessel of S/V = 1.2 cm^{-1}. However, the time available did not allow further work to be done. We hope that some other research workers will continue the study of the kinetics using this reaction vessel.

The activation energy for the temperature range 182°C and 214°C was calculated using the Arrhenius equation. The result is 13.92 $\pm$ 1.39 Kcal $mole^{-1}$. This is 2.36 Kcal $mole^{-1}$ less than the activation energy obtained by Pollard and Holbrook (1). However, if one considers the errors involved for both activation energies, the difference is not significant.

II. Pollard's rate expression

In the introduction of this thesis, we have mentioned that Pollard's rate expression may not fit their observations. This was discussed by D. Barton and Peter E. Yankwich (3).

An attempt was made to fit our data to equation (1) by calculating k'. This may be rewritten as

[1] $\frac{dx}{dt} = k_1 (A_o - x)(B_o - x) + k' (A_o - x)(B_o - x)(C_o + x)$

where $\frac{dx}{dt}$ denotes the rate at any time; x is the corresponding pressure change; k_1 the rate constant of the non-autrcatalytic second order reaction; k' the rate constant of the autocatalytic third order process; A_o, B_o, and C_o are initial reactant pressures of HCOOH, NO_2 and NO respectively,

It is clear from Tables III to VII that k' so calculated varies throughout the course of the reaction. Therefore,

our results do not fit Pollard's rate expression.

In the next section the method of finding how the autocatalytic term of the rate expression depends upon [HCOOH], $[NO_2]$ and [NO] will be described.

III. Autocatalytic term in the rate expression

i. Dependence of rate upon the concentration of nitric oxide

The type C runs were used to determine the dependence of rate upon the concentration of nitric oxide. Due to the existence of the induction period which is present in all of the type C experiments (See figures 12 and 13), the initial rate of the reaction could not be measured. An alternate differential method of treating the data was adopted. If one assumes that the simple stoichiometry is valid throughout the reaction, all instantaneous partial pressures are simply a function of initial pressures and ΔP. Then, the rate of reaction at any time is

$$[9] \quad R = M + X$$

where $R = \frac{dx}{dt}$, X is the whole autocatalytic term, and the form of M is assumed to be $k_1(A_0 - x)(B_0 - x)$ throughout the course of the reaction. The curves of R against P_{NO} are plotted in Figures 20 and 21 at ΔP = 4 mm Hg, 10 mm Hg, and 14 mm Hg.

First, the data obtained at 214°C was treated. The R values were obtained by measuring slopes from the recorder charts of individual runs at the pressure changes, ΔP = 4 mm Hg,

10 mm Hg, and 14 mm Hg. (These were Type C runs with constant initial pressures of formic acid and nitrogen dioxide and with various initial pressures of nitric oxide.) The M values were calculated using $K_1 = 1.034 \times 10^{-5}$ mm $Hg^{-1}sec^{-1}$ at a particular ΔP. Hence, the X values were obtained from equation [9]. X is expected to be a function of only P_{NO} at a certain ΔP, since the pressures of NO_2 and HCOOH are fixed.

The resulting plot of X against P_{NO} (Figure 22) at the particular ΔP values shows in every case a curve which is concave downward over a very wide range of nitric oxide pressure. Instead of being first order, as originally proposed (1), it is obvious that the order with respect to nitric oxide is less than one as was later suggested (3). The curvature is particularly noticable at ΔP = 10 mm Hg and 14 mm Hg.

In addition, the double logarithmic plot of X vs P_{NO} (Figure 23) is curved. Definitely, our experimental evidence shows that the autocatalytic term is not simply a function which is proportional to P_{NO} raised to some power. Instead, it is more complex.

The order was previously reported to be approximately 2/3 with respect to nitric oxide (3). This fractional value can be obtained from the data shown in Figure 23, using the least-squares method, taking the log-log plot to be linear. Because this treatment is not adequate for treating our experimental facts, the simple relationship $X = B[NO]^{2/3}$, as suggested by D. Barton and Peter E. Yankwich (3), is merely an approximation.

The trial expression [10] is the simplest which could show a variation of order with respect to nitric oxide. The expression would give a rate which varies linearly with P_{NO} at low P_{NO}, whereas at higher P_{NO}, this relationship no longer would hold and the rate would become nearly independent of P_{NO}.

$$[10] \qquad \frac{X}{} = \frac{a\ (C_o + x)}{b + c\ (C_o + x)}$$

This is consistent with the data in Figure 22, in a qualitative way. The parameters a, b and c contain rate constants and perhaps concentrations of formic acid and nitrogen dioxide. The expression can be written as

$$\frac{(C_o + x)}{X} = \frac{b}{a} + \frac{c}{a}(C_o + x)$$

The plot of $\frac{(C_o + x)}{X}$ vs $(C_o + x)$ is shown in Figure 24. Although the points show some scatter, the plot was treated as a straight line. Both c/a (slope) and b/a (intercept) values were calculated by the least-squares method. They are listed below.

ΔP (mm Hg)	c/a (slope)	b/a (intercept)
4	11.04 ± 0.58	1487 ± 66
10	15.99 ± 0.81	1830 ± 95
14	25.47 ± 1.32	2641 ±170

Although the data (Figures 25 and 26) are relatively few, the type C experiments at 182°C were similarly treated. The results are given below.

ΔP mm Hg	c/a (slope)	b/a (intercept)
4	39.19 ± 1.88	2807 ± 117
6	46.45 ± 2.49	2853 ± 160
8	57.59 ± 3.92	3097 ± 258
10	69.03 ± 4.62	3770 ± 313
12	90.34 ± 6.10	4847 ± 425

Apparently, equation [10] is an adequate description of the dependence of rate upon the concentration of nitric oxide.

ii. Dependence of rate upon the concentration of nitrogen dioxide

In the type D experiments the initial nitric oxide and formic acid pressures were fixed and the initial nitrogen dioxide pressure was varied. The pressure-time curves were treated by the method explained in the foregoing section. The plots of X against P_{NO_2} (Figures 27, 28 and 29) show that the kinetic order is less than one. There seems to be no tendency for the reaction to become zero order at high NO_2 pressure, indicating that the required expression is not similar to expression [10]. Instead, a straight line was

obtained from the plot of log X vs log P_{NO_2} (Figures 30, 31 and 32). The orders obtained are given below.

ΔP mm Hg	Order with respect to NO_2
4	0.36 ± 0.02
10	0.41 ± 0.03
14	0.38 ± 0.02

The orders show no drift with the increase of ΔP and are approximately 2/5. The X term can now be written as

$$[11] \quad X = \frac{a' (C_o + x)}{b' + c' (C_o + x)} (B_o - x)^{2/5}$$

where a', b' and c' may be functions of [HCOOH].

This unusually low order should be noted.

iii. Dependence of rate upon the concentration of formic acid

Type E experiments were obtained by keeping the initial pressures of NO and NO_2 at a constant value and by varying the initial pressure of formic acid. The results were treated by the same method as explained in sections (i) and (ii). The plot of X against P_{FA} at ΔP = 4 mm Hg (Figure 33) is more or less a straight line. At ΔP = 10 mm Hg, the data are highly scattered and the plot of X vs P_{FA} (Figure 34) curves slightly upward. A linear relationship was at first assumed. The X term would then be

$$[12]\quad X = \frac{k'_a\ (C_o + x)\ (B_o - x)^{2/5}\ \ (A_o - x)}{k'_b + k_c\ (C_o + x)}$$

where k'_a, k'_b and k_c are constants.

Consequently, the complete rate expression could be written

$$[13]\quad \frac{dx}{dt} = k_1\ (A_o - x)\ (B_o - x) + \frac{k'_a\ (C_o + x)(B_o - x)^{2/5}(A_o - x)}{k'_b + k_c\ (C_o + x)}$$

An attempt was made, using equation [13] and calculated values of k'_a, k'_b and k_c to fit the curves of rates as a function of pressure change, obtained from the type A and B experiments. The fit is reasonable up to the maximum rate, but it does not at all fit the curve after the maximum rate. The calculated values are much too low. It was proposed that equation [13] could be modified by making k_c a function of $1/[NO_2]^r$ or $1/[HCOOH]^q$ It was shown in the preceeding section that the order with respect to NO_2 is approximately 2/5; one can exclude the possibility of k_c being a function of $1/[NO_2]^r$. Since the dependence of rate upon [HCOOH] was not entirely clear, (see preceeding section) it was proposed that the problem was connected with HCOOH, and $1/[HCOOH]^q$ was suggested. The effect of $1/[HCOOH]^q$ would be greatest at large concentrations of NO, i.e. later in the reaction, because the second part of the denominator would be

$$[14]\quad k'_c\ \frac{[NO]}{[HCOOH]^q}$$

The plot of X vs P_{FA} (Figure 35) at P = 14 mm Hg was then examined and it could be definitely seen to curve upward. The double logarithmic plot of X vs P_{FA} (Figure 36) is still curved upwards, indicating that the dependence of rate upon HCOOH is not of the form $[HCOOH]^p$, but that the order increases as [HCOOH] increases. The slope at low formic acid pressure was measured roughly and found to be about 1, whereas at high formic acid pressure it increased to about 3/2. The following trial function for the autocatalytic term was then proposed:

$$[15] \qquad X = \frac{k_a' \ (C_o + x) \ (B_o - x)^{2/5} \ (A_o - x)}{k_b' + k_c' \ \dfrac{(C_o - x)}{(A_o - x)^{1/2}}}$$

iv. Evaluation of k_c'/k_a' and k_b'/k_a'

Both c/a and b/a which were measured using the type C data, can be expressed as a function of [HCOOH], $[NO_2]$, k_a', k_b' and k_c':

$$[16] \qquad \frac{c}{a} = \frac{k_c'}{k_a' \ (A_o - x)^{3/2} \ (B_o - x)^{2/5}}$$

$$[17] \qquad \frac{b}{a} = \frac{k_b'}{k_a' \ (A_o - x) \ (B_o - x)^{2/5}}$$

Using the values of the initial pressures of reactants (A_o, B_o and C_o, and $\Delta P = x$), one can calculate k'_c/k'_a and k'_b/k'_a from equations [16] and [17]. For example, from run 105 (214°C) A_o = 31.99 mm Hg, B_o = 23.20 mm Hg and C_o = 41.45 mm Hg.

At ΔP = 4 mm Hg, c/a = 11.04 and b/a = 1.49×10^3.

Therefore $11.04 = \frac{k'_c}{k'_a} \frac{1}{(A_o - x)^{3/2} (B_o - x)^{2/5}}$

$$k'_c/k'_a = 11.04 \times (27.99)^{3/2} (19.02)^{2/5}$$

$$= 5332.05$$

and $k'_b/k'_a = 1.49 \times 10^3 (27.99) (19.02) = 1.37 \times 10^5$.

At ΔP = 10 mm Hg, c/a = 16, b/a = 1.83×10^3,

$$k'_c/k'_a = 16 \times (21.99)^{3/2} (13.20)^{2/5}$$

$$= 4629.27,$$

and $k'_b/k'_a = 1.83 \times 10^3 (21.99) (13.20)^{2/5}$

$$= 1.13 \times 10^5.$$

At ΔP = 14 mm Hg, c/a = 25.5, b/a = 2.64×10^3,

$$k'_c/k'_a = 25.5 (17.99)^{3/2} (9.20)^{2/5}$$

$$= 4665.60,$$

and $k'_b/k'_a = 2.64 \times 10^3 (17.99) (9.20)^{2/5}$

$$= 1.15 \times 10^5.$$

Similarly from run 42 (182°C),

A_o = 29.08 mm Hg,

B_o = 30.83 mm Hg,

and C_o = 39.49 mm Hg.

At ΔP = 4 mm Hg, c/a = 39.19, b/a = 2.81×10^3,

$$k'_c/k'_a = 39.19 \times 25.08 \times 5.01 \times 3.72$$
$$= 0.193 \times 10^5$$

and $$k'_b/k'_a = 2.81 \times 10^3 \times 25.08 \times 3.725$$
$$= 2.62 \times 10^5.$$

At ΔP = 6 mm Hg, c/a = 46.45, b/a = 2.85×10^3

$$k'_c/k'_a = 46.45 \times 23.08 \times 4.80 \times 3.61$$
$$= 0.186 \times 10^5$$

and $$k'_b/k'_a = 2.85 \times 10^3 \times 23.08 \times 3.61$$
$$= 2.38 \times 10^5.$$

At ΔP = 8 mm Hg, c/a = 57.59, b/a = 3.10×10^3

$$k'_c/k'_a = 57.59 \times 21.08 \times 4.59 \times 3.49$$
$$= 0.194 \times 10^5$$

and $$k'_b/k'_a = 3.10 \times 10^3 \times 21.08 \times 3.49$$
$$= 2.28 \times 10^5.$$

At ΔP = 10 mm Hg, c/a = 69.04, b/a = 3.77×10^3

$$k'_c/k'_a = 69.04 \times 19.08 \times 4.37 \times 3.37$$
$$= 3.37 \times 10^5$$

and $$k'_b/k'_a = 3.77 \times 10^3 \times 19.08 \times 3.37$$
$$= 2.424 \times 10^5.$$

At ΔP = 12 mm Hg, c/a = 90.34, b/a = 4.85×10^3

$$k'_c/k'_a = 90.34 \times 17.08 \times 413 \times 3.23$$
$$= 0.206 \times 10^5$$

and $$k'_b/k'_a = 4.85 \times 17.08 \times 3.23$$
$$= 2.674 \times 10^5.$$

Hence, the average values of k'_c/k'_a and k'_b/k'_a obtained from the above calculations are tabulated below.

Temperature ^oC	k'_c/k'_a	k'_b/k'_a
182	$0.193 \pm 0.007 \times 10^5$	$2.48 \pm 0.14 \times 10^5$
214	$4.88 \pm 0.30 \times 10^3$	$1.17 \pm 0.09 \times 10^5$

Next, using these rate constant ratios in the rate expression

$$[18]\ R = k_1\ [HCOOH]\ [NO_2] + \frac{k'_a\ [HCOOH]\ [NO_2]^{2/5}\ [NO]}{k'_b + k'_c \frac{[NO]}{[HCOOH]^{1/2}}}$$

The rate was calculated as a function of ΔP for forty-four experiments and compared with the experimental rates. In order to carry out a good test, the experimental results were tested

over a variety of conditions. In some cases, calculations were carried out at ΔP = 4, 10 and 14 mm Hg and in some cases the whole curve was calculated. The results are shown in Figures 37 to 51 and Tables VIII to XI.

v. Comments on curve-fitting

For experiments at 214°C with no nitric oxide added initially, experimental and calculated rates were compared for three cases:

(i) with high initial nitrogen dioxide pressure,

(ii) with moderate initial pressures of both formic acid and nitrogen dioxide,

(iii) with high initial formic acid pressure.

The results are shown in Figures 37, 38, and 39. The calculated and experimental rates differ by at most 5%. Since this is within the rate measurement and instrumental errors, the fit was considered to be perfect.

For experiments at 214°C with nitric oxide present initially, experimental and calculated rates were compared for nine cases:

(i) with high initial formic acid pressure,

(ii) with moderate initial formic acid pressure,

(iii) with low initial formic adic pressure,

(iv) with high initial NO_2 pressure,

(v) with moderate initial NO_2 pressure,

(vi) with low initial NO_2 pressure,

(vii) with high initial NO pressure,

(viii) with low initial NO pressure, and

(ix) with moderate initial NO pressure.

The results are shown in Figures 40, 41, 42, 43, 44, 45, 46, 47, and 48. In all cases the experimental rate is less than the calculated rate before the maximum rate. The agreement between calculated and experimental results is excellent after the maximum rate. In runs 123, 124, 73, 74, 72, 75 and 125 an interesting sharp decrease in rate occurs at about 80% reaction. (See section 1 of the RESULTS AND DISCUSSION SECTION) It is not clear whether or not the rate expression fits this portion because of the large error caused by the small $(A_o - x)$ and $(B_o - x)$ terms. It should also be recalled that in these runs the maximum rate occurs at about 20% reaction but not at zero time. It is important to distinguish between these experiments and the type B experiments with high formic acid pressures without nitric oxide added initially: the maximum rate occurs at about 50% reaction, but there is perfect agreement between the calculated rate and the experimental rate.

Similarly, in experiments at 182°C, with nitric oxide present initially, experimental and calculated rates were compared for three cases:

(i) with high initial NO pressure,

(ii) with moderate initial pressures of HCOOH, NO and NO_2, and

(iii) with low initial NO pressure.

The results are shown in Figures 49, 50 and 51. The agreement between calculated and experimental results is also excellent after the maximum, but not before the maximum rate.

In addition, the fitting of the calculated rate to the experimental rate at 214°C with nitric oxide added initially for three ΔP points, is excellent for thirty-one experiments.

5. Concluding Remarks

Non-autocatalytic reaction

The main points in the evidence presented by Pollard and Holbrook (1), related to the non-autocatalytic reaction, are listed below.

1. The order of the reaction with respect to formic acid and nitrogen dioxide was approximately one.
2. The pre-exponential factor was found to be $10^{6.73} \pm 0.25$ 1 $mole^{-1} sec^{-1}$ and the activation energy was found to be 16.276 ± 0.559 kcal $mole^{-1}$.
3. The major products were CO_2, H_2O and NO.

The proposed mechanism is

[2] $HCOOH + NO_2 \rightarrow [HCOOH.NO_2] \rightarrow COOH + HNO_2$

[3] $COOH + NO_2 \rightarrow CO_2 + HNO_2$

[4] $2HNO_2 \rightarrow NO + H_2O + NO_2$

The proposed rate-controlling step is formation of $[HCOOH.NO_2]$ by reaction between adsorbed formic acid and NO_2 in the gas phase. Such a reaction would be accompanied by a

negative entropy of activation, resulting in a low pre-exponential factor as observed. This surface reaction might also have a low activation energy. It is not clear whether the intermediate [$HCOOH.NO_2$] should decompose to COOH or to HCOO radical although each could plausibly occur in this system.

D. Barton and Peter E. Yankwich have suggested hydrogen abstraction reactions such as

[19] $HCOOH + NO_2 \rightarrow COOH + HONO$

[20] $HCOOH + NO_2 \rightarrow HCOO + HONO$

instead of Pollard's reaction [2]. The evidence for hydrogen abstraction at both positions is that the hydrogen isotope effects are $k_{hh}/k_{dh} = 1.48 \pm 0.12$ and $k_{hh}/k_{hd} = 1.39 \pm 0.99$ in the non-autocatalytic reaction which are nearly equal. Such steps have also been postulated in reactions of NO_2 with other hydrogen containing compounds. For example, see references (16) and (17).

It was mentioned in the RESULTS and DISCUSSION section that the rate of the non-autocatalytic reaction might not be affected by changing the s/v ratio. Our inference was that perhaps the non-autocatalytic reaction does occur in the gas phase rather than at the surface. In contradiction of this Pollard reported that the initial rate, i.e. the non-autocatalytic rate, was increased in packed vessels. However, no data was reported; this aspect of the reaction clearly requires further study.

Autocatalytic reaction

It is interesting to speculate on some of the possible reactions which could be consistent with the rate expression.

The study of the dependence of rate upon the concentration of nitric oxide showed that the rate seems to reach a maximum when a large amount of nitric oxide is added. This definitely eliminates the mechanism

[5] $NO + NO_2 \rightarrow N_2O_3$

[6] $N_2O_3 \rightarrow NO + NO_2$

[7] $HCOOH + N_2O_3 \rightarrow COOH + NO + HNO_2$

proposed by Pollard. This is because the equilibrium constant for the reaction $N_2O_3 \rightleftharpoons NO + NO_2$ is so favourable to dissociation of N_2O_3 that the relationship between N_2O_3 concentration and NO concentration is a linear one, at this temperature. Therefore, the reaction would be first order with respect to nitric oxide.

On the other hand, the mechanism could probably include two extreme types of reaction, i.e. catalysis as well as inhibition by nitric oxide.

The procedure for finding a suitable mechanism might be to first consider the effect of NO on pyrolysis reactions. This subject has been reviewed by Szabo (18) who discussed the following general mechanism.

Propagation steps:

[21] $R + NO \rightarrow RNO$

[22] $A + R \rightarrow E + R$

[23] $A + RNO \rightarrow E + RNO$

Termination steps:

[24] $R + R \rightarrow R - R$

[25] $R + RNO \rightarrow R\text{-}R + NO$ (low NO concentration)

[26] $RNO + RNO \rightarrow R\text{-}R + 2NO$ (High NO concentration)

Catalysis by NO would result if the rate ratio of propagation step [23] to termination step [25] (or [26]) is greater than the rate ratio of propagation step [22]to termination step [24]. It is not yet known whether or not this principle could apply to the reaction between HCOOH and NO_2. Nevertheless, the dependence of rate upon NO does suggest this type of mechanism.

The order with respect to NO_2 is 2/5. It would be difficult to find a mechanism for this strange order. However, orders of this kind have been found in surface reactions. If the rate is proportional to the coverage $[A]_{ads}$ of the surface, which in turn is proportional to some low power of the gas phase concentration of reactants $[A]^n$, the order with respectto A would be n. Such a reaction, the catalyzed formation of NH_3 from N_2 and H_2 has been discussed by Ashmore (19). The first possibility is perhaps, that NO_2 is adsorbed and reacts on the surface. Another possibility may be that an intermediate is adsorbed and reacts at the surface, which could be reflected

in the 2/5 order with respect to NO_2. However, since the degree of coverage is affected by temperature, one would expect a change in order with a temperature change. No information on the absorption of NO_2 was obtained.

In conclusion, it can be said that a rate expression has been determined for the reaction between formic acid and nitrogen dioxide, which fits the experimental rate over a considerable range of conditions. A suitable mechanism has not yet been found because it is a very complex rate expression.

TABLE I

Initial rate in type A and B reactions at 182°C

Run No.	$P_{(FA)_i}$ mm Hg.	$P_{(NO_2)_i}$ mm Hg.	$(\frac{dP}{dt})_i \times 10^3$ mm Hg/sec
17	30.4700	7.67	0.75
21	28.48	21.46	2.49
9	29.65	32.45	3.63
12	30.11	39.45	4.27
13	30.30	42.10	5.94
14	29.92	48.26	5.16
10	29.83	48.51	5.84
20	29.91	59.43	7.01
15	28.53	71.17	7.28
22	28.75	94.73	10.14
24	18.87	29.49	2.52
27	39.10	30.21	4.55
25	48.62	29.99	5.81
33	56.86	29.44	6.76
30	57.45	29.43	7.05
26	68.21	30.31	9.64
31	79.96	28.96	9.95

TABLE II

Initial rate in type A and B reactions at 214°C

Run No.	$P_{(FA)_i}$ mm Hg.	$P_{(NO_2)_i}$ mm Hg.	$\left(\frac{dP}{dt}\right)_i \times 10^2$ mm Hg/sec
83	29.11	36.70	1.05
82	30.59	37.14	1.13
50	30.68	38.47	1.14
81	29.45	47.73	1.27
88	30.06	49.34	1.35
49	29.28	59.80	1.71
87	30.51	64.00	1.85
120	30.38	65.67	1.85
54	28.96	69.96	1.83
80	31.08	77.93	2.26
86	29.70	90.86	2.71
127	15.16	30.00	0.50
128	20.15	29.69	0.62
131	37.85	30.41	1.21
130	38.42	29.92	1.20
126	38.55	30.12	1.18
129	39.42	30.25	1.33
117	52.10	29.92	1.81
122	71.59	29.64	2.73
114	71.61	29.98	2.72

TABLE III

Data for run # 30

Temperature $214^{o}C$

Initial FA pressure 38.42 mm Hg

Initial NO_2 pressure 29.92 mm Hg

$k_1 = 1.034 \times 10^{-5}$ mm $Hg^{-1}sec^{-1}$

No.	Total pressure change (mm Hg)	$\frac{dp}{dt} \times 10^2$ mm Hg/sec	$k'_{cal.} \times 10^6$ mm $Hg^{-2}sec^{-1}$
1	2.23	1.24	0.91
2	2.78	1.24	0.90
3	10.17	1.28	1.24
4	17.39	1.05	1.69
5	19.56	0.89	1.80
6	21.30	0.74	1.88
7	22.74	0.66	2.12
8	23.90	0.54	2.15

TABLE IV

Data for run # 125

Temperature 214°C

Initial FA pressure 32.06 mm Hg

Initial NO_2 pressure 23.79 mm Hg

Initial NO pressure 297.98 mm Hg

$k_1 = 1.034 \times 10^{-5}$ mm $Hg^{-1} sec^{-1}$

No.	Total pressure change (mm Hg)	$\frac{dp}{dt} \times 10^2$ mm Hg/sec	$k'_{cal.} \times 10^6$ mm $Hg^{-2} sec$
1	0.76	5.51	0.22
2	1.56	6.23	0.27
3	2.70	6.93	0.33
4	4.00	7.13	0.39
5	6.31	6.43	0.43
6	7.56	5.94	0.45
7	10.00	4.95	0.49
8	11.28	4.15	0.48
9	14.00	3.03	0.52
10	16.05	2.23	0.53
11	17.09	1.98	0.59

TABLE V

Data for run # 73

Temperature 214°C

Initial FA pressure 81.18 mm Hg

Initial NO_2 pressure 22.91 mm Hg

Initial NO pressure 33.21 mm Hg

$k_1 = 1.034 \times 10^{-5}$ mm $Hg^{-1} sec^{-1}$

No.	Total pressure change (mm Hg)	$\frac{dP}{dt} \times 10^2$ mm Hg/sec	$k'_{cal.} \times 10^6$ mm Hg^{-2}/sec
1	0.45	5.44	0.58
2	1.67	6.36	0.78
3	2.71	6.53	0.85
4	4.00	7.13	1.03
5	7.25	7.11	1.26
6	10.00	6.93	1.50
7	14.00	5.94	1.88
8	16.22	4.94	2.09
9	18.45	3.96	2.53
10	19.83	3.56	3.36
11	20.67	1.86	2.35

TABLE VI

Data for run # 42

Temperature 182°C

Initial Pressure of FA 29.08 mm Hg

Initial pressure of NO_2 30.83 mm Hg

Initial NO pressure 39.49 mm Hg

$k_1 = 0.402 \times 10^{-5}$ mm Hg $^{-1}$sec^{-1}

No.	Total pressure change (mm Hg)	$\frac{dP}{dt} \times 10^2$ mm Hg/sec	$k'_{cal.} \times 10^6$ mm Hg^{-2}sec^{-1}
1	0.32	1.06	0.20
2	1.03	1.17	0.25
3	2.38	1.32	0.32
4	4.00	1.23	0.33
5	6.00	1.19	0.37
6	8.00	1.04	0.37
7	10.00	0.89	0.37
8	12.00	0.69	0.34
9	15.20	0.50	0.34
10	17.55	0.40	0.38
11	20.40	0.25	0.39

TABLE VII

Data for run # 46

Temperature 182°C

Initial FA pressure 28.33 mm Hg

Initial NO_2 pressure 29.85 mm Hg

Initial NO pressure 18.95 mm Hg

$k_1 = 0.402 \times 10^5$ mm $Hg^{-1} sec^{-1}$

No.	Total pressure change (mm Hg)	$\frac{dP}{dt} \times 10^2$ mm Hg/sec	$k'_{cal.} \times 10^6$ mm $Hg^{-2} sec^{-1}$
1	0.61	0.74	0.26
2	1.56	0.85	0.35
3	2.39	0.89	0.40
4	4.00	0.85	0.41
5	6.00	0.81	0.45
6	8.00	0.74	0.47
7	10.00	0.63	0.46
8	12.00	0.50	0.42
9	13.29	0.46	0.44
10	16.50	0.30	0.42
11	18.82	0.20	0.41
12	20.12	0.16	0.42

TABLE VIII

Comparison of calculated and experimental rates at 214°C for Type C experiments

Run	Initial pressure (mm Hg)			Δp = 4 (mm Hg)		ΔP = 10 (mm Hg)		ΔP = 14 (mm Hg)	
	FA	NO_2	NO	$R_{obs.}$[a]	$R_{calc.}$	$R_{obs.}$	$R_{calc.}$	$R_{obs.}$	$R_{calc.}$
116	32.30	23.01	13.44	1.78	1.77	1.49	1.33	0.94	0.98
107	32.09	22.81	14.77	1.78	1.81	1.56	1.36	1.06	0.99
102	32.06	22.93	22.84	2.12	2.27	1.78	1.62	1.18	1.17
103	32.29	23.16	23.59	2.23	2.34	1.78	1.68	1.31	1.21
98	32.00	23.35	30.08	2.40	2.66	1.91	1.87	1.35	1.33
105	31.99	23.20	41.45	2.88	3.16	2.28	2.16	1.49	1.59
101	32.13	23.10	52.86	3.14	3.63	2.47	2.44	1.77	1.68
100	31.83	24.21	53.21	3.34	3.69	2.47	2.50	1.78	1.74
106	32.18	23.84	63.56	3.64	4.08	2.82	2.64	1.95	1.90
104	31.80	23.69	68.51	3.47	4.17	2.77	2.75	1.91	1.89
96	32.14	23.03	70.33	3.49	4.24	2.72	2.77	1.86	1.90
99	31.99	22.85	84.96	3.71	4.59	2.64	2.98	1.80	2.01
123	32.47	23.64	139.87	5.13	6.01	3.91	3.85	2.60	2.60
124	32.09	26.74	203.49	6.13	7.26	4.57	4.67	3.10	3.21
125	32.06	23.79	297.98	7.13	7.65	4.95	4.75	3.05	3.14

[a] Units are mm Hg/sec x 10^2

TABLE IX

Comparison of calculated and experimental rates at 214°C for Type D experiments

Run	Initial pressure (mm Hg)			ΔP = 4 (mm Hg)		ΔP = 10 (mm Hg)		Δp = 14 (mm Hg)	
	FA	NO_2	NO	$R_{obs.}$ [a]	$R_{cal.}$	$R_{obs.}$	$R_{cal.}$	$R_{obs.}$	$R_{cal.}$
112	32.10	15.99	32.67	2.04	2.19	1.32	1.33	0.68	0.57
133	31.82	23.41	33.71	2.48	2.81	1.88	1.95	1.35	1.38
111	32.07	32.16	32.61	3.17	3.40	2.69	2.52	1.96	1.91
113	32.00	41.34	32.59	3.56	3.97	2.74	2.99	2.19	2.35
109	31.89	41.60	33.20	3.67	4.00	3.18	3.03	2.50	2.36
110	32.22	60.81	32.91	4.64	5.13	4.05	4.00	3.43	3.21
136	32.30	75.27	32.92	5.23	5.88	4.83	4.65	4.05	3.77
108	31.94	83.74	32.86	5.44	6.21	4.98	4.92	4.22	3.97
135	32.14	84.62	32.59	5.73	6.30	4.76	4.98	4.13	4.05

[a] Units are mm Hg sec^{-1} x 10^2

TABLE X

Comparison of calculated and experimental rates at 214°C for Type E experiments

Run	Initial pressure (mm Hg)			ΔP = 4 (mm Hg)		ΔP = 10 (mm Hg)		ΔP = 14 (mm Hg)	
	FA	NO_2	NO	$R^{a}_{obs.}$	$R_{cal.}$	$R_{obs.}$	$R_{cal.}$	$R_{obs.}$	$R_{cal.}$
91	19.93	23.04	33.17	1.44	1.50	0.81	0.78		0.374
95	28.58	22.77	32.70	2.23	2.37	1.40	1.57	1.02	1.05
69	32.15	21.75	33.07	2.38	2.69	1.79	1.85	1.19	1.28
70	38.95	22.33	33.12	3.08	3.47	2.38	2.55	1.76	1.90
66	47.01	22.08	33.58	3.79	4.34	3.34	3.33	2.62	2.57
67	48.49	22.67	33.18	4.08	4.54	3.34	3.53	2.64	2.77
90	54.79	21.90	32.75	4.16	5.09	3.64	4.03	2.72	3.18
85	58.56	21.69	32.93	5.01	5.59	4.45	4.37	3.04	3.63
68	59.25	23.02	32.82	4.950	5.75	3.72		3.14	
92	65.70	22.57	34.10	5.76	6.55	5.40	5.34	3.81	4.37
93	66/46	23.29	33.08	5.52	6.64	5.09	5.49	3.71	4.54
64	74.17	22.79	33.44	6.68	7.46	5.94	6.20	4.95	5.17
73	81.18	22.91	33.21	7.13	8.33	6.93	7.05	5.94	5.93
72	82.12	23.21	34.79	6.93	8.66	7.17	7.35	5.94	6.17
75	82.74	22.52	33.78	7.17	8.44	7.03	7.09	5.94	5.92
74	82.77	24.20	33.14	7.24	8.69	7.27	7.45	6.00	6.38

TABLE XI

Comparison of calculated and experimental rates at 182°C for Type C experiments

Run	Initial Pressure (mm Hg)			Δp (mm Hg)									
				4		6		8		10		12	
	FA	NO_2	NO	$R^a_{obs.}$	$R_{cal.}$	$R_{obs.}$	$R_{cal.}$	$R_{obs.}$	$R_{cal.}$	$R_{obs.}$	$R_{cal.}$	$R_{obs.}$	$R_{cal.}$
46	28.33	29.85	18.95	0.85	0.86	0.81	0.78	0.74	0.70	0.63	0.60	0.49	0.52
38	29.91	31.63	27.29	1.06	1.12	0.10	1.02	0.87	0.90	0.74	0.79	0.62	0.68
42	29.08	30.83	39.49	1.27	1.25	1.19	1.11	1.04	0.98	0.89	0.84	0.69	0.71
45	28.59	28.92	52.00	1.39	1.32	1.27	1.16	1.14	1.00	0.94	0.86	0.74	0.71
41	28.06	30.25	86.87	1.67	1.59	1.49	1.38	1.27	1.18	1.06	0.10	0.83	0.82
40	29.02	28.15	88.29	1.67	1.61	1.52	1.40	1.27	1.20	1.06	1.02	0.83	0.84

TABLE XII

Calibration of Thermocouples

Thermocouple # 6 (while freezing)

e.m.f.	time
9.4116 m. volts	
9.4122 "	
9.4122 "	
9.4124 "	
9.4124 "	
9.4130 "	
9.4136 "	
9.4136 "	
9.4138 "	
9.4138 "	
9.4138 "	
9.4138 "	
9.4138 "	
9.4138 "	
9.4154 "	
9.4154 "	
9.4154 "	
9.4154 "	
9.4160 "	
9.4160 "	
9.4164 "	
9.4164 "	for 1976 seconds

.... contd.

TABLE XII (Contd.)

Calibration of Thermocouples

Thermocouple # 6 (while freezing)

e.m.f.	time
9.4174 m. volts	
9.4174 "	
9.4190 "	
9.4176 "	
9.4196 "	
9.4203 "	
9.4215 "	
9.4215 "	
9.4160 "	

Average = 9.415 millivolts

TABLE XIII

Calibration of Thermocouples

Thermocouple # 4 (while freezing)

e.m.f.	time
9.4104 m. volts	
9.4105 "	
9.4100 "	
9.4101 "	
9.4112 "	
9.4121 "	
9.4121 "	
9.4121 "	
9.4129 "	
9.4135 "	
9.4141 "	
9.4141 "	
9.4143 "	
9.4143 "	
9.4148 "	
9.4157 "	
9.4159 "	
9.4164 "	
9.4171 "	
9.4185	for 2052 seconds

.... contd.

TABLE XIII (contd.)

Calibration of Thermocouples

Thermocouple # 4 (while freezing)

e.m.f.		time
9.4200	m. volts	
9.4205	"	
9.4229	"	
9.4246	"	
9.4263	"	
9.4241	"	
9.4154	"	for 2052 seconds

Average = 9.4157 millivolts

TABLE XIV

Calibration of Thermocouples

Thermocouple # 3 (while freezing)

e.m.f.	time
9.4126 m. volts	
9.4139 "	
9.4139 "	
9.4140 "	
9.4138 "	
9.4138 "	
9.4135 "	
9.4131 "	
9.4134 "	
9.4134 "	
9.4136 "	
9.4136 "	
9.4134 "	
9.4134 "	
9.4136 "	
9.4136 "	
9.4135 "	
9.4135 "	
9.4139 "	
9.4133 "	
9.4141 "	for 2038 seconds

Average = 9.4138 millivolts

.... contd.

TABLE XIV

Calibration of Thermocouples

Thermocouple # 3 (while freezing)

e.m.f.		time
9.4142	m. volts	
9.4149	"	
9.4155	"	
9.4133	"	for 2038 seconds

Average = 9.4138 millivolts

TABLE XV

Calibration of Thermocouples

Thermocouple # 2 (while freezing)

e.m.f.	time
9.4115 m. volts	
9.4115 "	
9.4115 "	
9.4115 "	
9.4116 "	
9.4115 "	
9.4172 "	
9.4146 "	
9.4146 "	
9.4116 "	
9.4140 "	
9.4130 "	
9.4128 "	
9.4128 "	
9.4128 "	
9.4128 "	
9.4128 "	
9.4134 "	
9.4145 "	

.... contd.

TABLE XV

Calibration of Thermocouples

Thermocouple # 2 (while freezing)

e.m.f.		time
9.4139	m. volts	
9.4141	"	
9.4142	"	
9.4150	"	
9.4150	"	
9.4151	"	
9.4156	"	
9.4156	"	
9.4110	"	
9.4107	"	for 1961 seconds

Average = 9.4137 millivolts

FIGURE 1

A schematic diagram of the apparatus used

B - Bulb

C - Column (P_2O_5)

D - Diffusion pump

F - Furnace

G - Spoon gauge

M - Manometer or Mcleod gauge

R - Reaction vessel

S - Stopcock

S_t - Teflon stopcock

ST - Storage

T - Trap

TH - Thermocouple gauge

TR - Toepler pump

S - Joint

U - U-trap

W - Thermocouple well

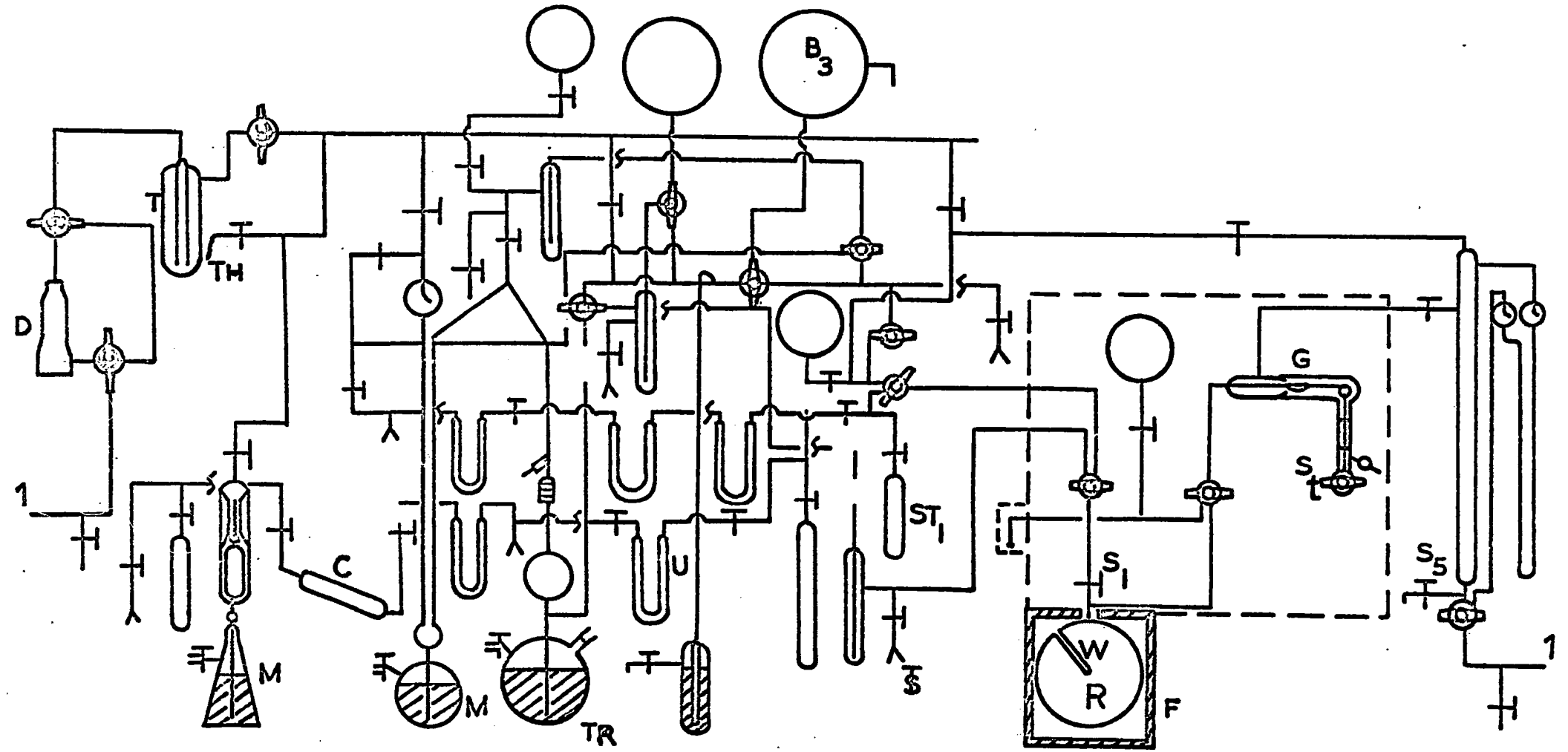
B3
T
TH
D
1
C
M
M
TR
U
ST1
S
S1
W
R
F
G
St
S5
1

FIGURE 2

Reactor and Thermocouple Positions

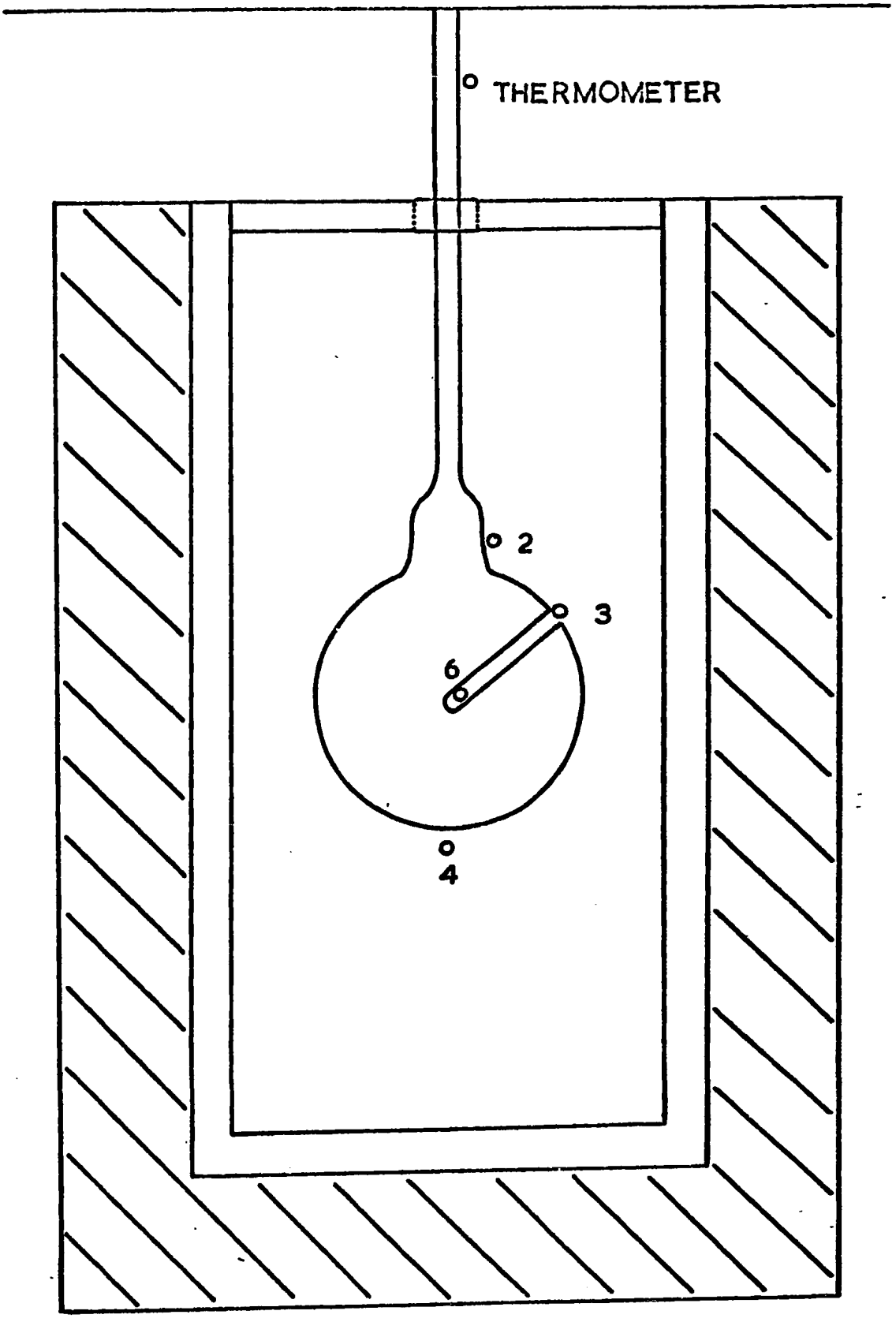
THERMOMETER
2
3
6
4

FIGURE 3

a - Air furnace

b - To reactor

c - To manifold

d - To pump

e - Amplifier

f - Millivolt recorder

G - Spoon gauge

M - Manometer

M
c
S5
d
D
a
G
S4
e
f

FIGURE 4

Diagram of Recording Spoon Gauge

1 - Antimagnetic spring

2 - Teflon screw

3 - LVDT core

4 - Transformer (LVDT)

5 - Antimagnetic steel rod

6 - Teflon rod

7 - Teflon stopcock

8 - To amplifier and recorder

9 - Transformer, schematic diagram

10 - A.C. input

11 - D.C. output

12 - Transformer (LVDT)

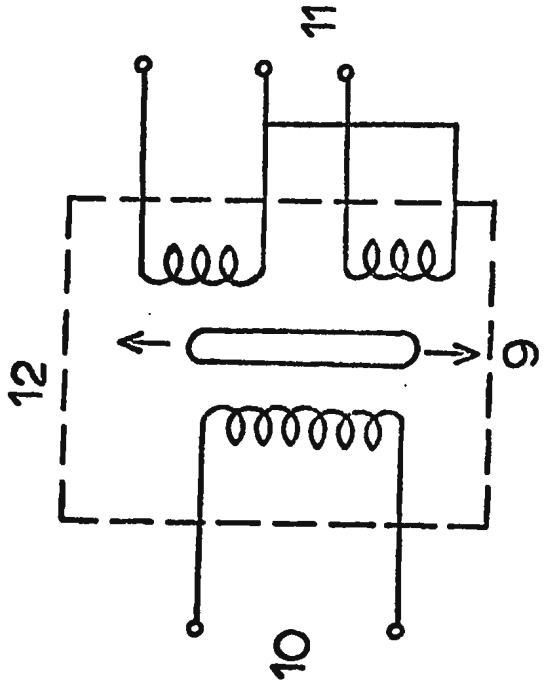
11
12
9
10

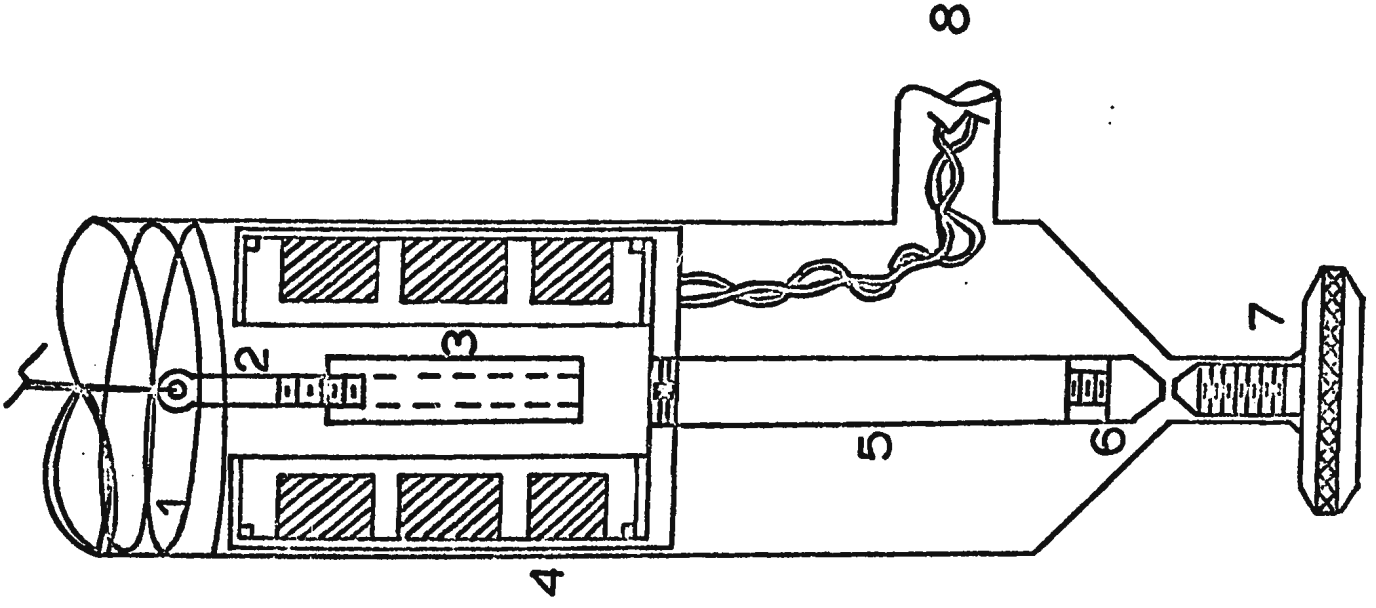
8
7
2
3
1
5
6
4

FIGURE 5

Calibration curve of recording spoon gauge

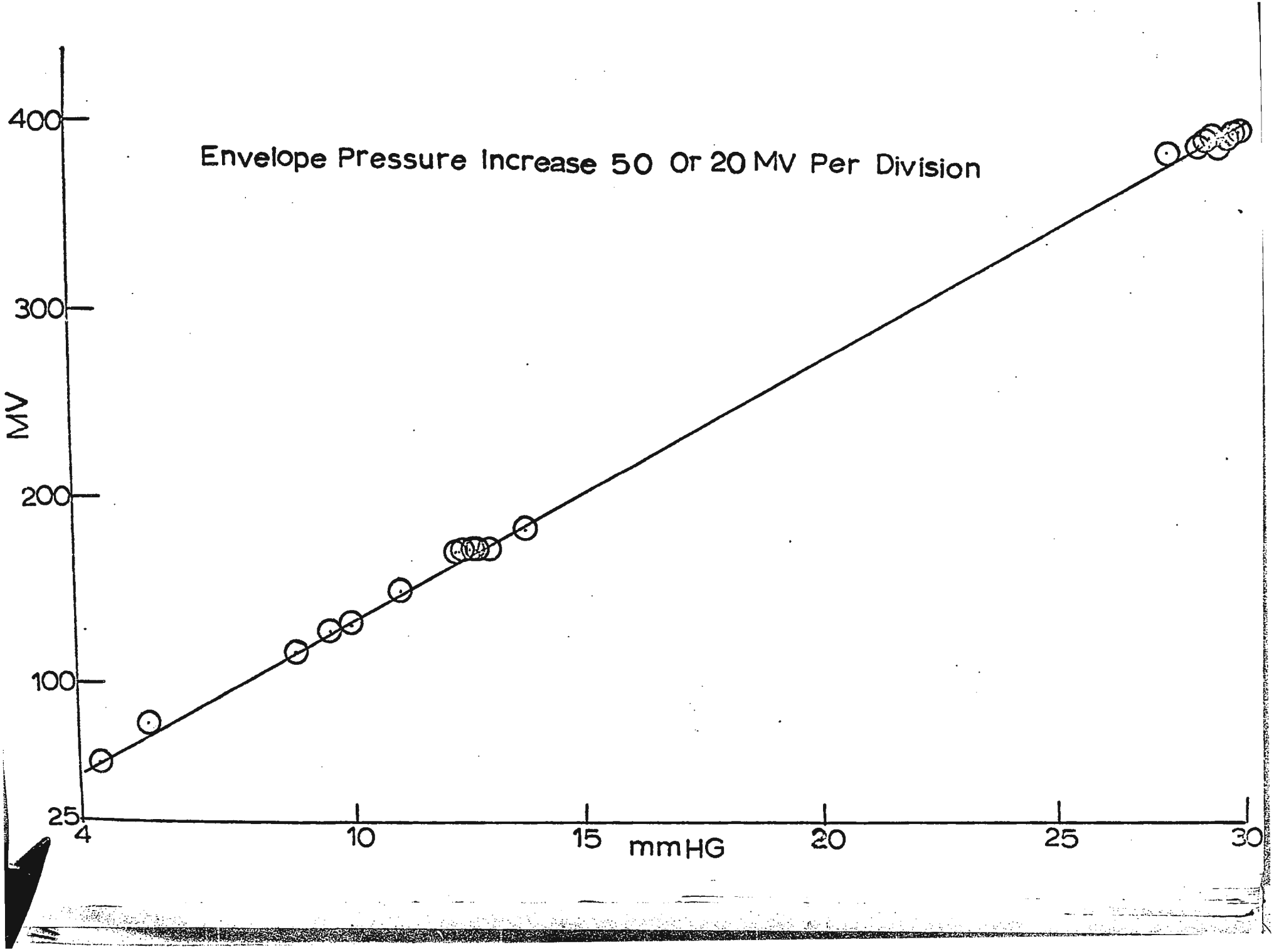
Envelope Pressure Increase 50 Or 20 MV Per Division
400
300
200
100
25
MV
4
10
15
mmHG
20
25
30

FIGURE 6

Pressure-time data (Type A) for determination of the order with respect to NO_2 (non-autocatalytic term) at 214°C.

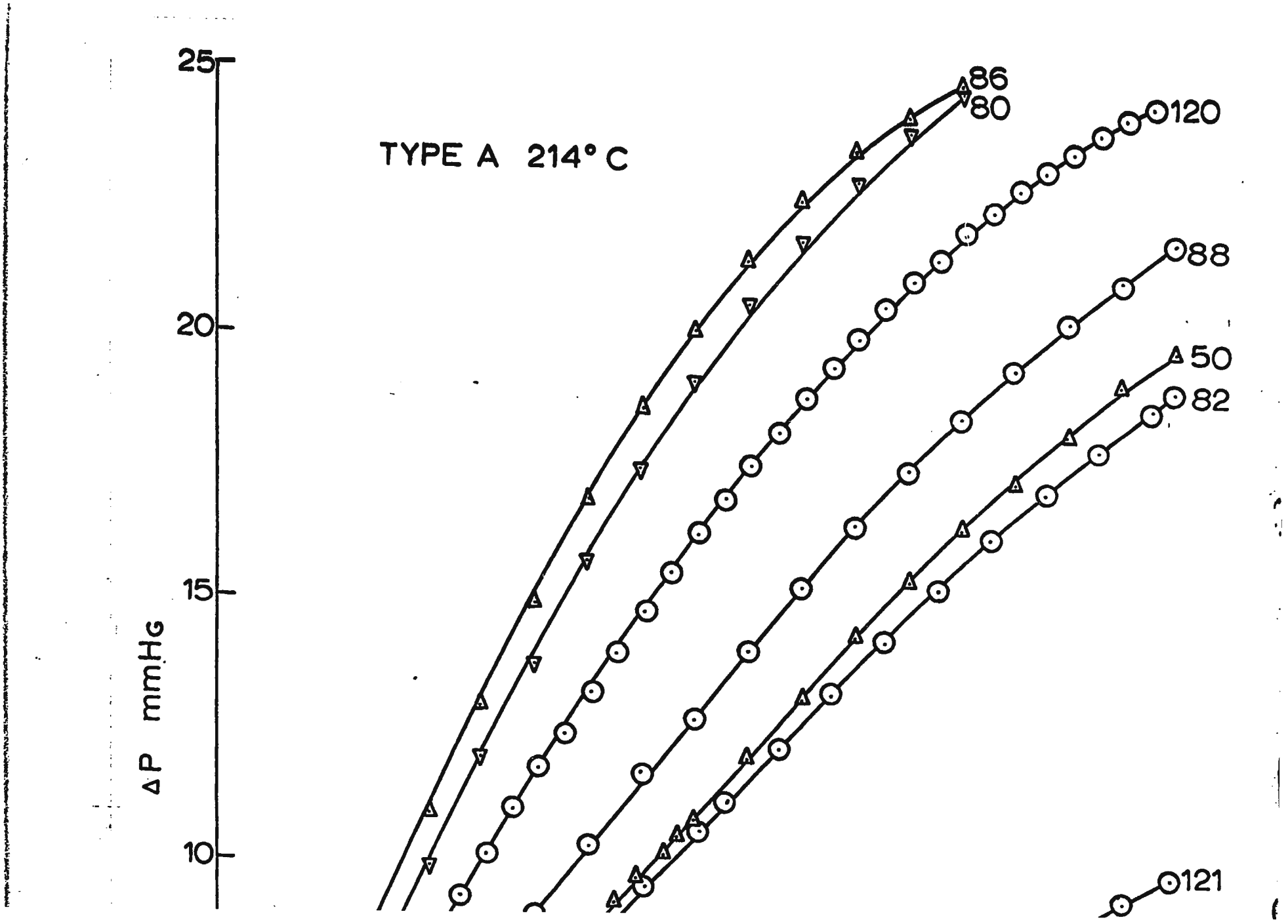
TYPE A 214° C
ΔP mmHg
25
20
15
10
86
80
120
88
50
82
121

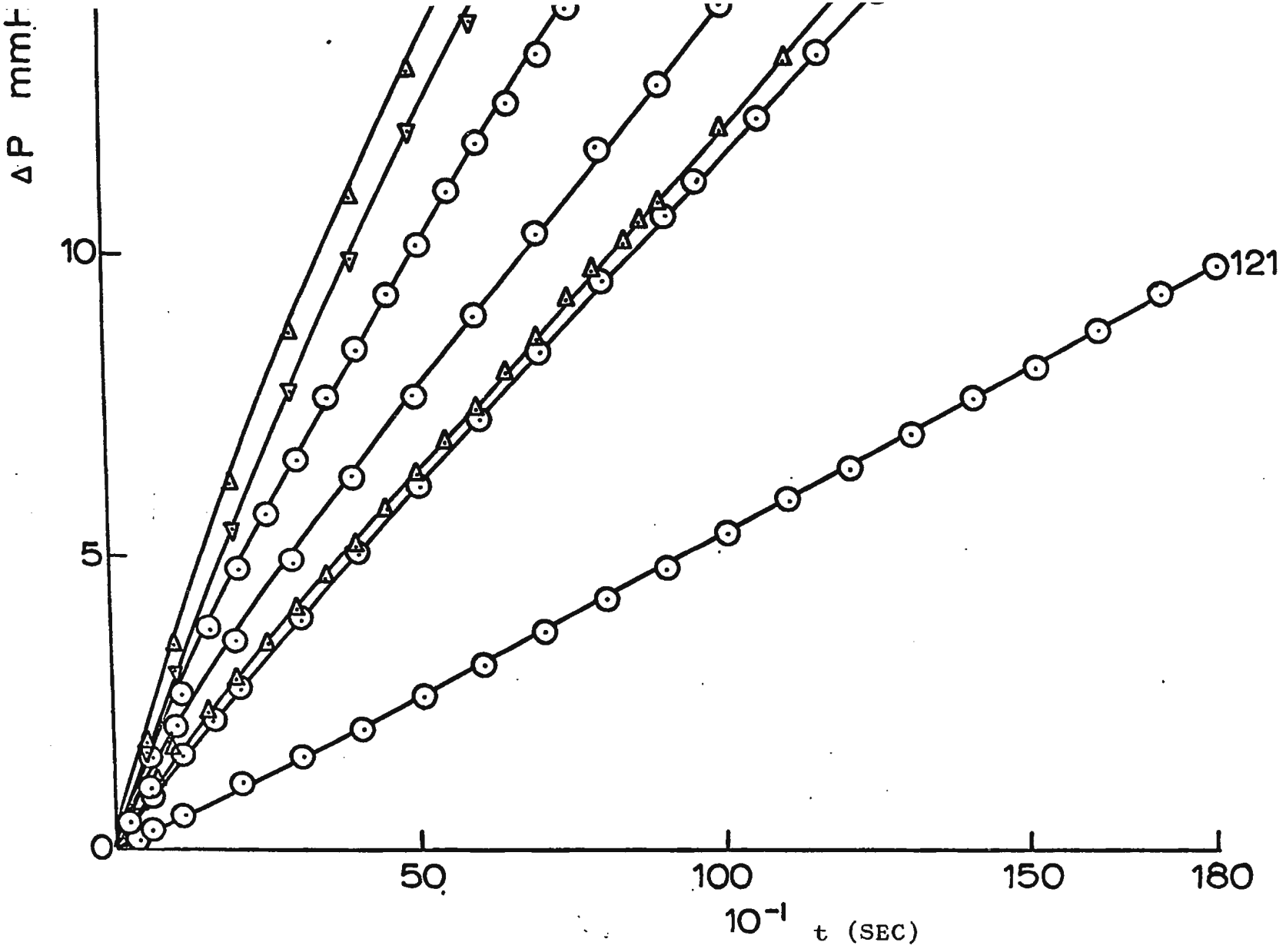
ΔP mmH
10
5
0
50
100
150
180
121
10⁻¹ t (SEC)

FIGURE 7

Pressure-time curves (214°C)

Run 50:

P_{FA} = 30.68 mm Hg P_{NO_2} = 38.47 mm Hg ΔP_F = 29.36 mm Hg

Run 126:

P_{FA} = 38.55 mm Hg P_{NO_2} = 30.12 mm Hg ΔP_F = 28.44 mm Hg

Run 129:

P_{FA} = 39.42 mm Hg P_{NO_2} = 30.25 mm Hg ΔP_F = 29.51 mm Hg

129
126
50
30
20
10
ΔP mmHg

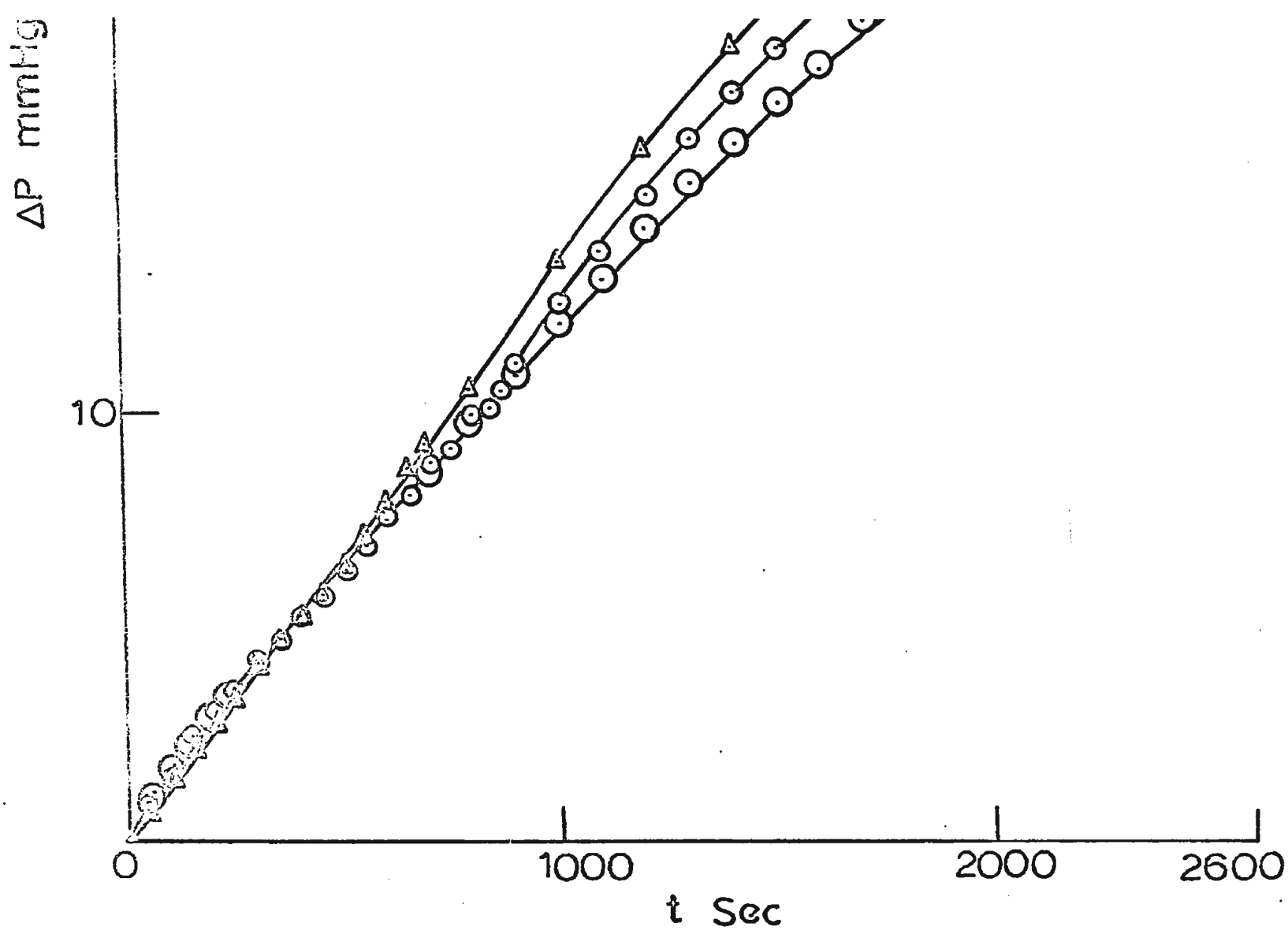
ΔP mmHg
10
0
1000
2000
2600
t Sec

FIGURE 8

Pressure-time curves (214°C)

Run 130:

P_{FA} = 38.42 mm Hg P_{NO_2} = 29.92 mm Hg ΔP_F = 29.29 mm Hg

Run 131:

P_{FA} = 38.75 mm Hg P_{NO_2} = 30.41 mm Hg ΔP_F = 30.40 mm Hg

130
131
30
20
10
ΔP mmHg

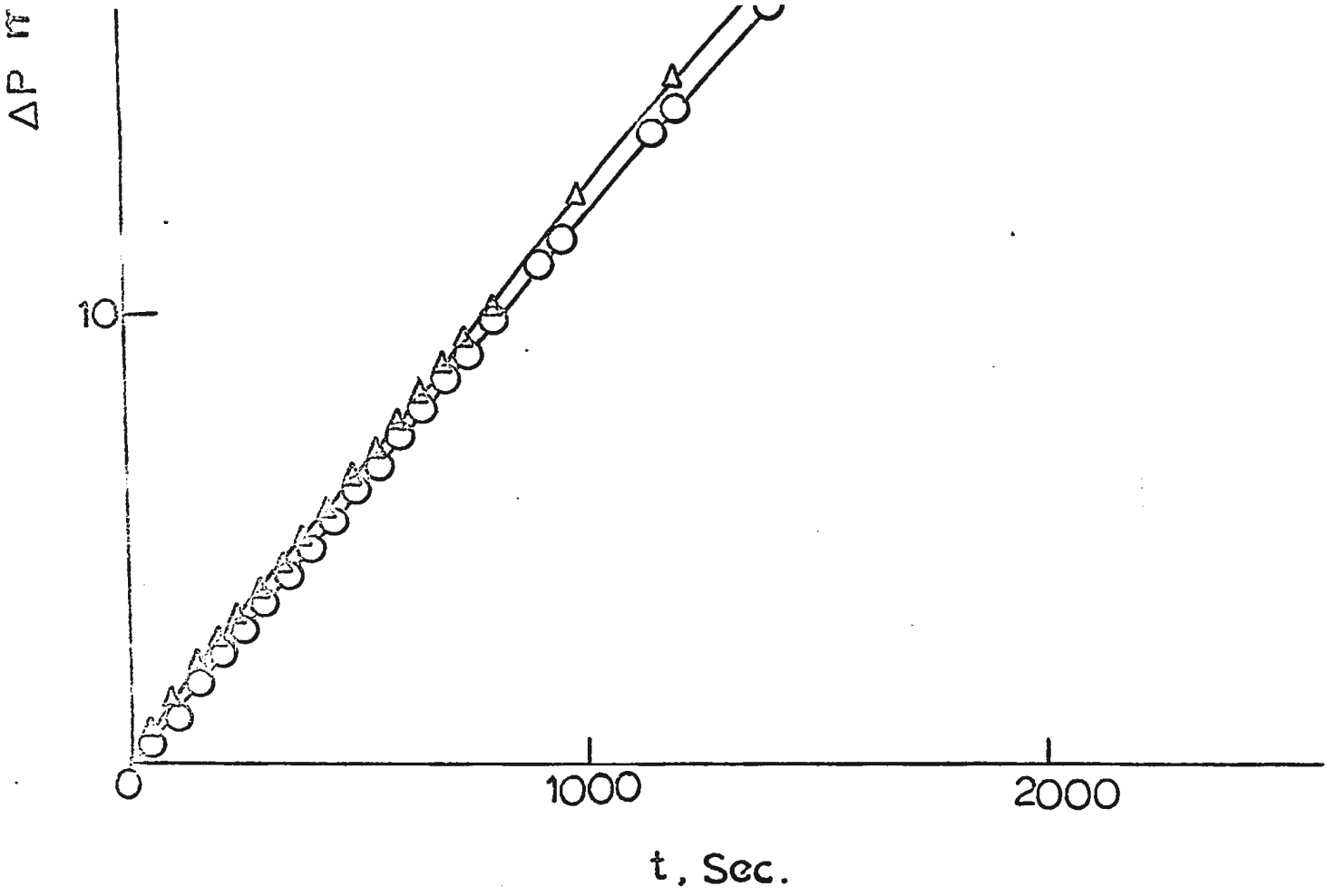
ΔP π
10
0
1000
2000
t, Sec.

FIGURE 9

Pressure-time curves (214°C)

Run 87, P_{FA} = 30.51 mm Hg P_{NO_2} = 64.00 mm Hg

Run 120, P_{FA} = 30.38 mm Hg P_{NO_2} = 65.67 mm Hg

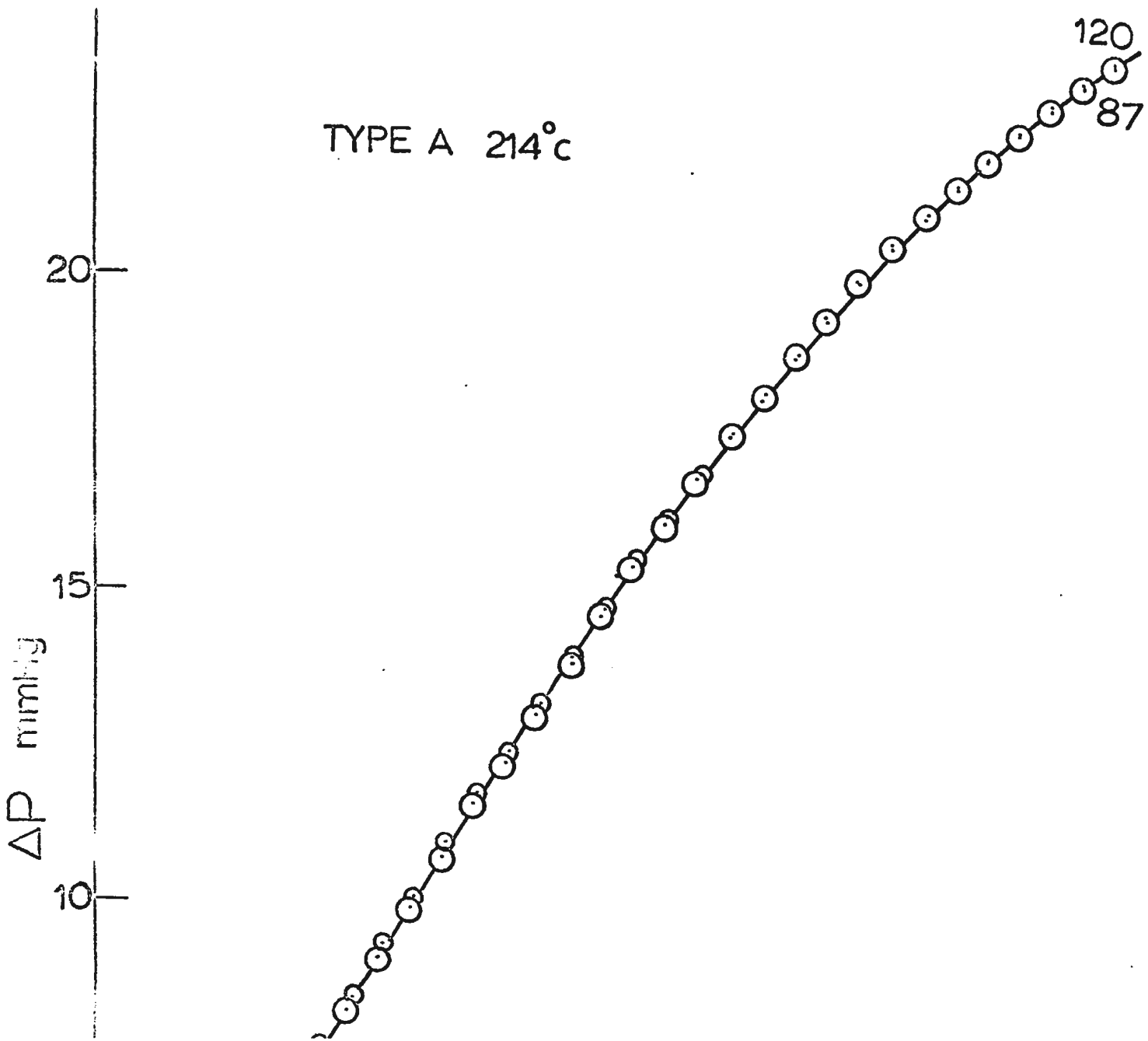
TYPE A 214°c
120
87
20
15
10
ΔP mmHg

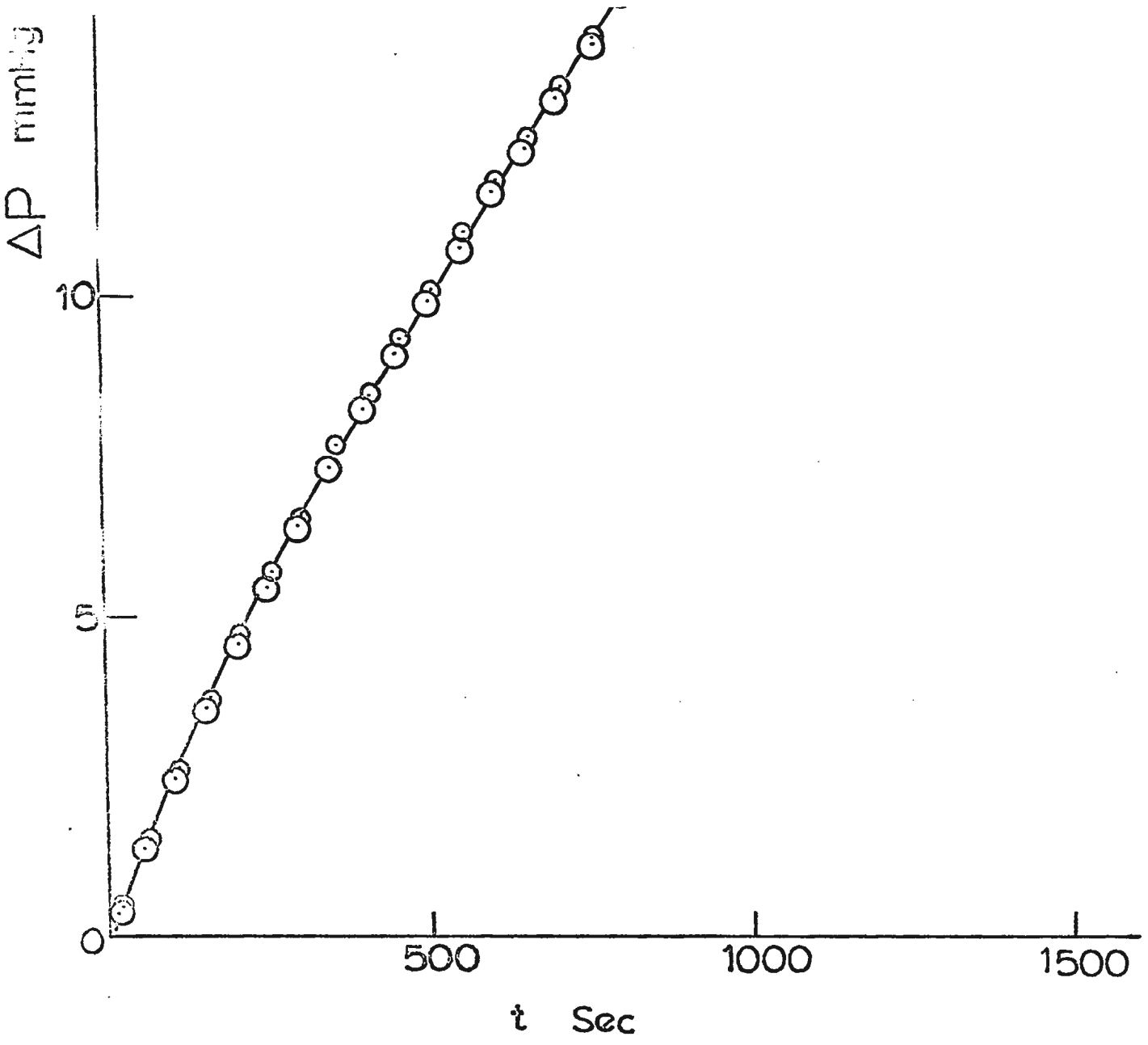
ΔP mmHg
10
0
500
1000
1500
t Sec

FIGURE 10

Pressure-time data (type B) for determination of the order with respect to formic acid (non-autocatalytic term) at 214°C.

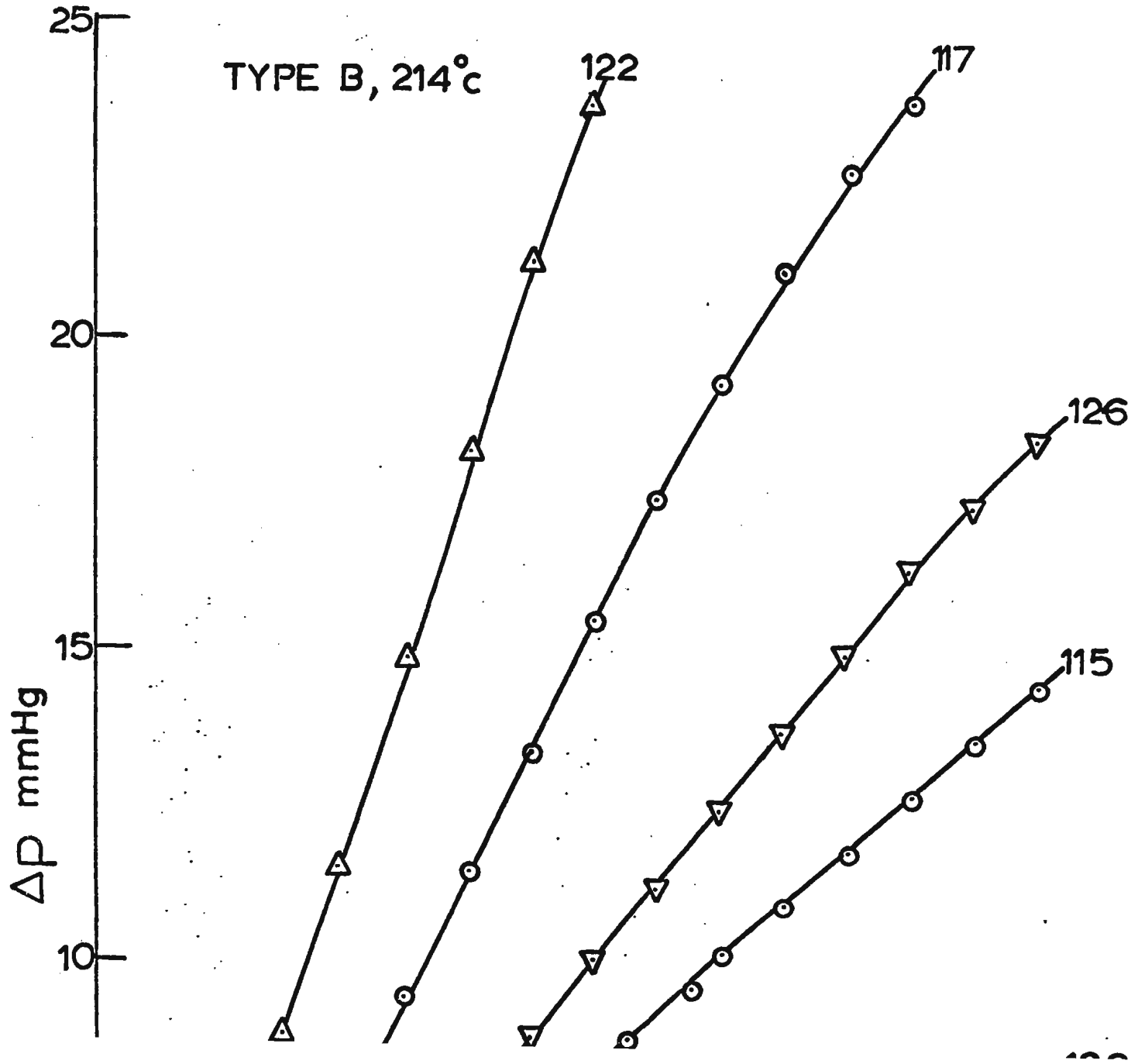
TYPE B, 214°c
25
20
15
10
ΔP mmHg
122
117
126
115

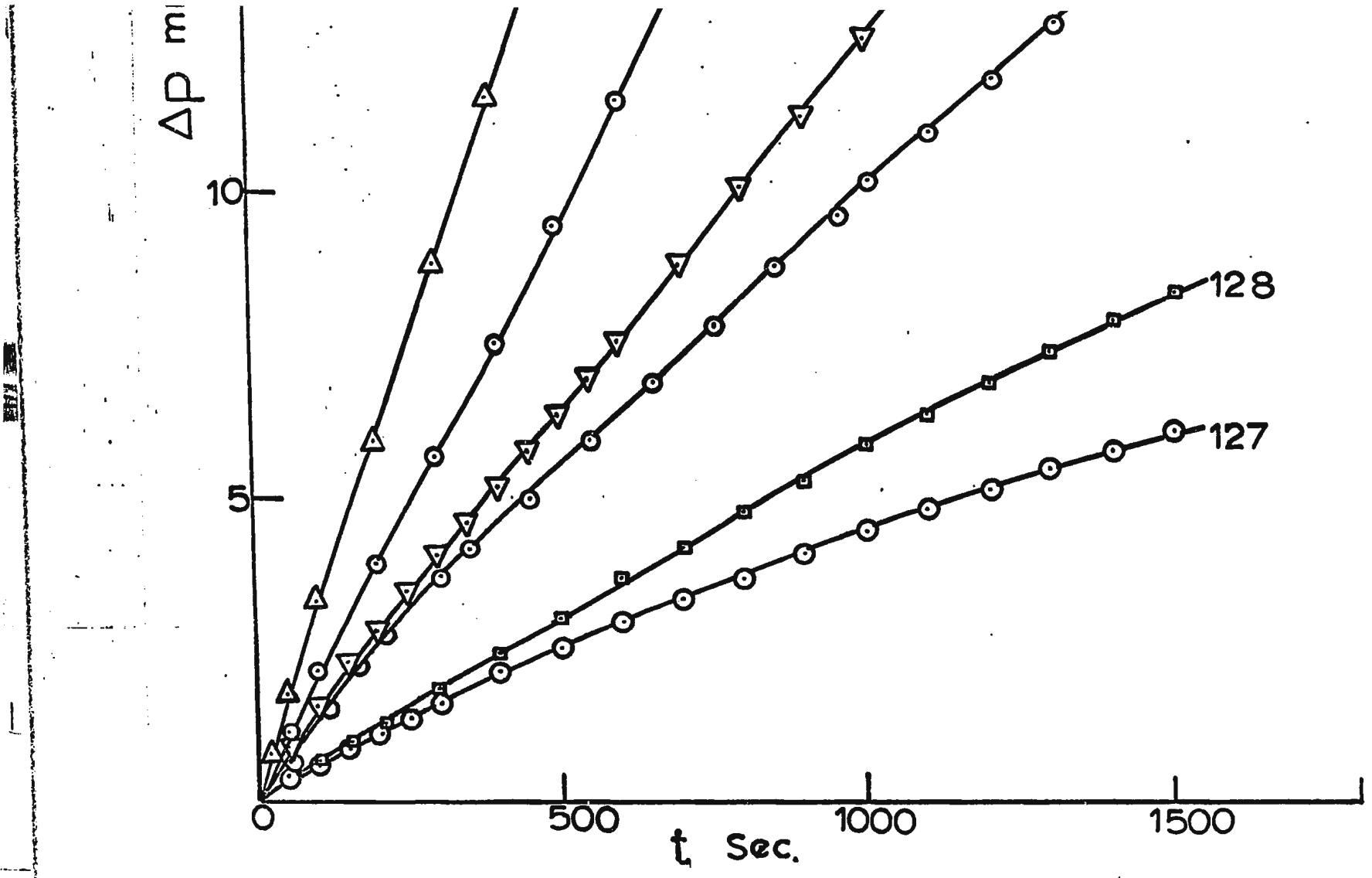
ΔP m
10
5
0
500
1000
1500
t Sec.
128
127

FIGURE 11

Pressure-time curves (214°C)

Run 114, P_{FA} = 71.61 mm Hg P_{NO_2} = 29.98 mm Hg

Run 122, P_{FA} = 71.59 mm Hg P_{NO_2} = 29.64 mm Hg

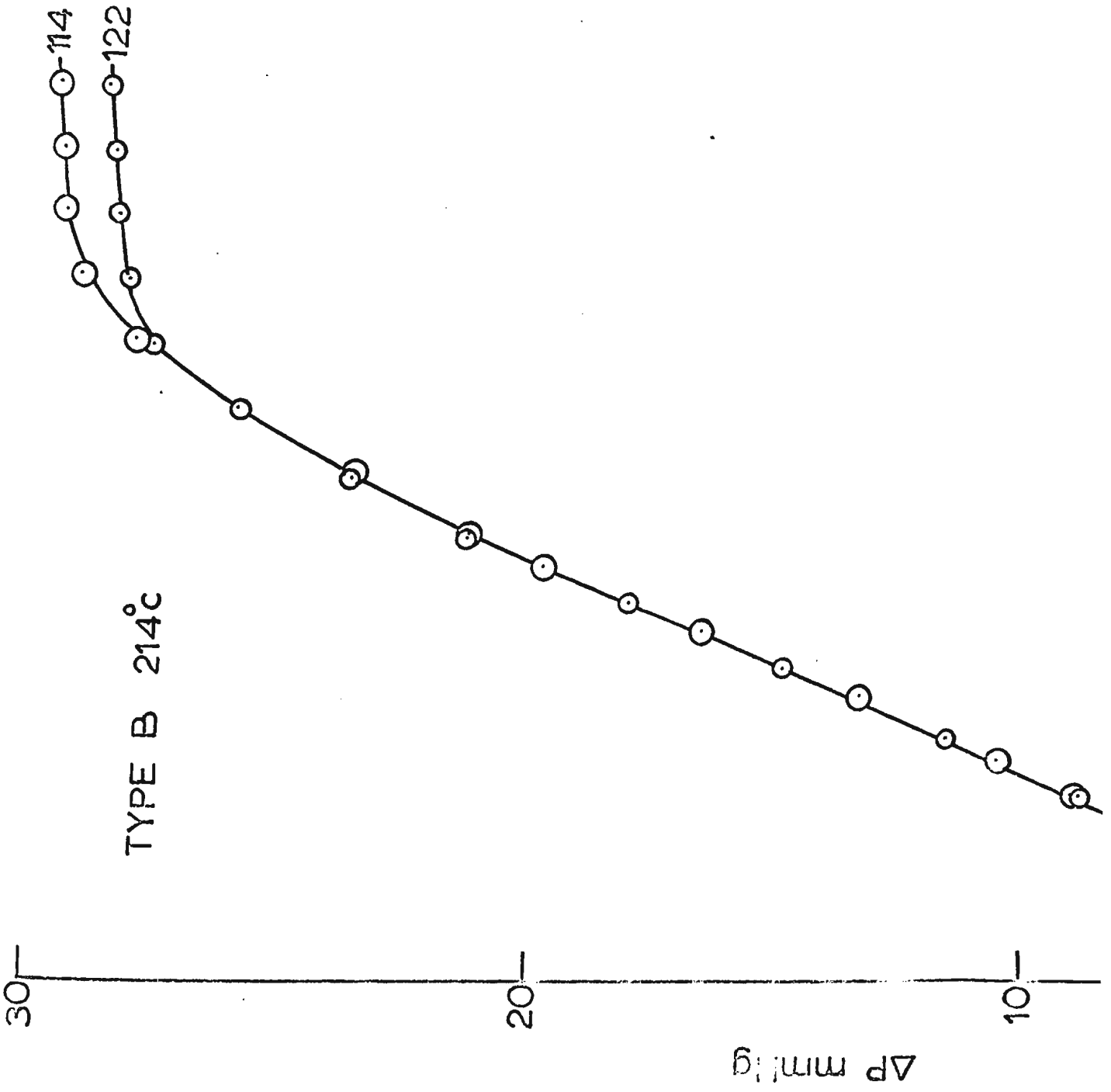
114
122
TYPE B 214°c
30
20
10
ΔP mm/g

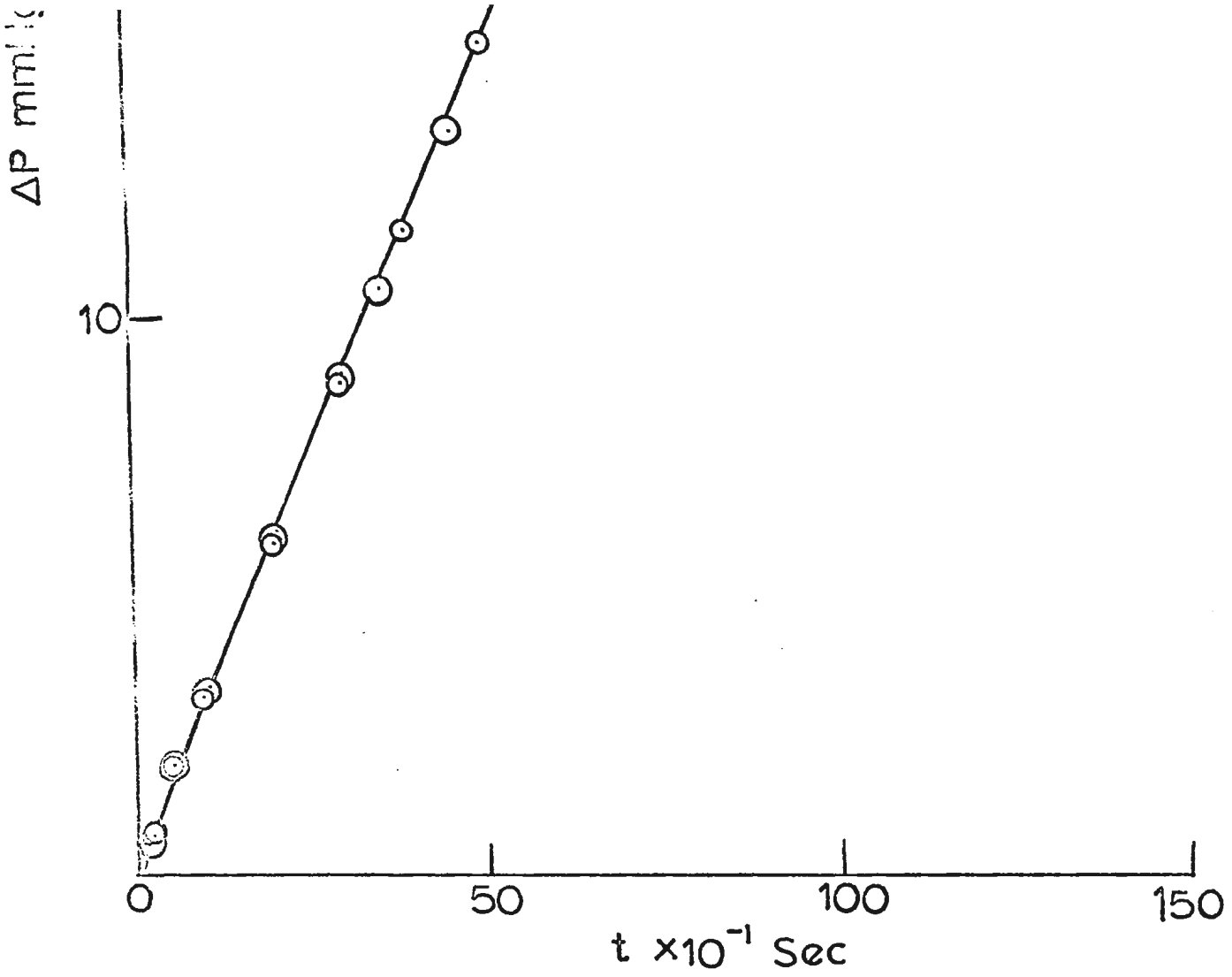
ΔP mm
10
0
50
100
150
t x10⁻¹ Sec

FIGURE 12

Pressure-time data (Type C at 214^{o}C) for determination of the dependence of rate upon the concentration of nitric oxide.

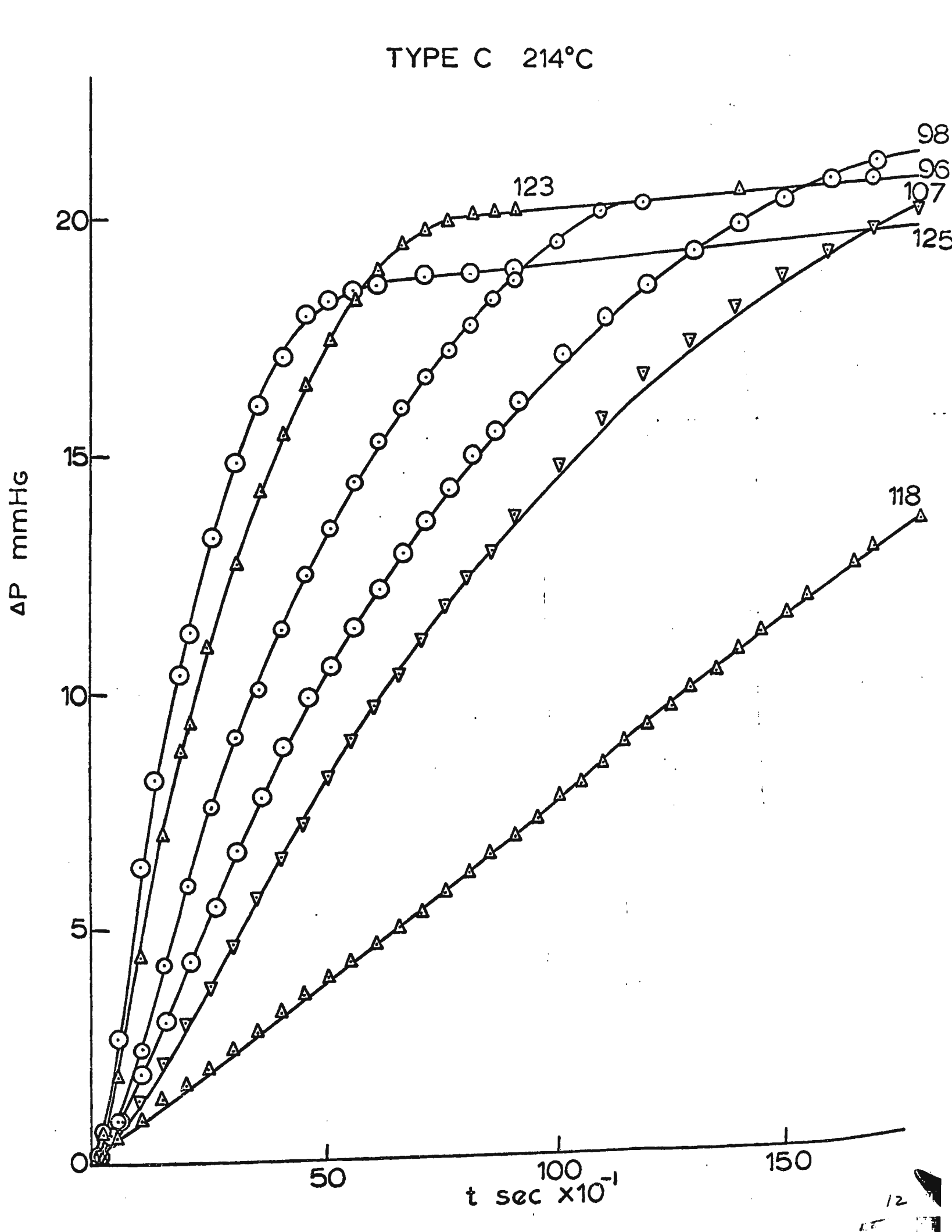
TYPE C 214°C
98
96
123
107
125
118
20
15
10
5
0
ΔP mmHg
50
100
150
t sec X10⁻¹

FIGURE 13

Pressure-time data (Type C at 182^{o}C) for determination of the dependence of rate upon the concentration of nitric oxide.

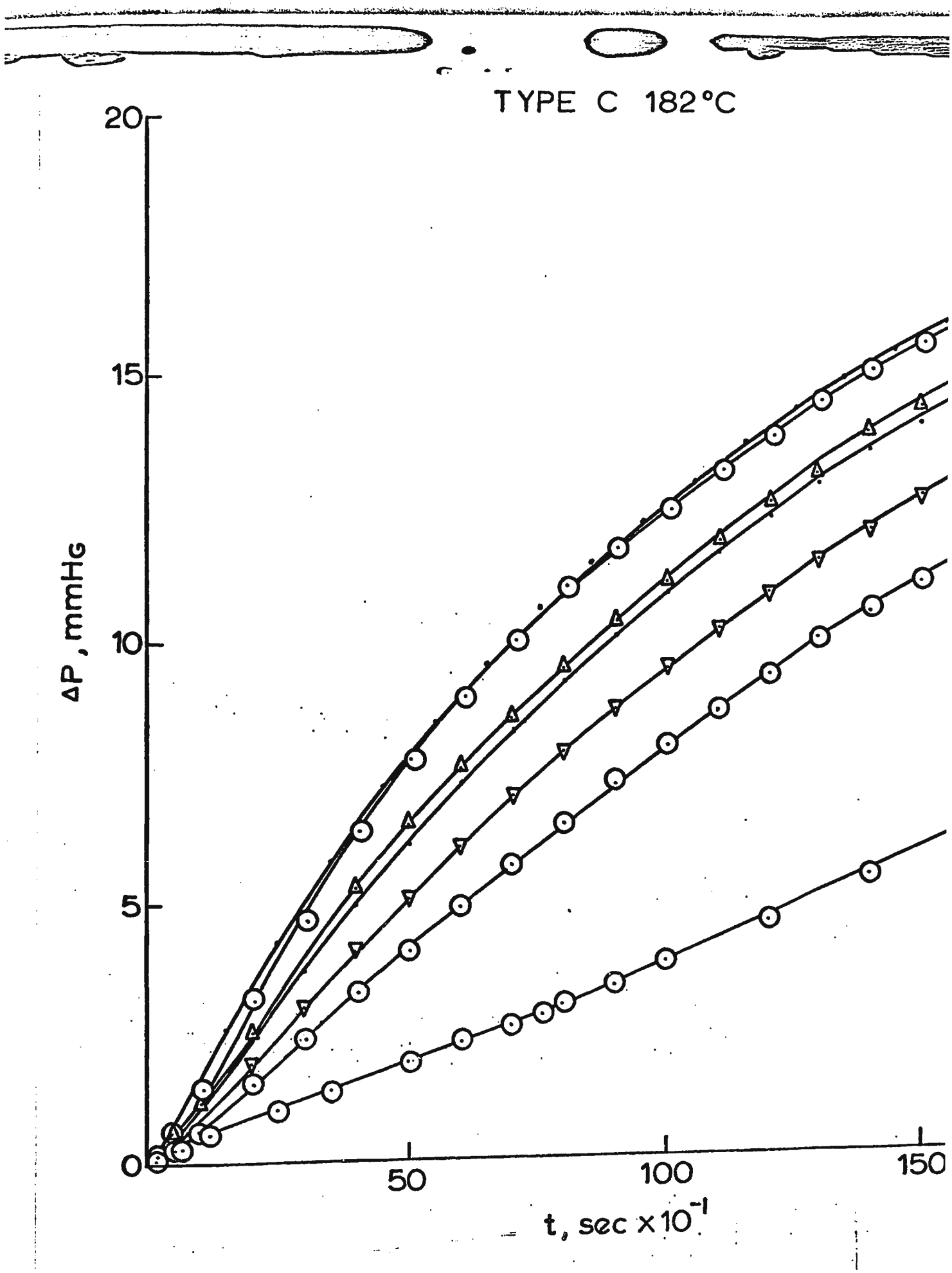
TYPE C 182°C
20
15
10
5
0
ΔP, mmHg
50
100
150
t, sec x 10⁻¹

TYPE C 182°C

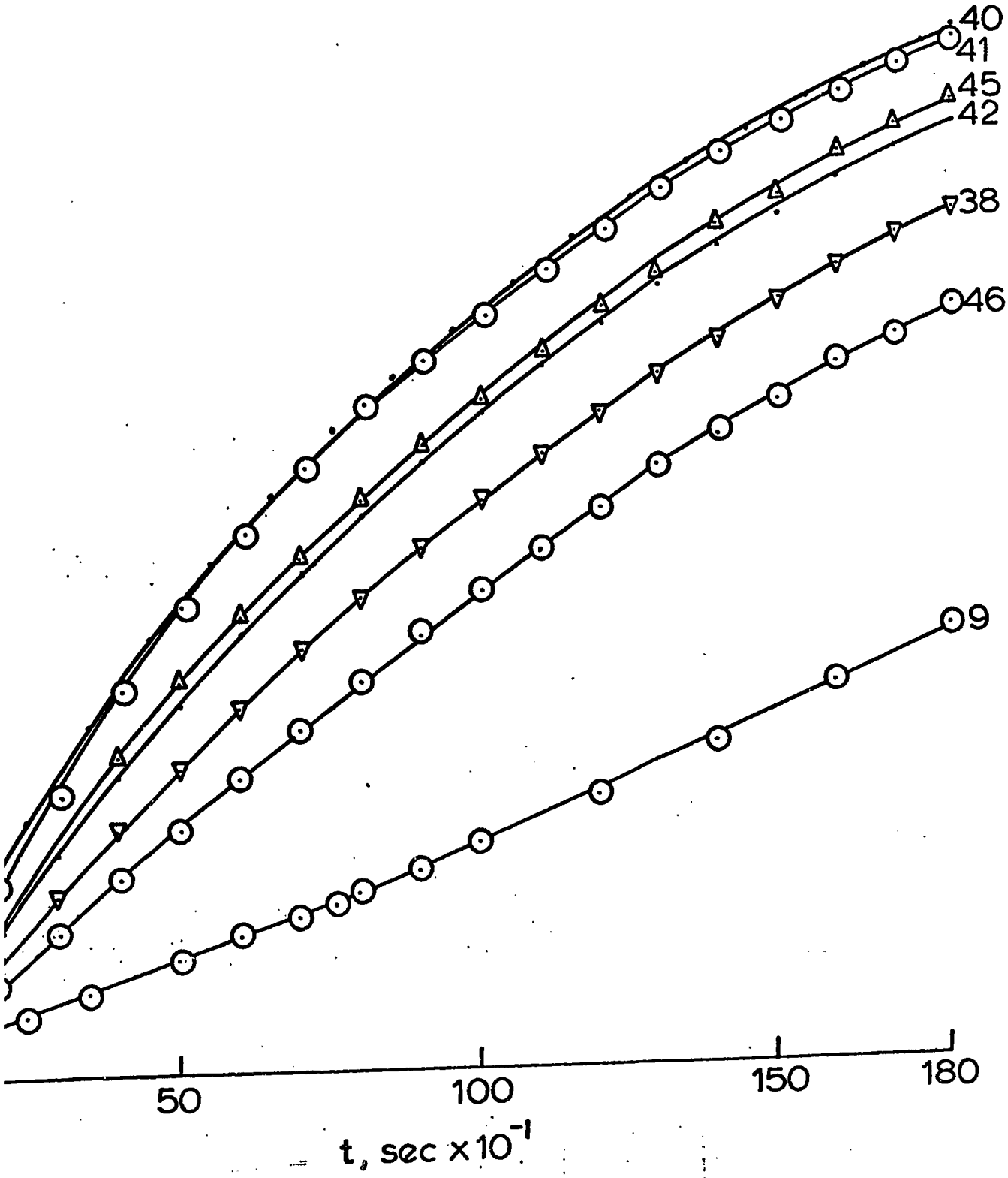

FIGURE 14

Pressure-time data (Type D, at 214^{o}C) for determination of the dependence of rate upon the concentration of nitrogen dioxide.

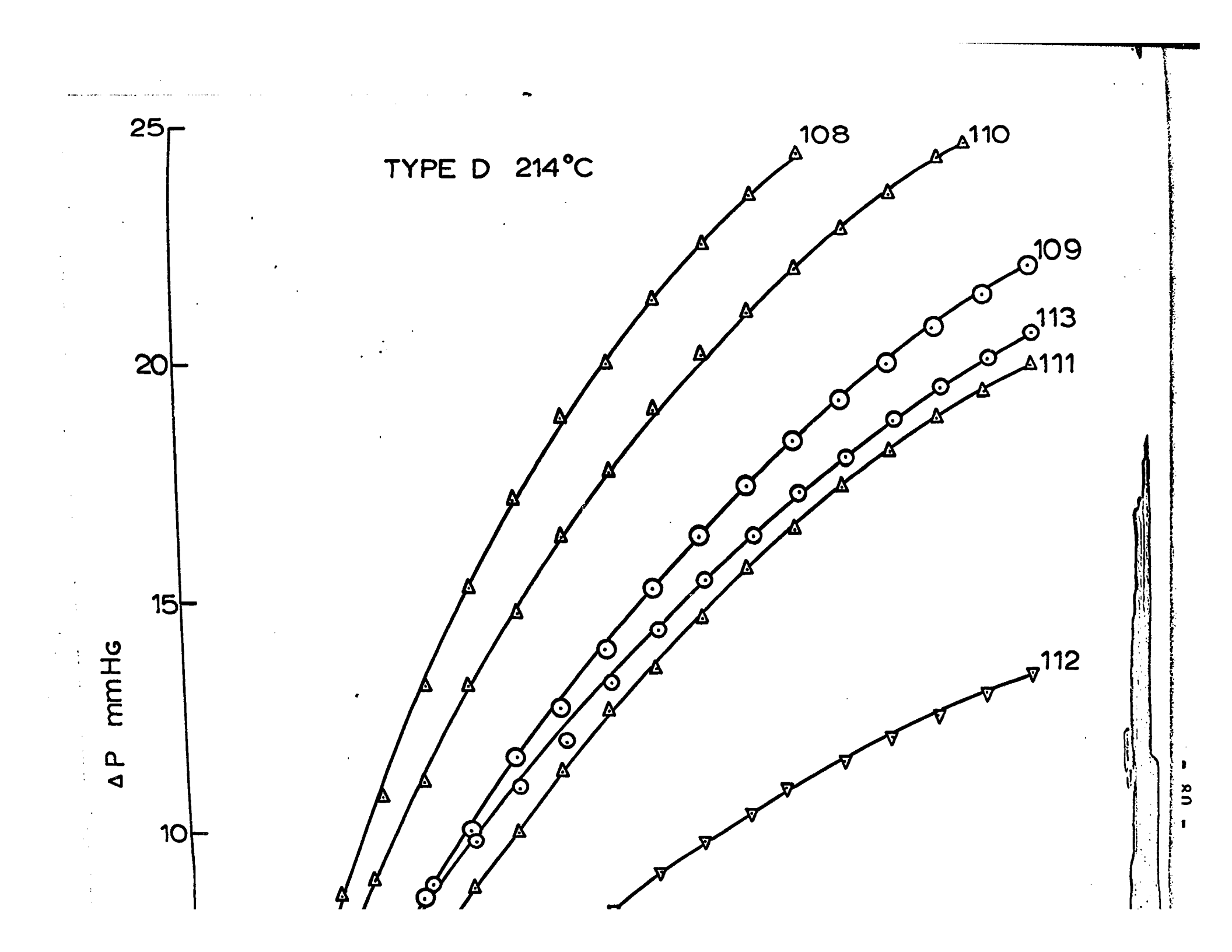
TYPE D 214°C
ΔP mmHg
25
20
15
10
108
110
109
113
111
112

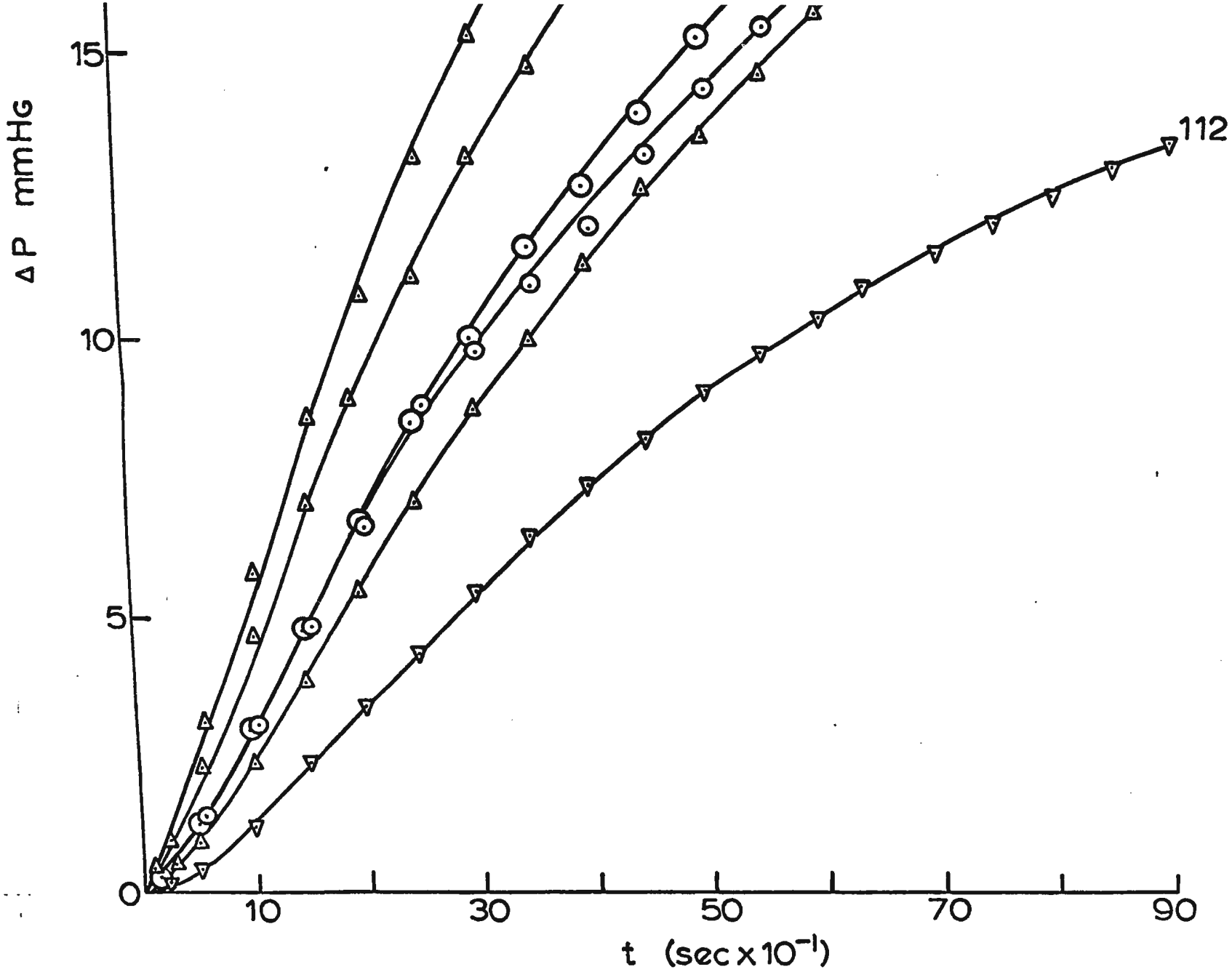
ΔP mmHg
15
10
5
0
10
30
50
70
90
t (sec x 10⁻¹)
112

FIGURE 15

Pressure-time data (Type E, at 214^{o}C) for determination of the dependence of rate upon the concentration of formic acid.

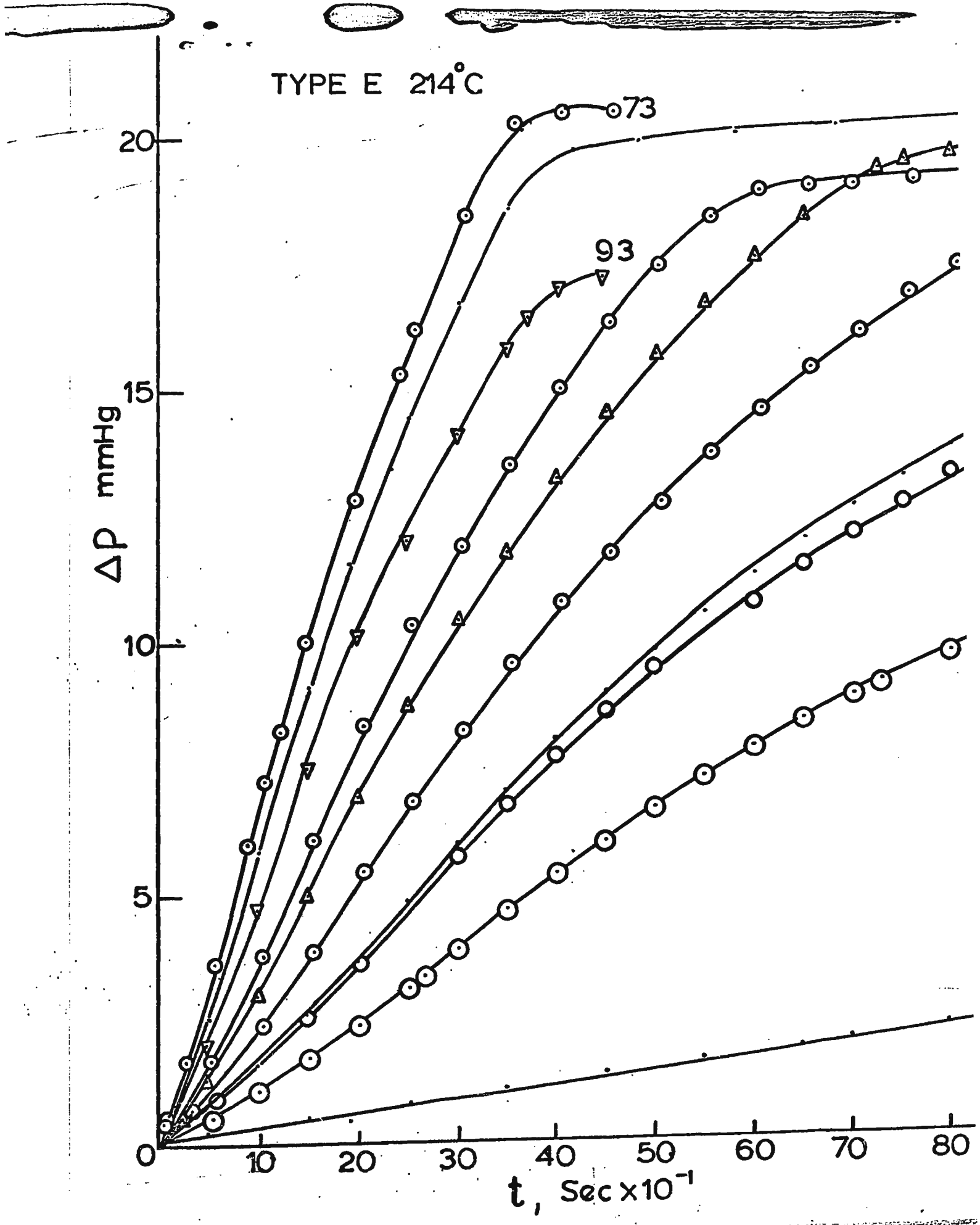
TYPE E 214°C
73
93
ΔP mmHg
0
5
10
15
20
10
20
30
40
50
60
70
80
t, Sec x 10⁻¹

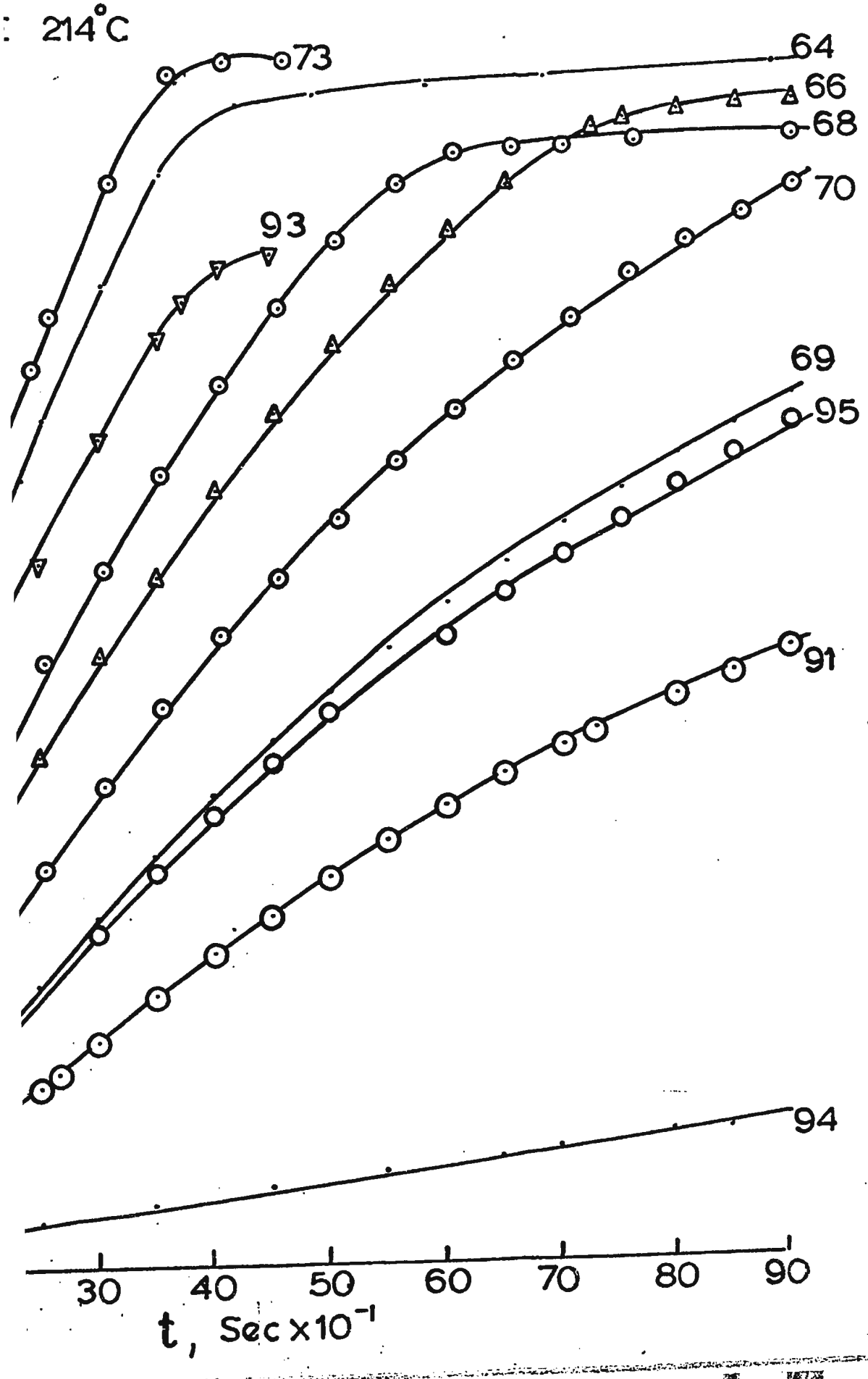
214°C
73
64
66
68
93
70
69
95
91
94
30
40
50
60
70
80
90
t, Sec x10⁻¹

FIGURE 16

Pressure-time curves (214°C)

Run 100:

P_{FA} = 31.83 mm Hg P_{NO_2} = 24.21 mm Hg P_{NO} = 53.21 mm Hg

Run 101:

P_{FA} = 33.13 mm Hg P_{NO_2} = 23.10 mm Hg P_{NO} = 52.86 mm Hg

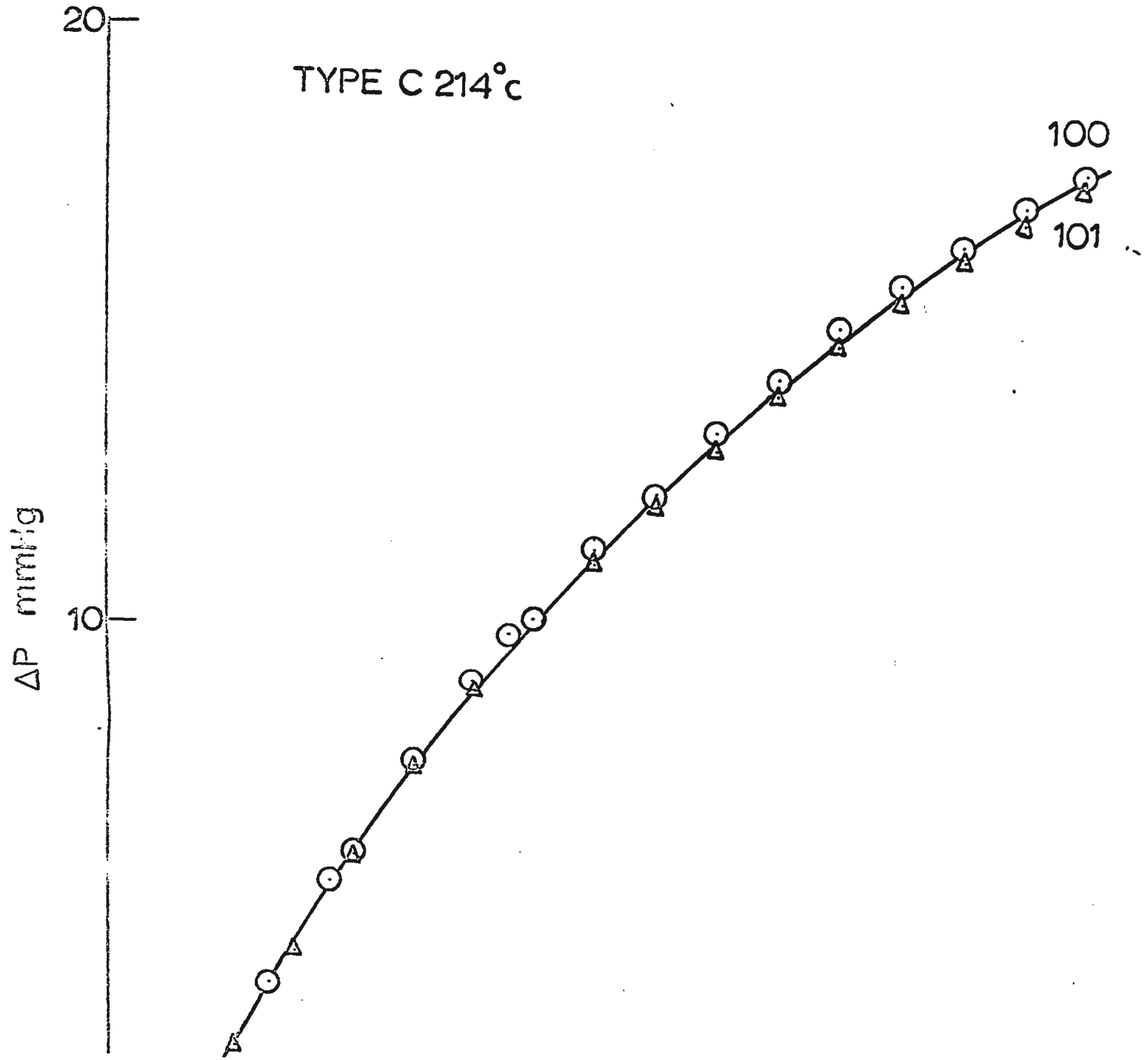
TYPE C 214°c
20
10
ΔP mm/g
100
101

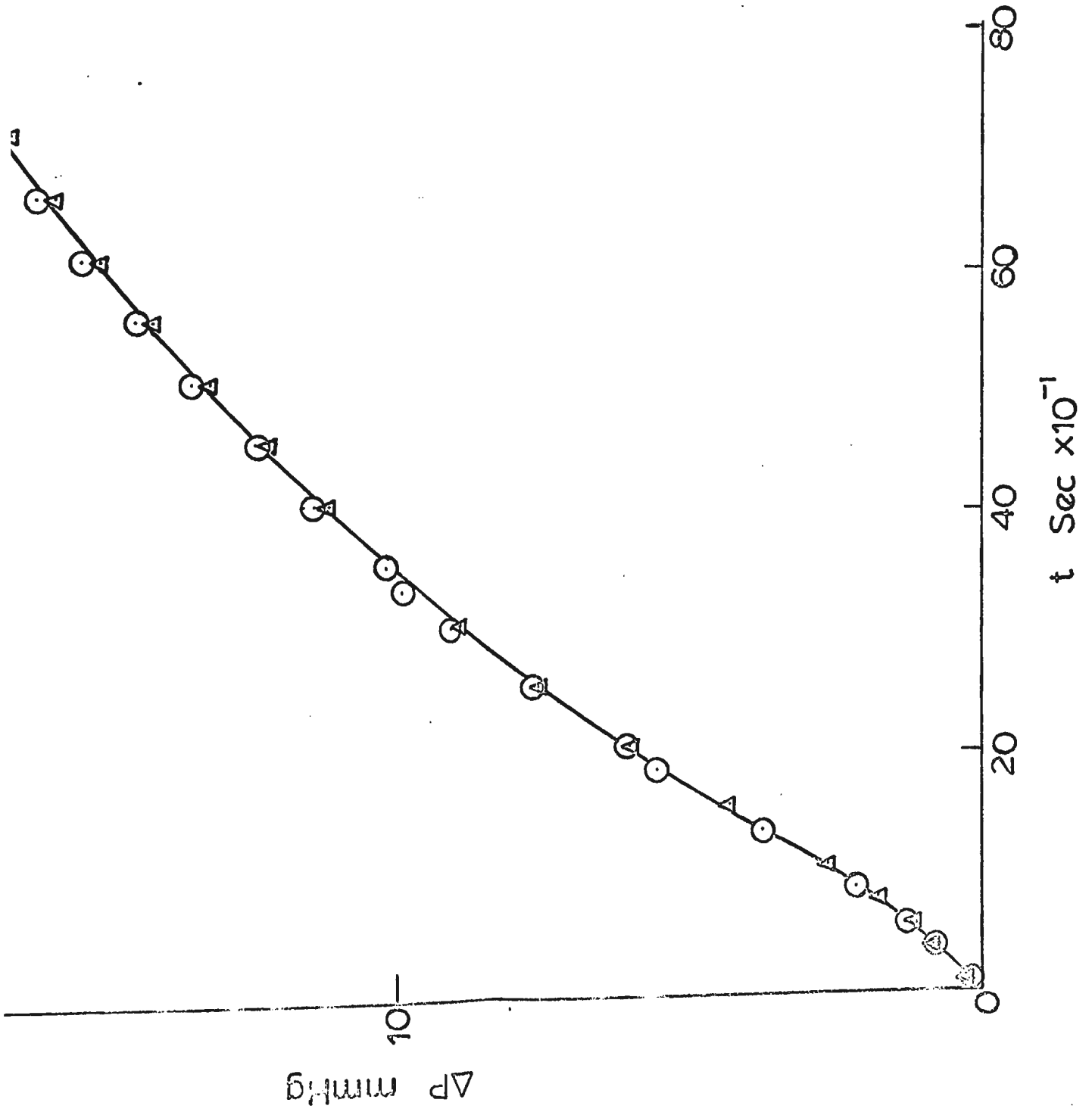
80
60
40
20
0
t Sec x10⁻¹
10
ΔP mmHg

FIGURE 17

Initial rate, as a function of initial pressure of NO_2 and HCOOH; Type A and B results at 214°C.

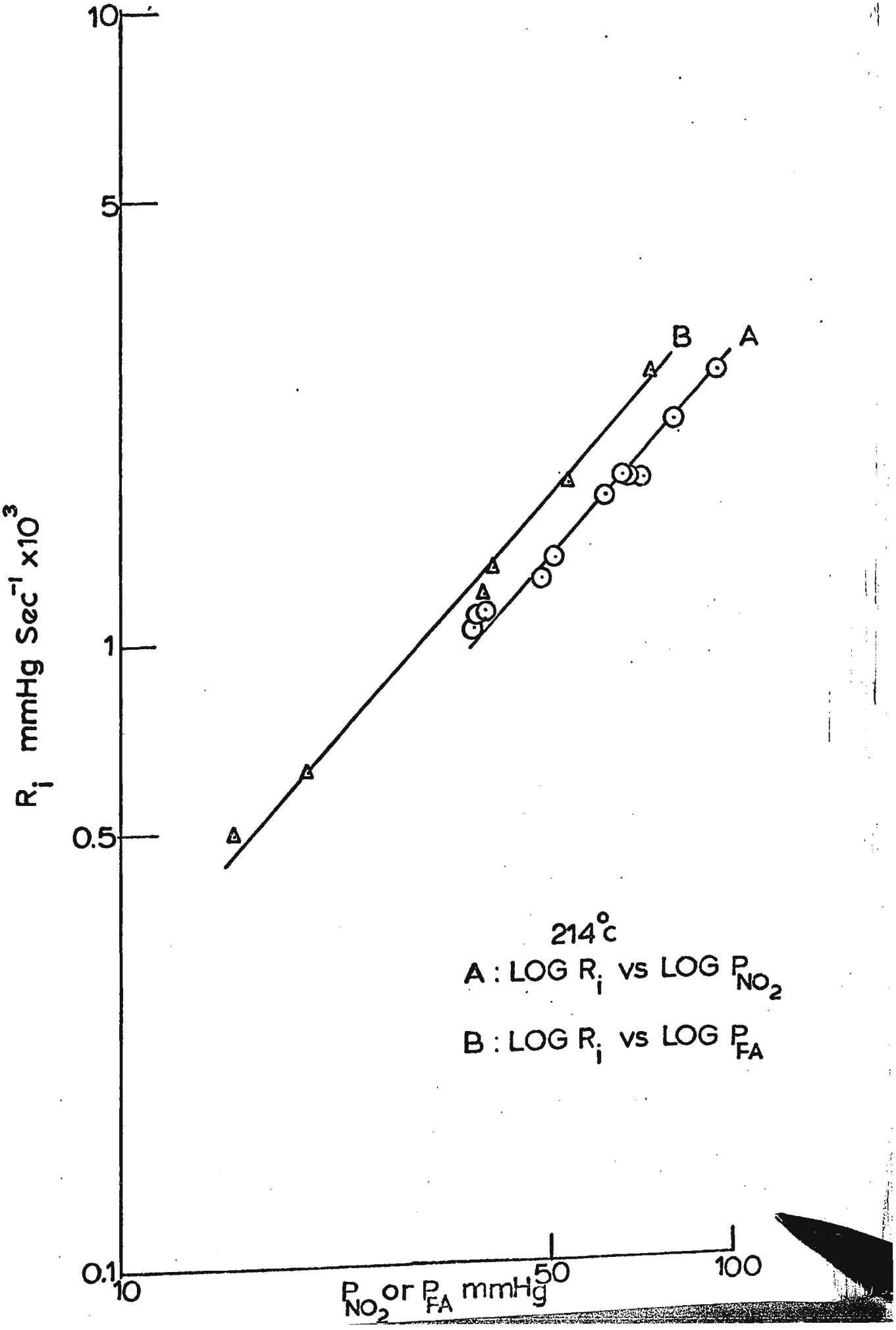
10
5
1
0.5
0.1
10
50
100
R_i mmHg Sec^{-1} x10^3
P_{NO_2} or P_{FA} mmHg
B
A
214°c
A : LOG R_i vs LOG P_{NO_2}
B : LOG R_i vs LOG P_{FA}

FIGURE 18

Initial rate as a function of initial pressure of NO_2, Type A results at 182°C.

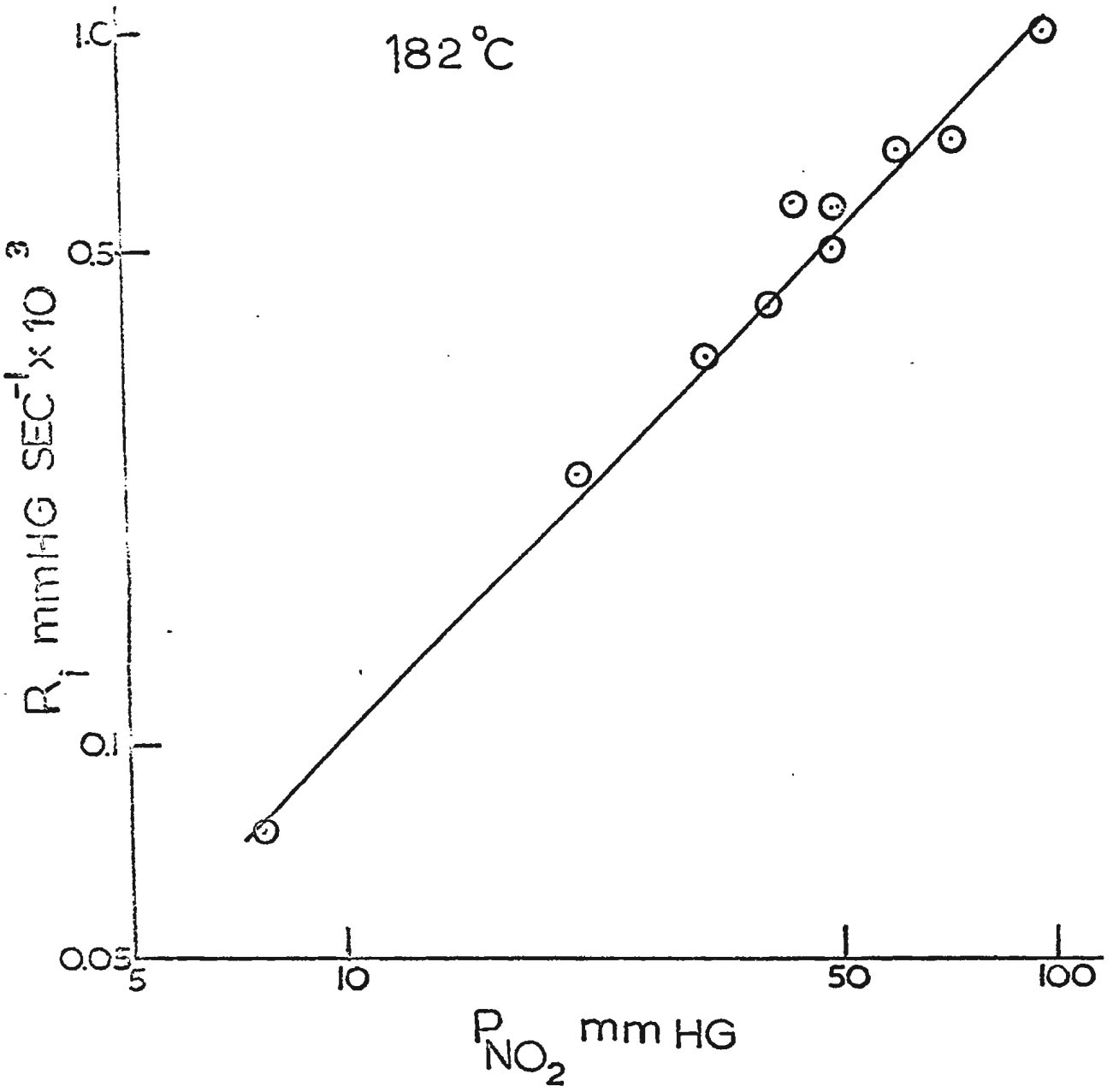
182 °C
1.0
0.5
0.1
0.05
R_i mmHG SEC^{-1} x 10^3
5
10
50
100
P_{NO_2} mm HG

FIGURE 19

Initial rate as a function of initial pressure of HCOOH, Type B results at 182°C.

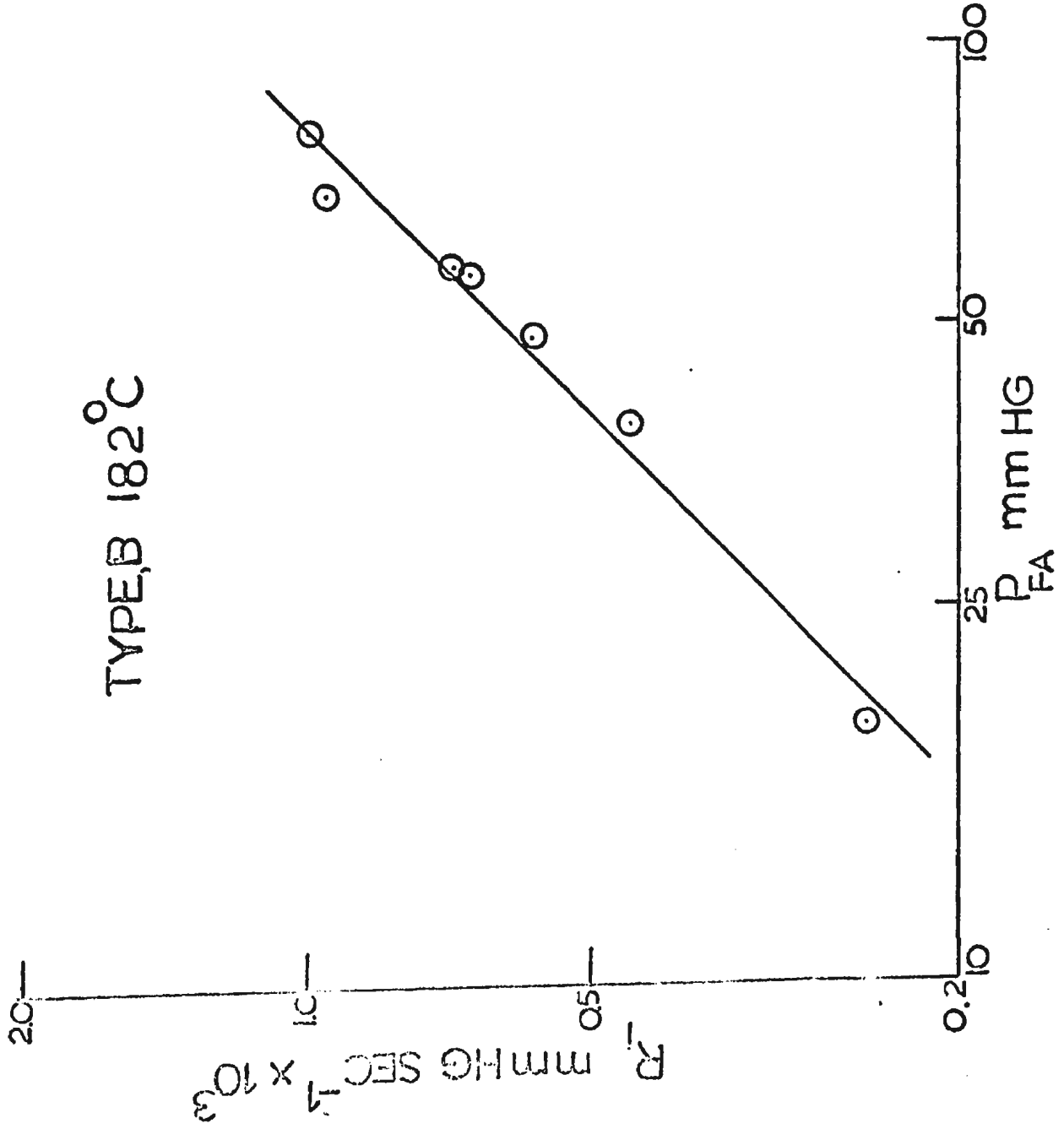
TYPE B 182°C
R_i mm HG SEC^{-1} x 10^3
2.0
1.0
0.5
0.2
10
25
50
100
P_{FA} mm HG

FIGURE 20

Total rate as a function of pressure of NO; type C results at 182°C. Initial values: $P_{FA} \cong 30$ mm Hg, $P_{NO_2} \cong 30$ mm Hg. The plots are for rates measured at the following values of ΔP: (1) $\Delta P = 4$ mm Hg, (2) $\Delta P = 6$ mm Hg, (3) $\Delta P = 8$ mm Hg, (4) $\Delta P = 10$ mm Hg, (5) $\Delta P = 12$ mm Hg.

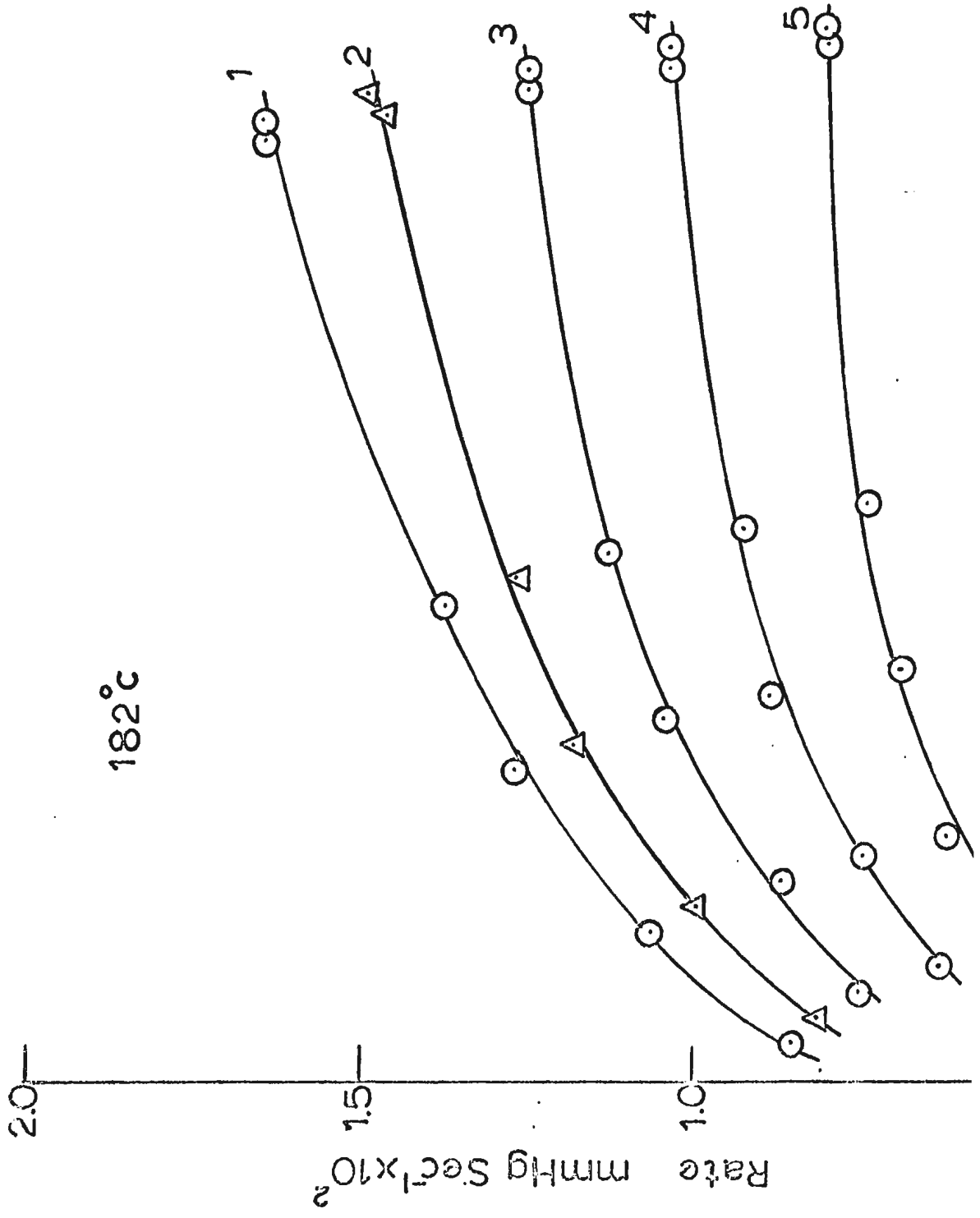
182°c
1
2
3
4
5
2.0
1.5
1.0
Rate mmHg Sec⁻¹x10²

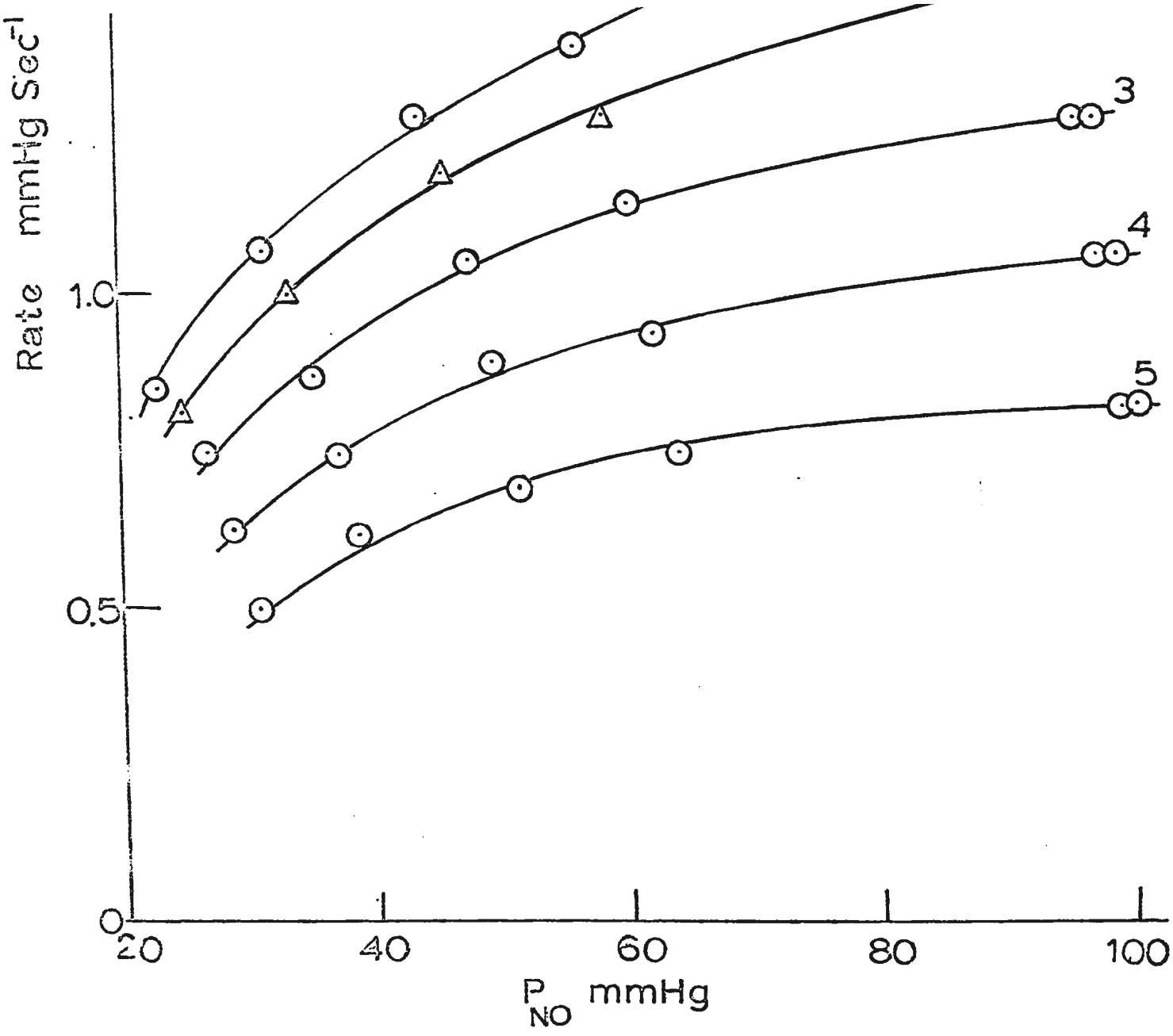
Rate mmHg Sec⁻¹
1.0
0.5
0
20
40
60
80
100
P NO mmHg
3
4
5

FIGURE 21

Total rate, as a function of P_{NO}; type C results (214°C) Initial values: $P_{FA} \cong 32$ mm Hg $P_{NO} \cong 23$ mm Hg. The plots are for rates measured at the following values of ΔP: $\Delta P = 4$ mm Hg, 10 mm Hg and 14 mm Hg.

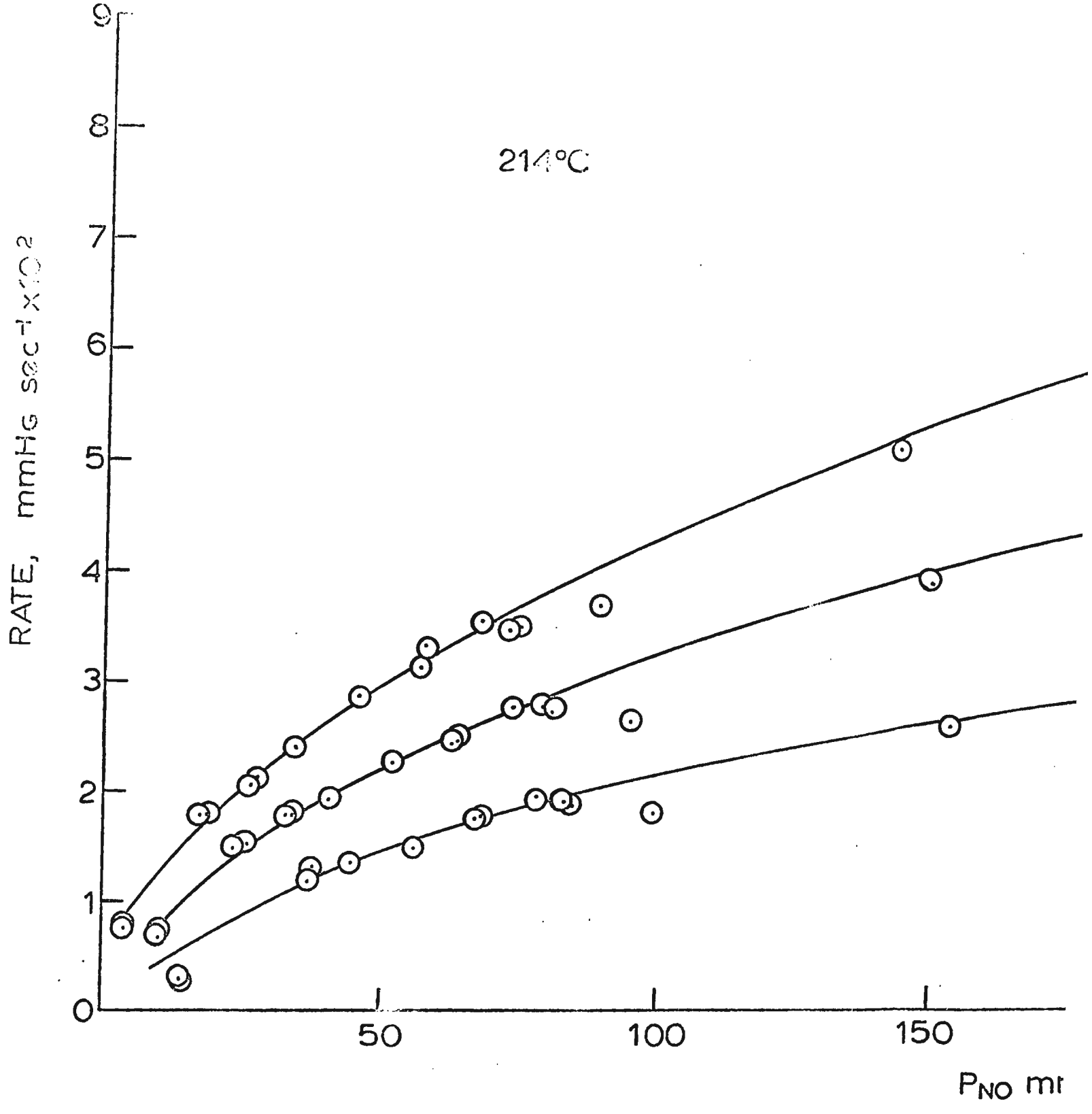
214°C
RATE, mmHg sec⁻¹ x10²
0
1
2
3
4
5
6
7
8
9
50
100
150
P_NO mr

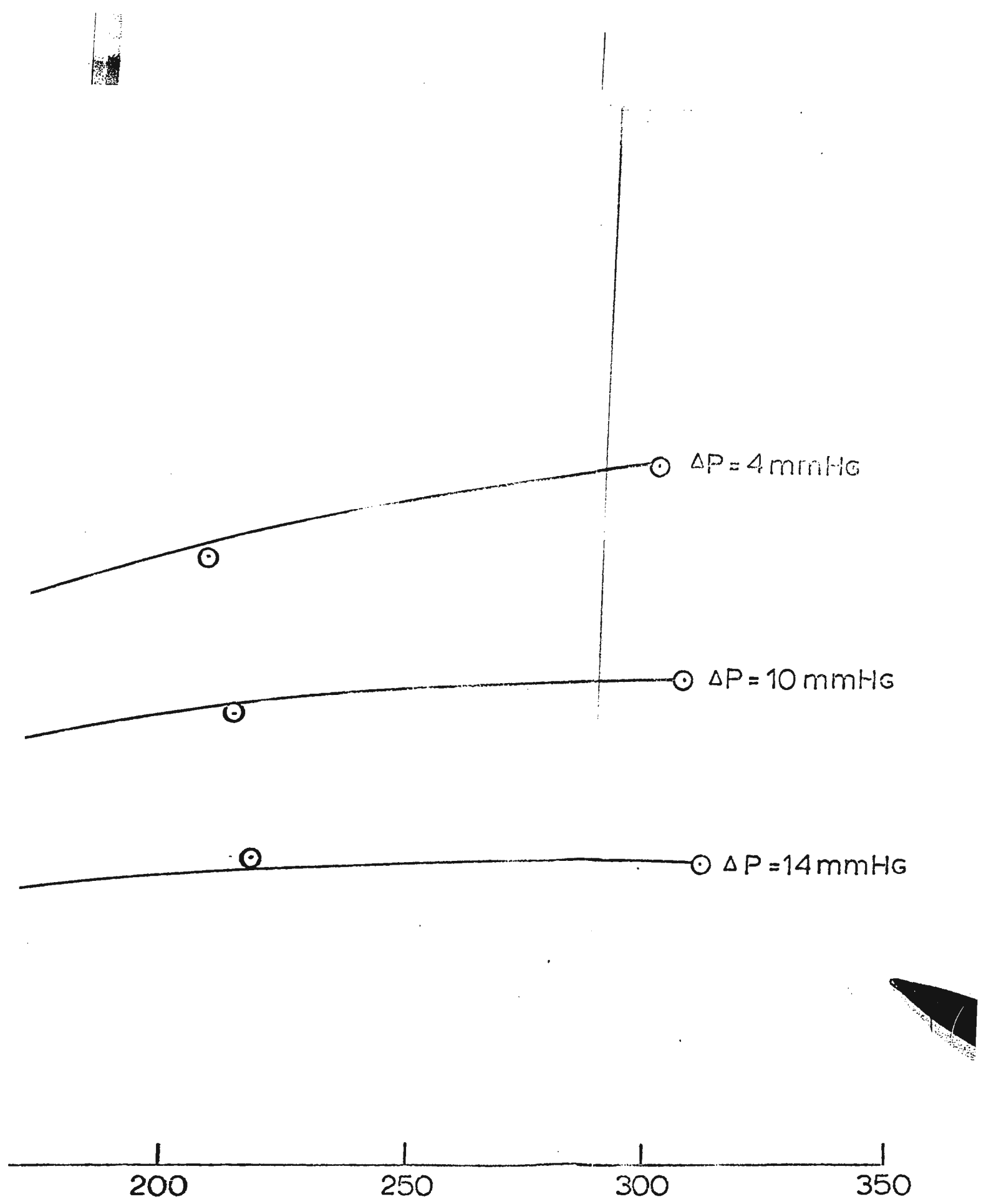
ΔP = 4 mmHg
ΔP = 10 mmHg
ΔP = 14 mmHg
200
250
300
350
mmHg

FIGURE 22

Autocatalytic contribution to the total rate as a function of P_{NO} at 214°C. The rates were measured at the following values of ΔP:
ΔP = 4 mm Hg, 10 mm Hg, and 14 mm Hg.

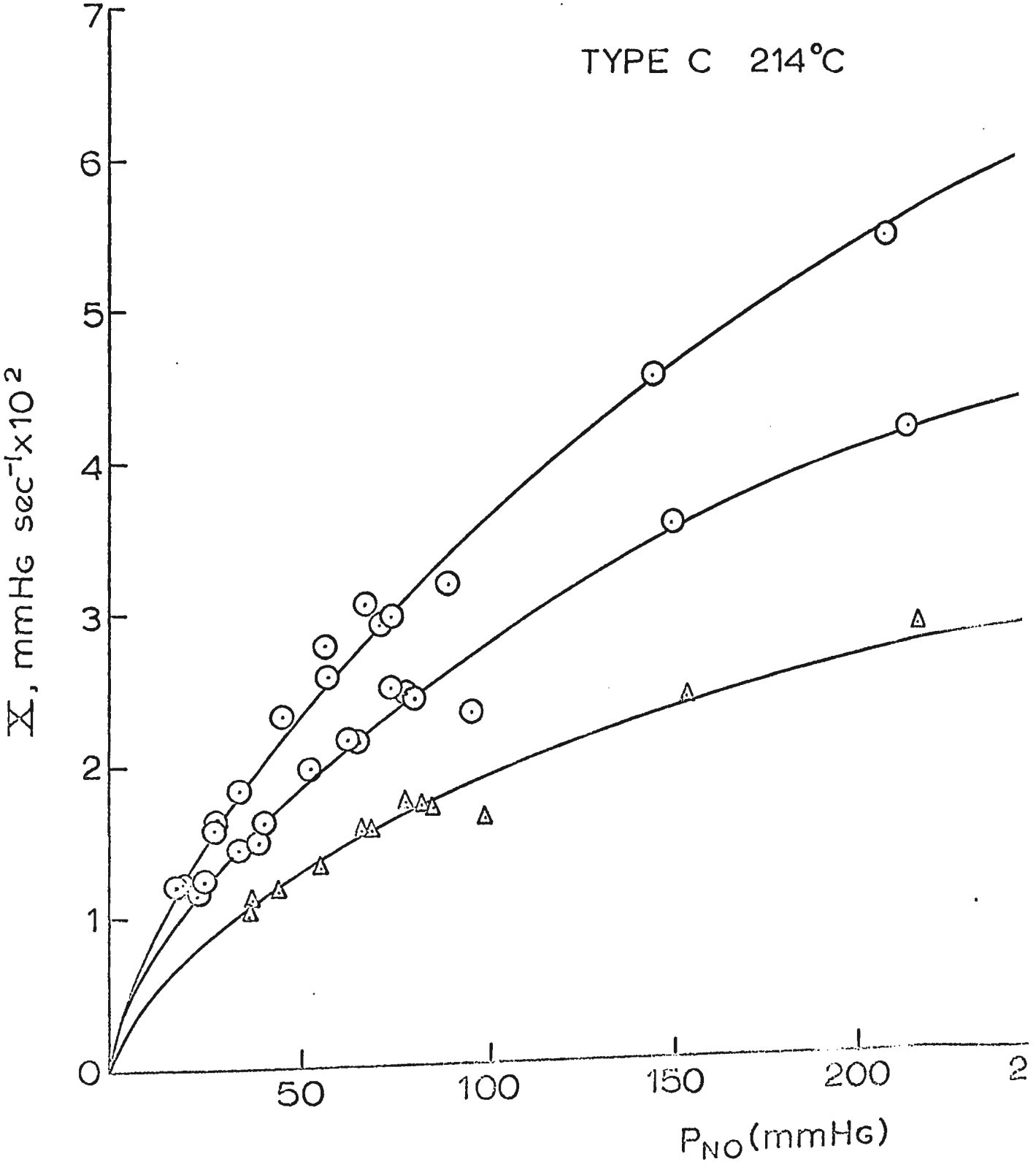
TYPE C 214°C
X, mmHg sec⁻¹x10²
P_NO(mmHg)
0
1
2
3
4
5
6
7
50
100
150
200

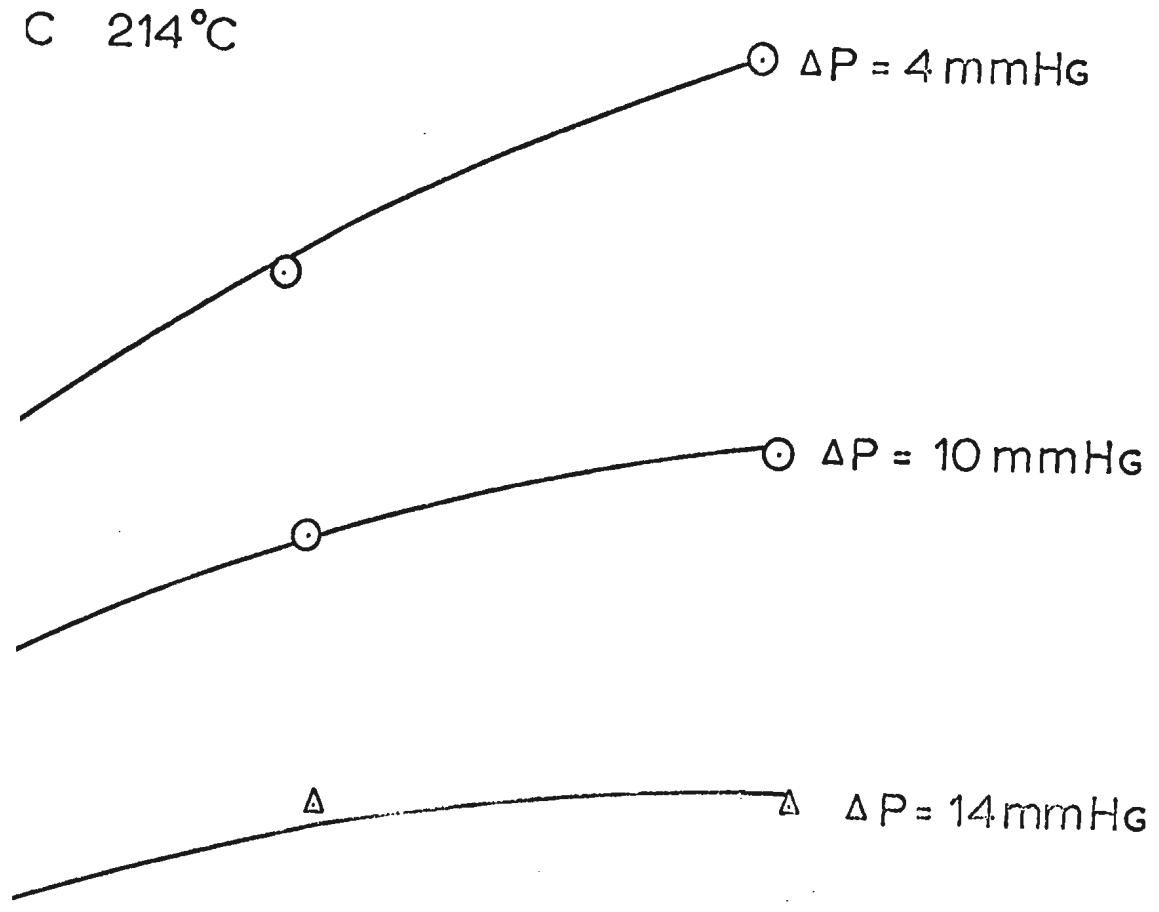

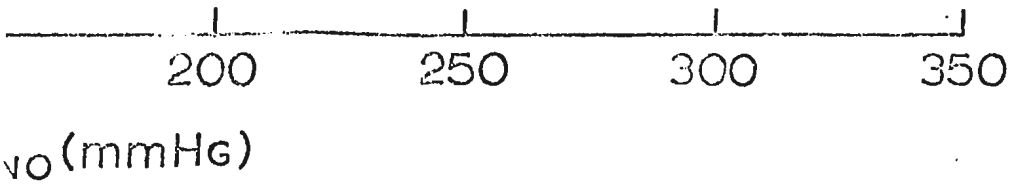

v_o (mmHG)

FIGURE 23

Autocatalytic contribution to the total rate at 214°C as a function of P_{NO} as a log-log plot. The rates were measured at the values of ΔP: 4 mm Hg, 10 mm Hg, and 14 mm Hg.

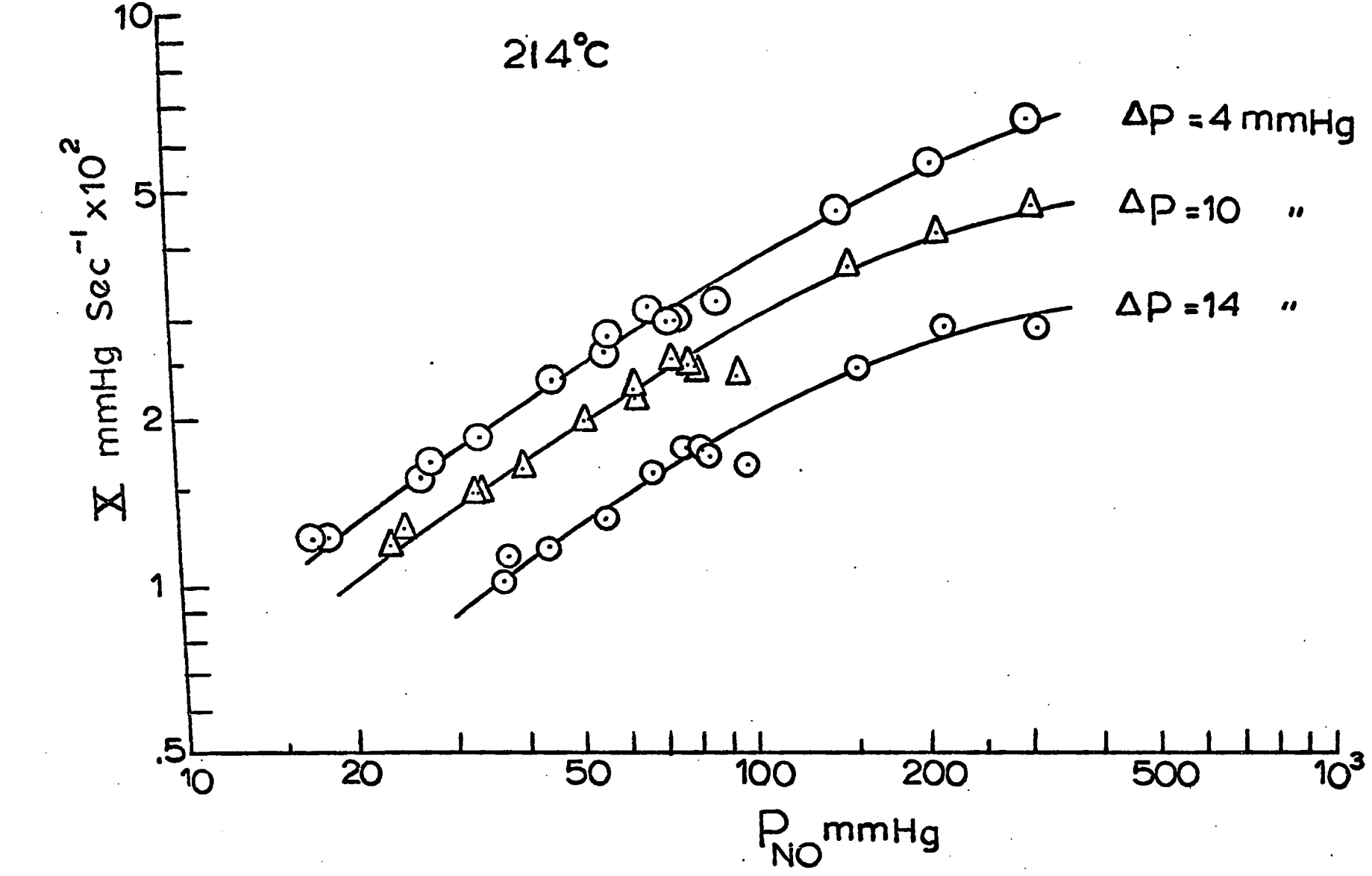
214°C
ΔP = 4 mmHg
ΔP = 10 "
ΔP = 14 "
X mmHg Sec⁻¹ x10²
10
5
2
1
.5
10
20
50
100
200
500
10³
P_NO mmHg

FIGURE 24

Plots of $\frac{P_{NO}}{X}$ vs P_{NO} at ΔP = 4 mm Hg, 10 mm Hg and 14 mm Hg at 214°C. Where X is the whole autocatalytic term.

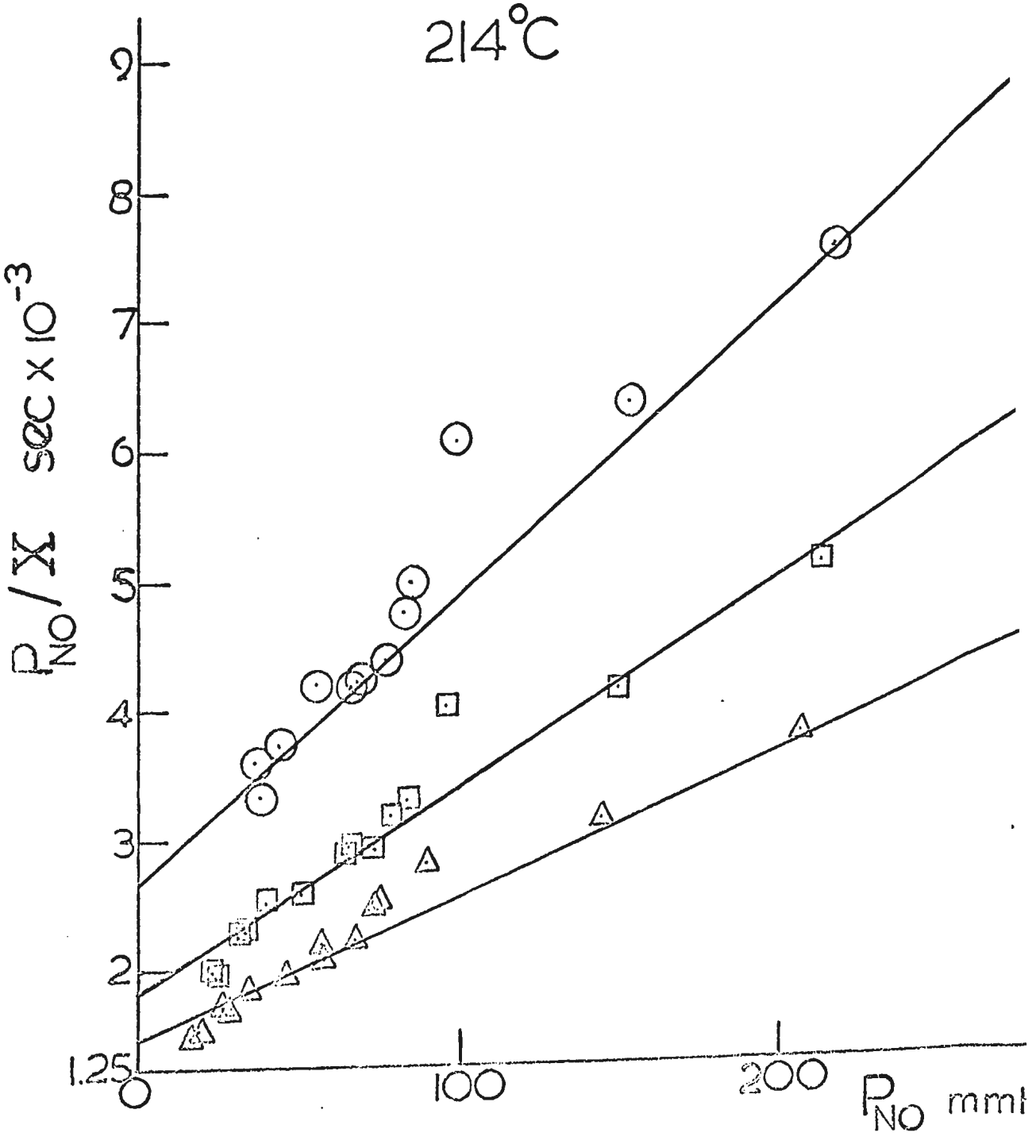
214°C
9
8
7
6
5
4
3
2
1.25
0
100
200
P_{NO} mm
P_{NO}/X sec x 10^{-3}

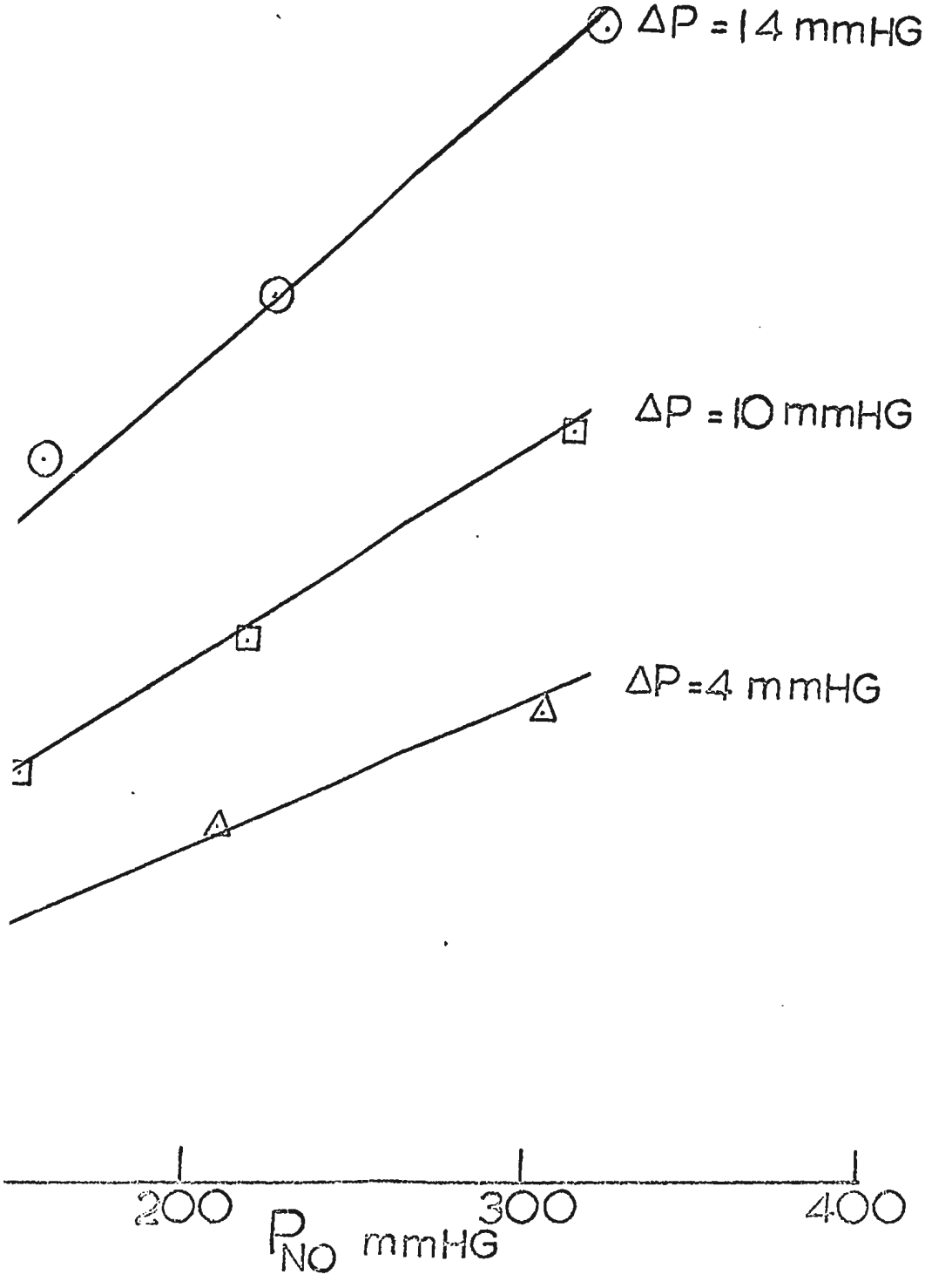
ΔP = 14 mmHG
ΔP = 10 mmHG
ΔP = 4 mmHG
200
300
400
P_{NO} mmHG

FIGURE 25

Autocatalytic contribution to total rate at 182°C as a function of P_{NO} as a log-log plot. The rates were measured at the values of ΔP 4, 6, 8, 10, and 12 mm Hg.

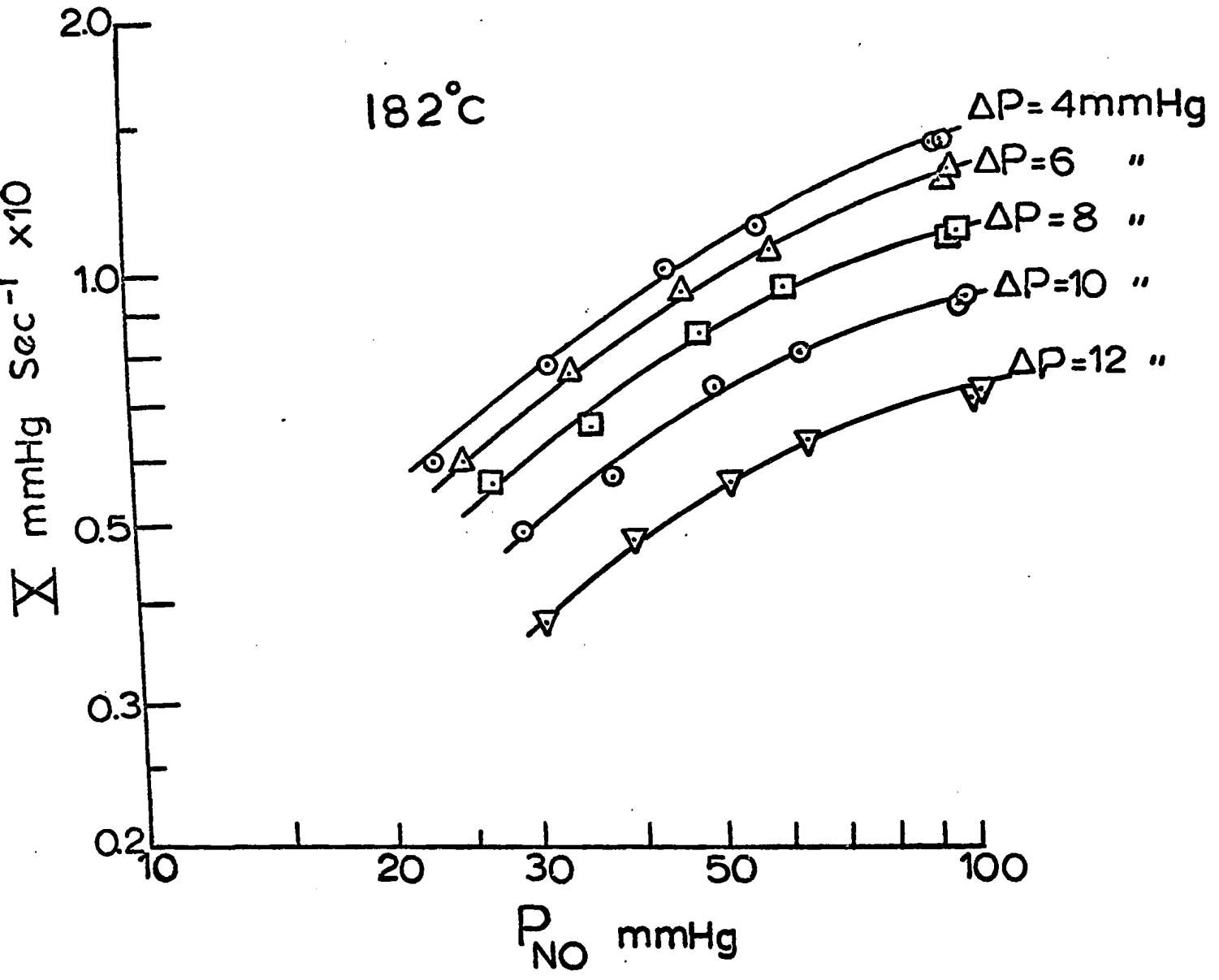
182°C
ΔP= 4mmHg
ΔP=6 "
ΔP=8 "
ΔP=10 "
ΔP=12 "
2.0
1.0
0.5
0.3
0.2
10
20
30
50
100
χ mmHg Sec⁻¹ x10²
P_NO mmHg

FIGURE 26

Plots of $\frac{P_{NO}}{X}$ vs P_{NO} at ΔP = 4, 6, 8, 10 and 12 mm Hg at 182°C.

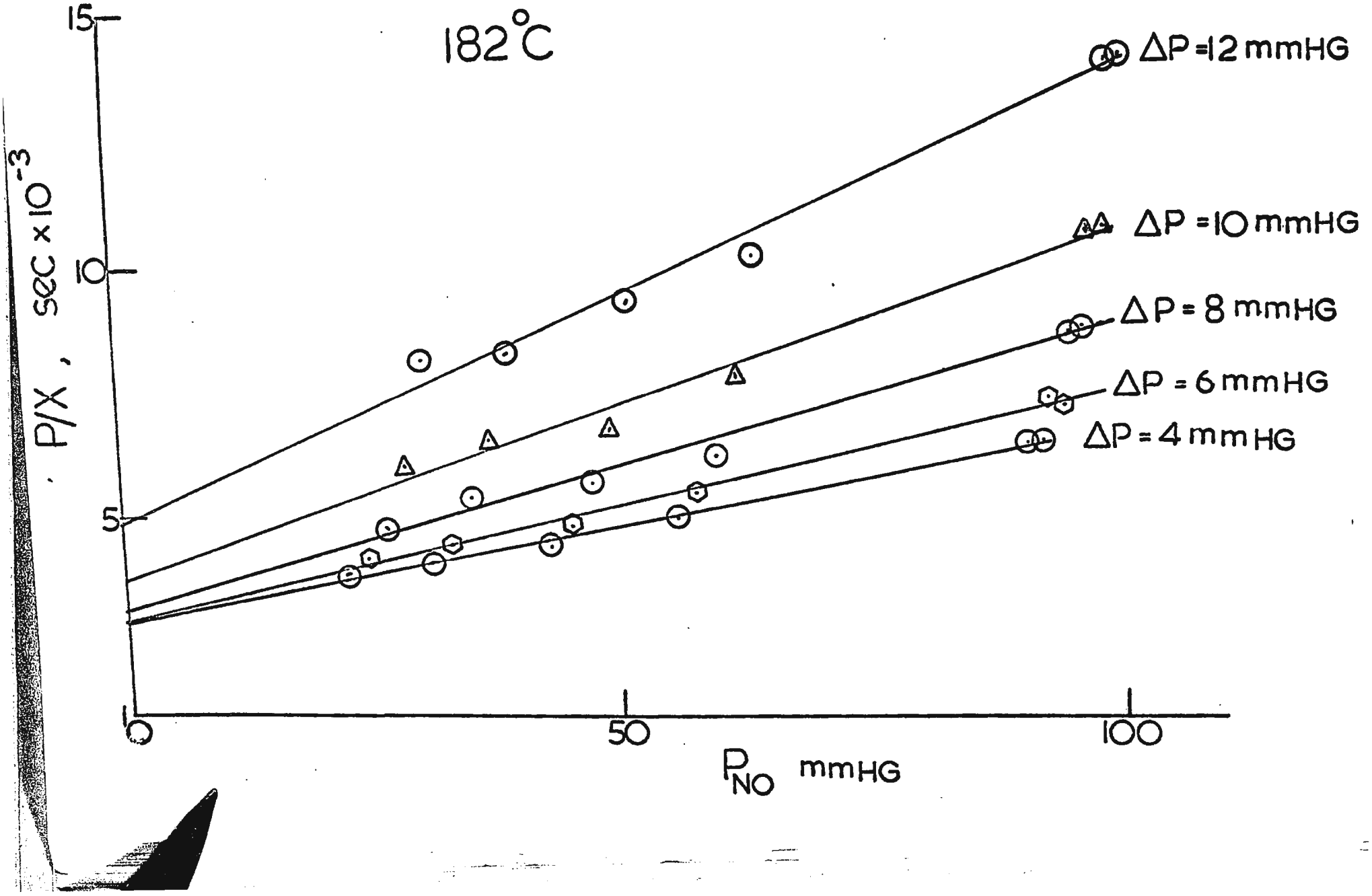
182°C
ΔP=12 mmHG
ΔP=10 mmHG
ΔP=8 mmHG
ΔP=6 mmHG
ΔP=4 mmHG
P/X, SEC x 10^-3
15
10
5
0
50
100
P_NO mmHG

FIGURE 27

Autocatalytic contribution to the total rate as a function of P_{NO_2} at 214°C and ΔP = 4 mm Hg.

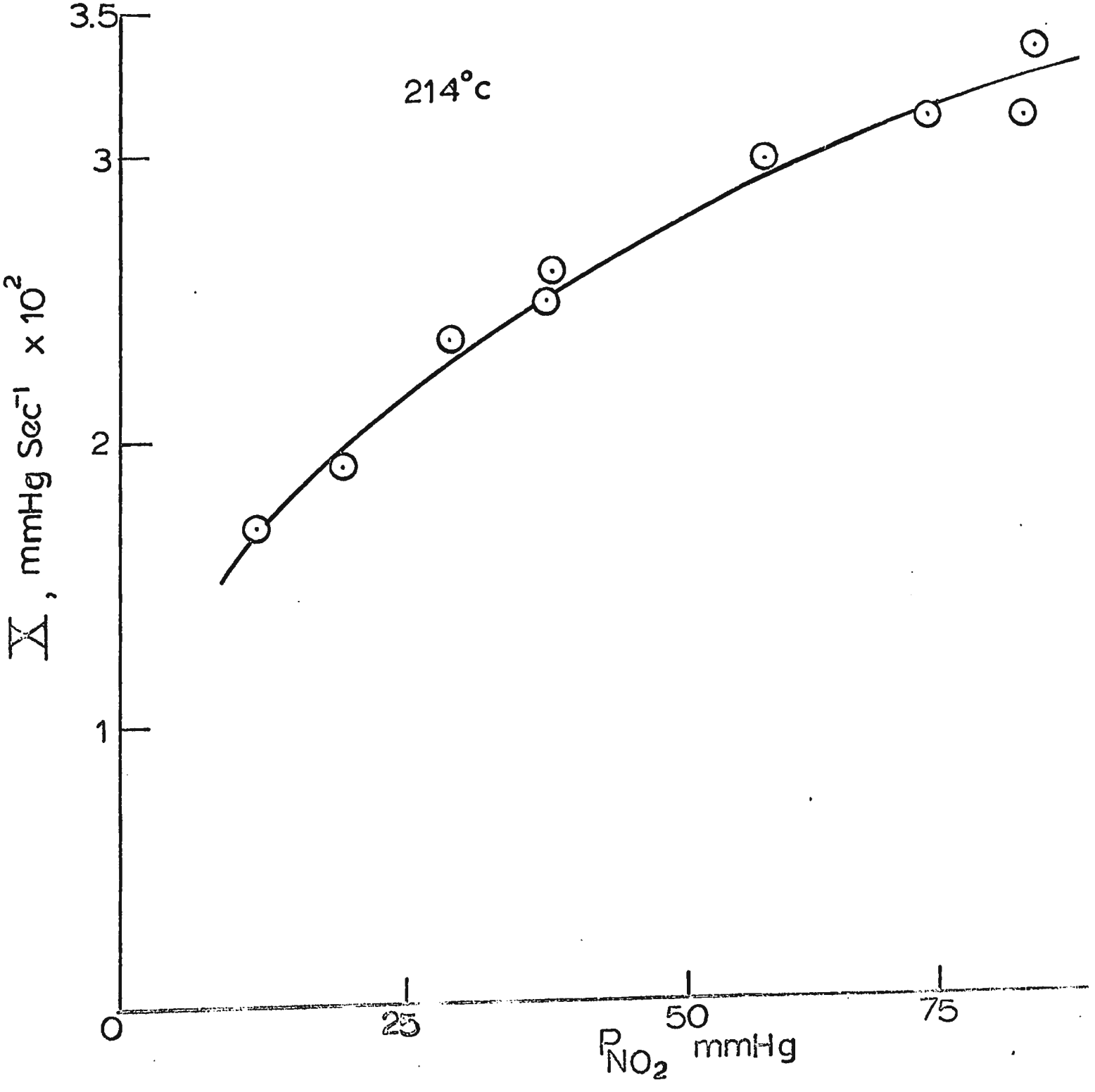
214°c
3.5
3
2
1
0
25
50
75
χ, mmHg Sec^{-1} x 10^2
P_{NO_2} mmHg

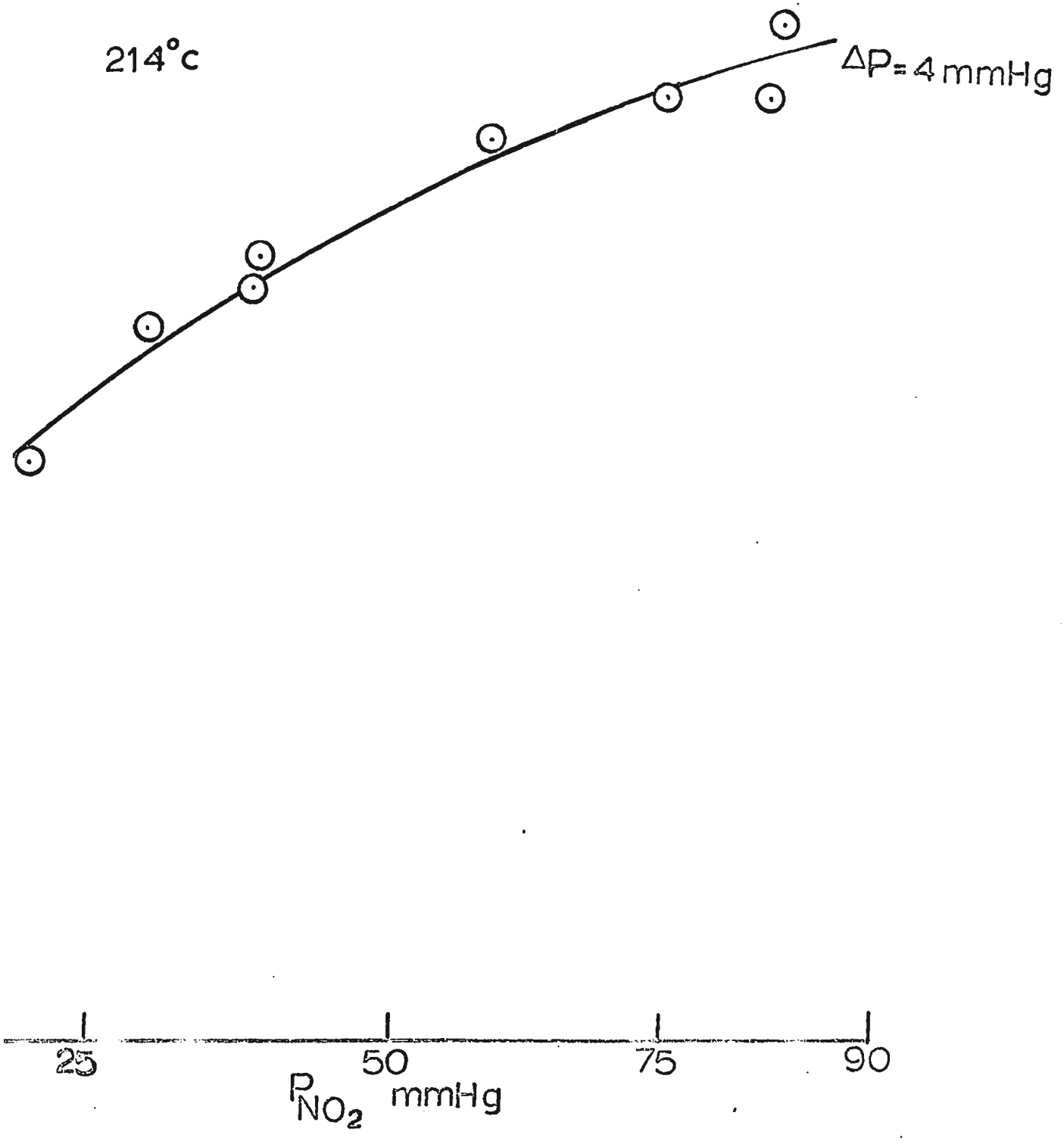
214°c
ΔP = 4 mmHg
25
50
75
90
P_{NO_2} mmHg

FIGURE 28

Autocatalytic contribution to the total rate as a function of P_{NO_2} at 214°C and ΔP = 10 mm Hg.

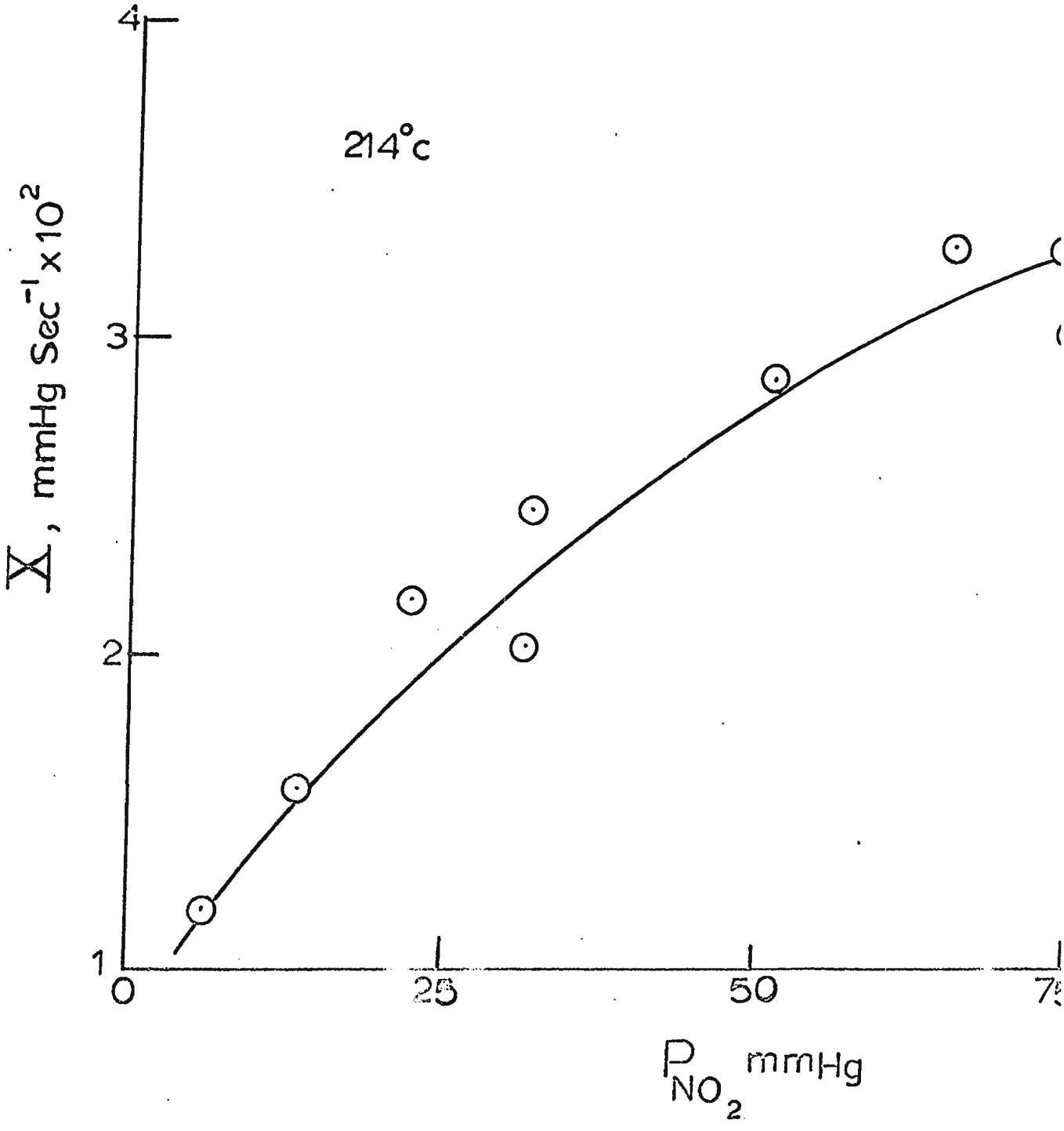
214°c
X, mmHg Sec⁻¹ x 10²
4
3
2
1
0
25
50
P NO₂ mmHg

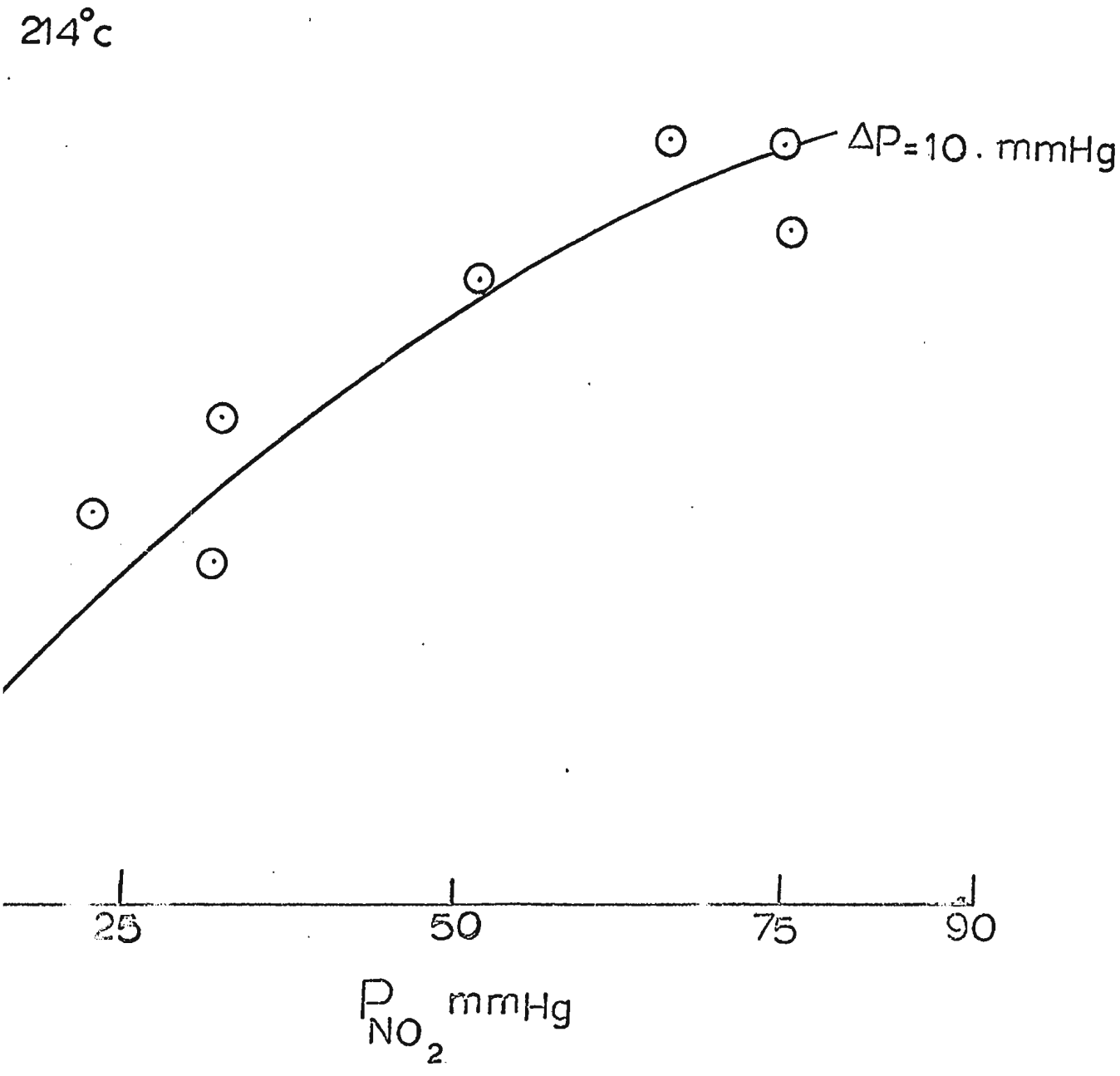
214°c
ΔP=10. mmHg
25
50
75
90
P NO2 mmHg

FIGURE 29

Autocatalytic contribution to the total rate as a function of P_{NO_2} at 214 °C and ΔP = 14 mm Hg.

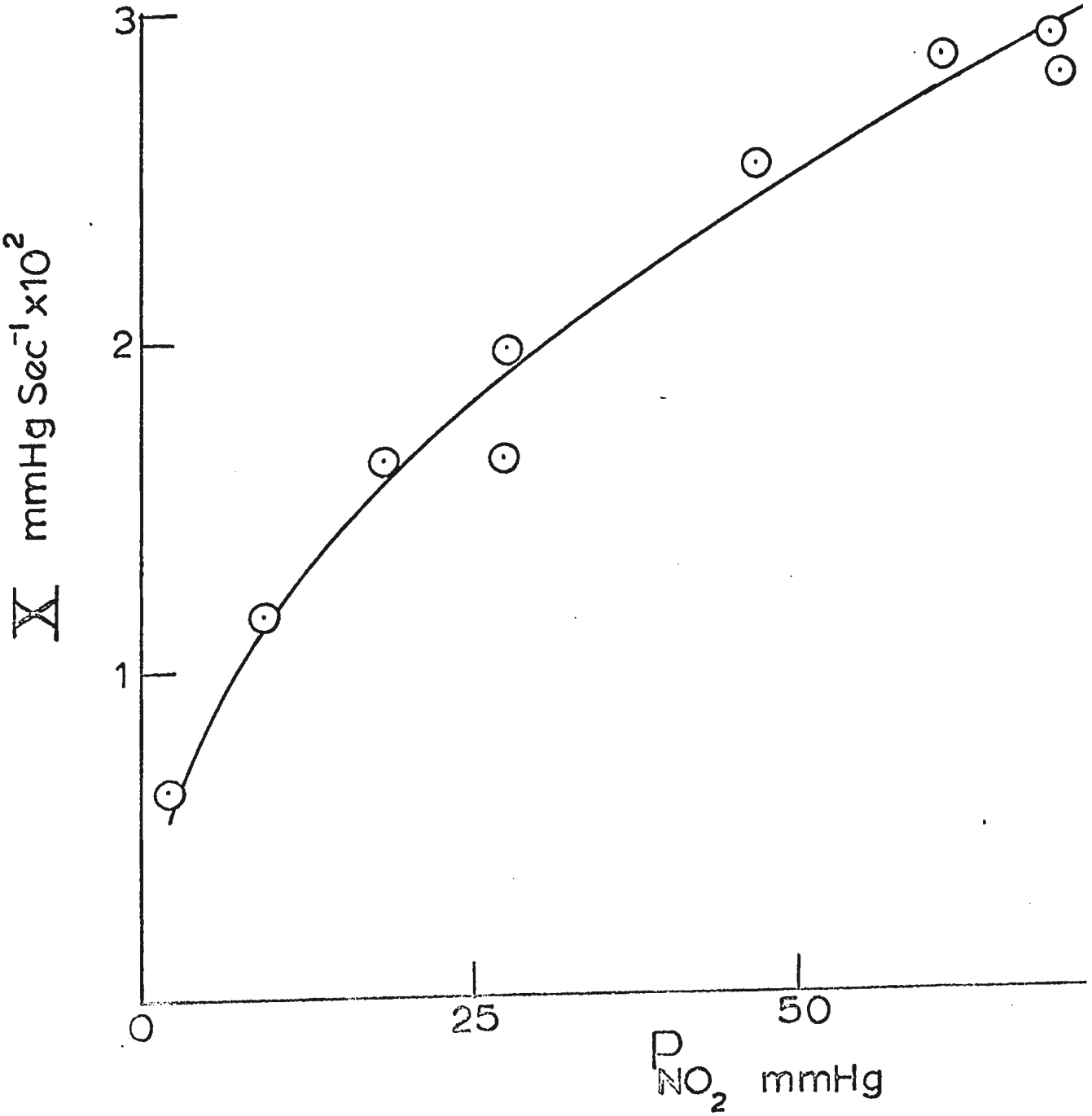
3
2
1
0
25
50
χ mmHg $Sec^{-1} \times 10^2$
P_{NO_2} mmHg

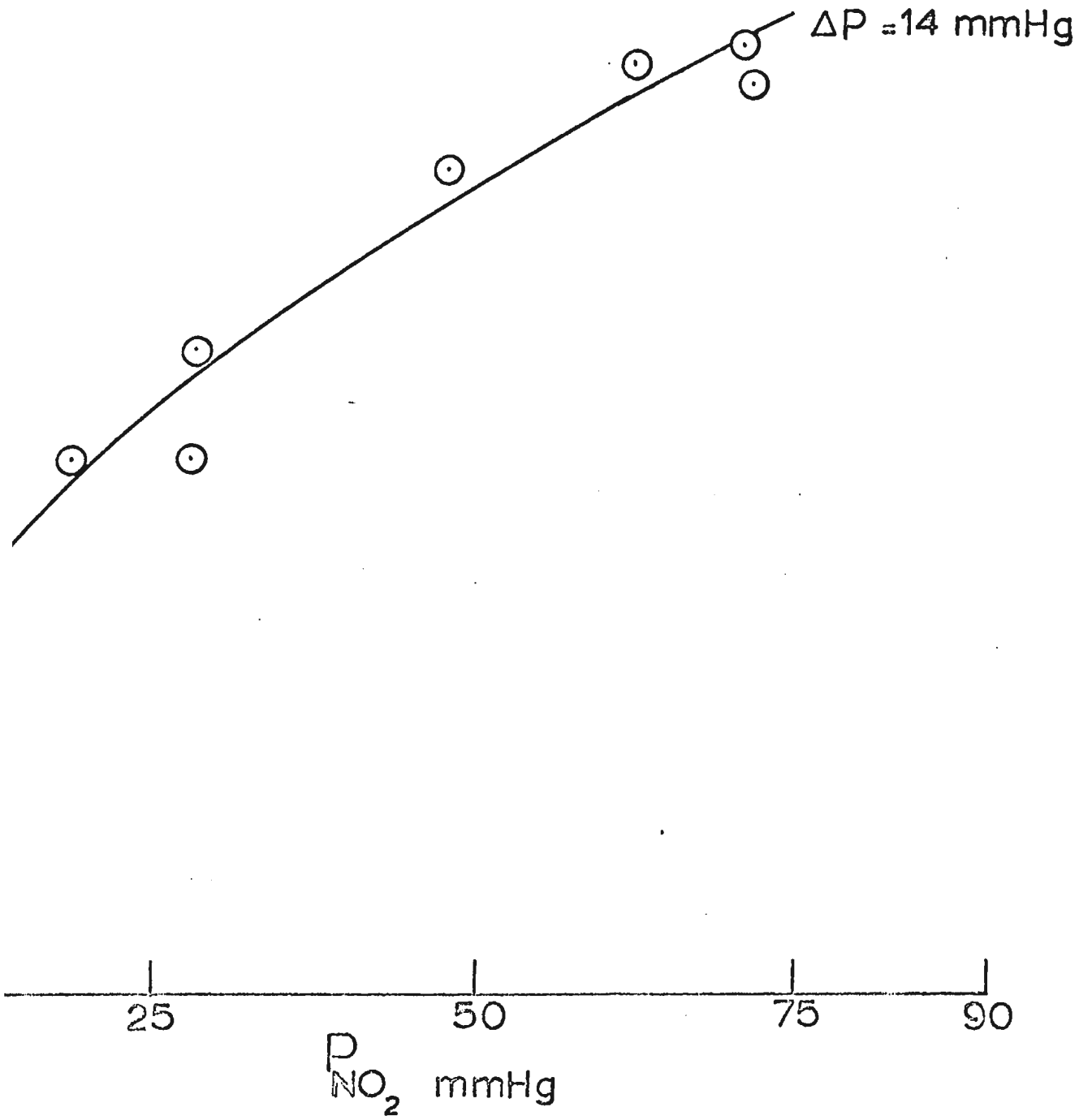
ΔP =14 mmHg
25
50
75
90
P
NO2 mmHg

FIGURE 30

Autocatalytic contribution to the total rate as a function of P_{NO_2} at 214°C and ΔP = 4 mm Hg as a log-log plot.

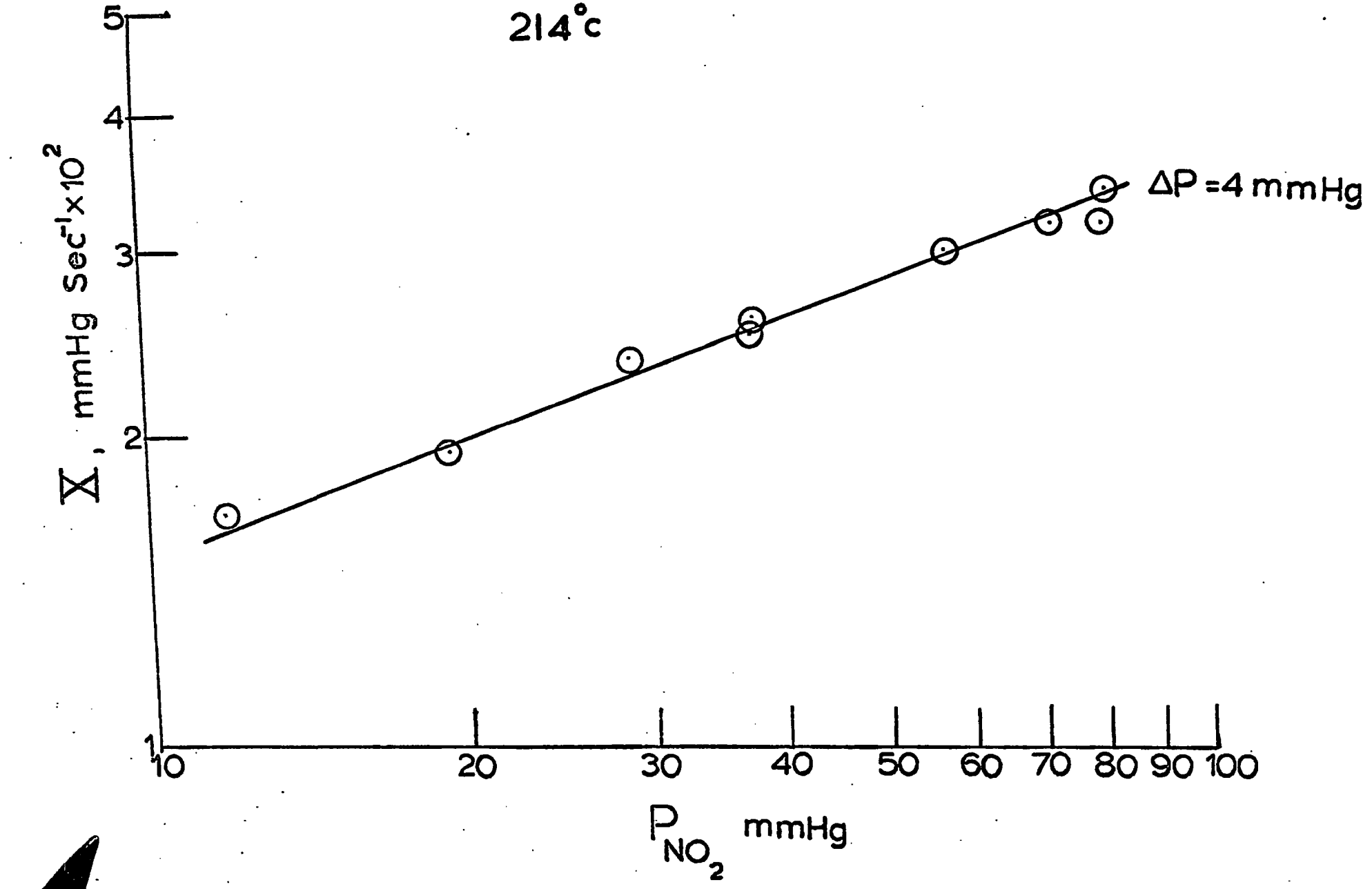
214°c
ΔP =4 mmHg
X, mmHg Sec⁻¹ x10²
5
4
3
2
1
10
20
30
40
50
60
70
80
90
100
P NO2 mmHg

FIGURE 31

Autocatalytic contribution to the total rate as a function of P_{NO_2} at 214°C and ΔP = 10 mm Hg as a log-log plot.

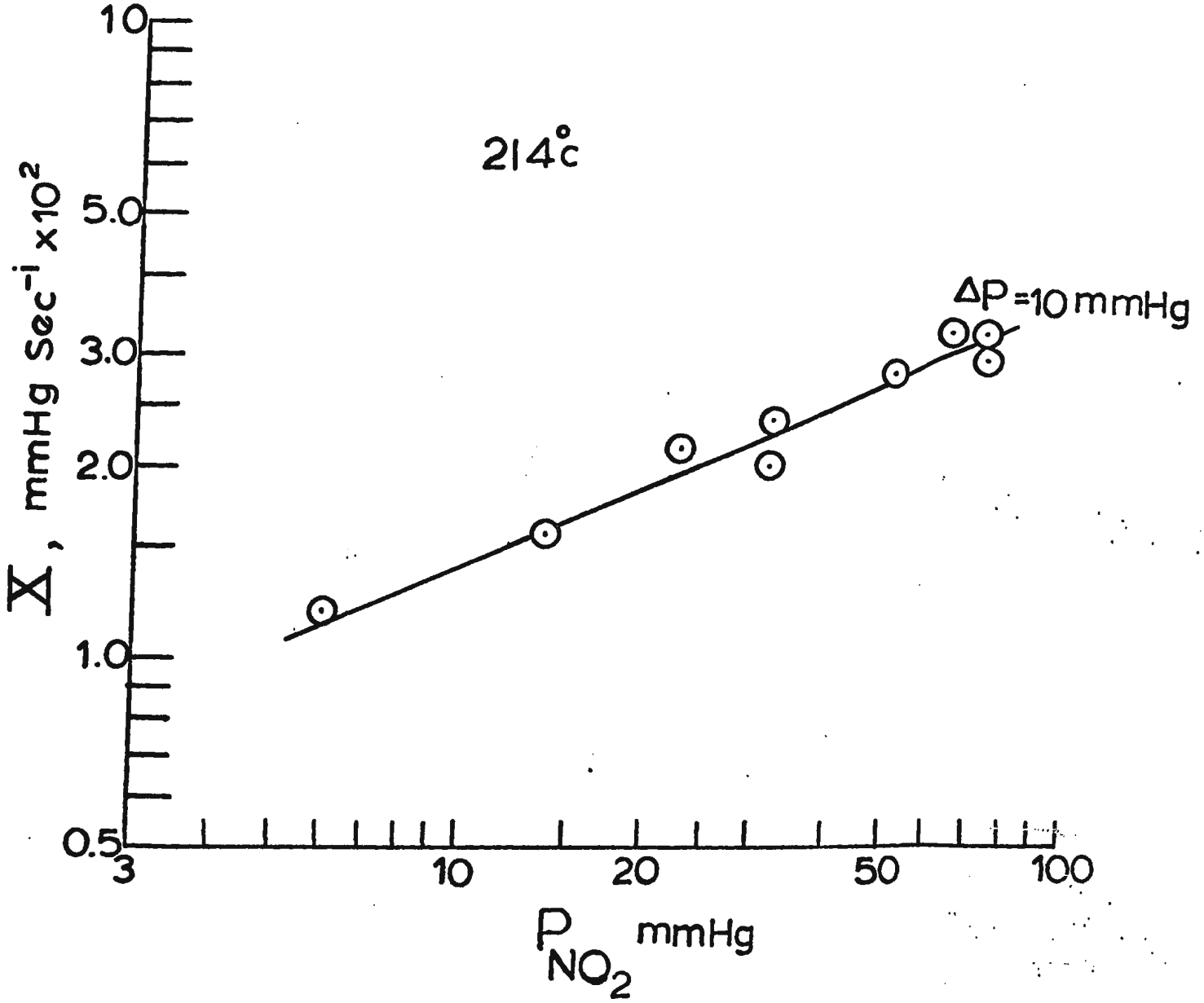
214°c
ΔP=10 mmHg
X, mmHg Sec⁻¹ x10²
10
5.0
3.0
2.0
1.0
0.5
3
10
20
50
100
P NO2 mmHg

FIGURE 32

Autocatalytic contribution to the total rate as a function of P_{NO_2} at 214°C and ΔP = 14 mm Hg as a log-log plot.

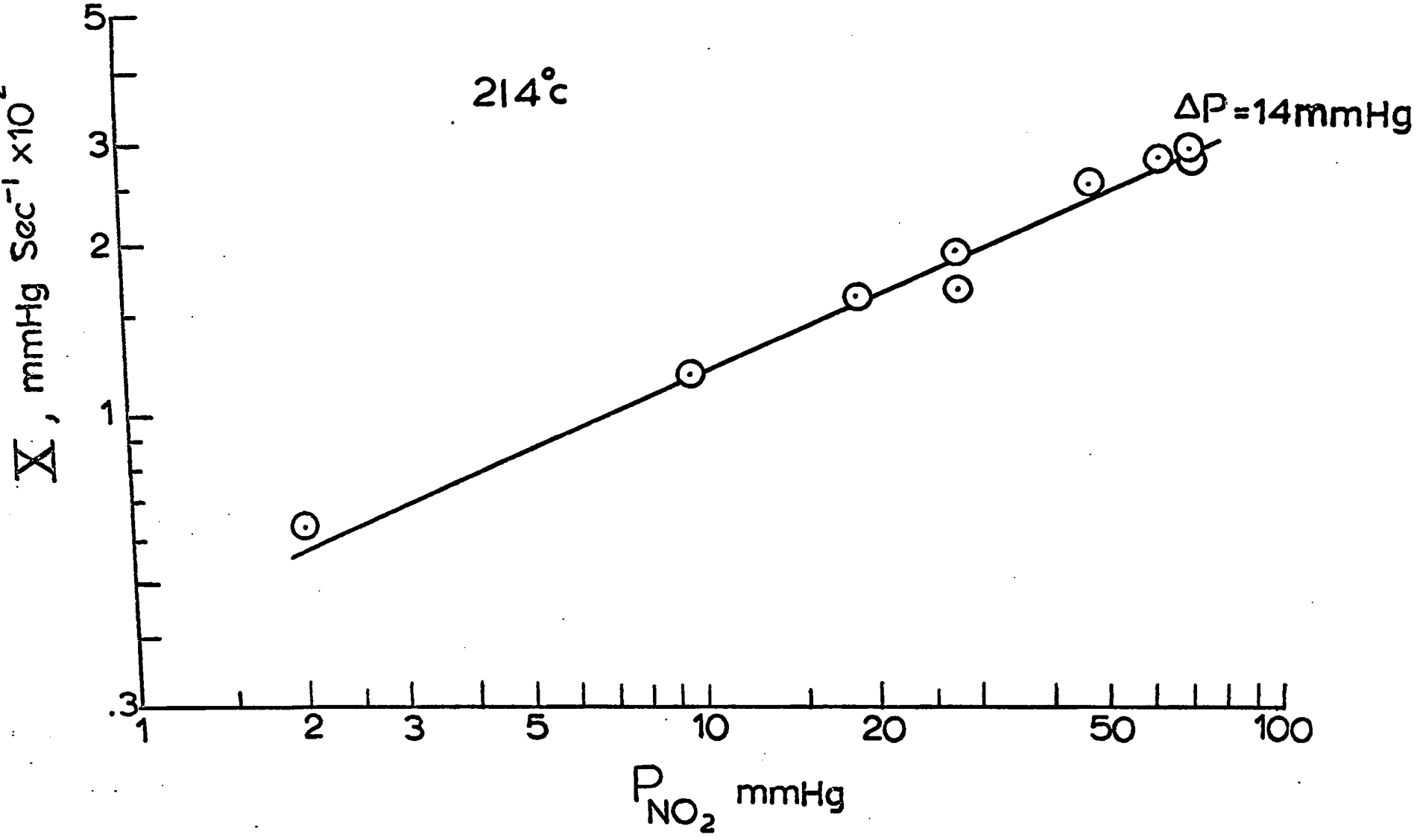
214°c
ΔP=14mmHg
X, mmHg Sec⁻¹ x10²
5
3
2
1
.3
1
2
3
5
10
20
50
100
P NO2 mmHg

FIGURE 33

Autocatalytic contribution to the total rate as a function of P_{FA} at 214°C and ΔP = 4 mm Hg.

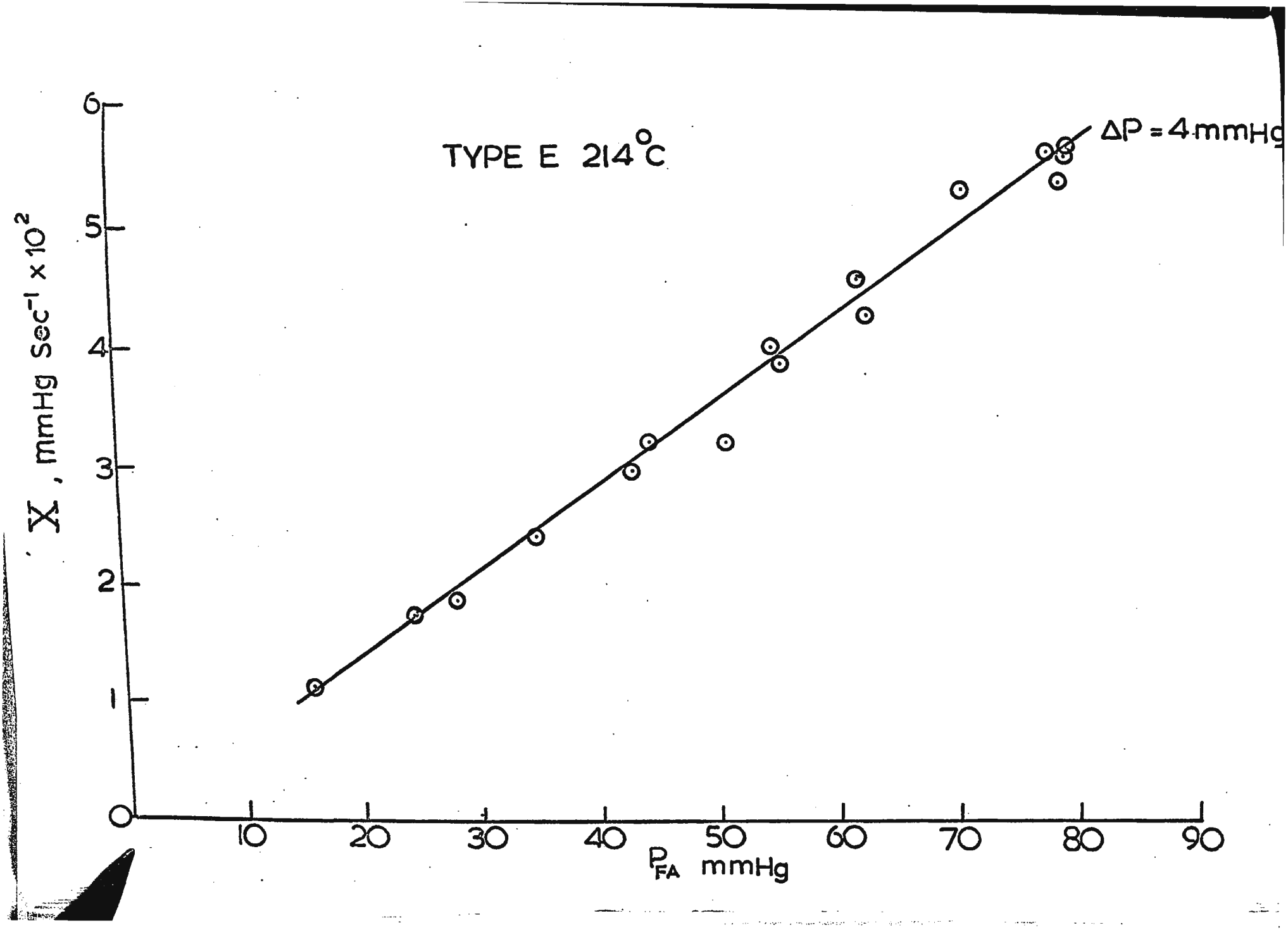
TYPE E 214°C
ΔP = 4 mmHg
X , mmHg Sec⁻¹ x 10²
0
1
2
3
4
5
6
10
20
30
40
50
60
70
80
90
P_FA mmHg

FIGURE 34

Autocatalytic contribution to the total rate as a function of P_{FA} at 214°C and ΔP = 10 mm Hg.

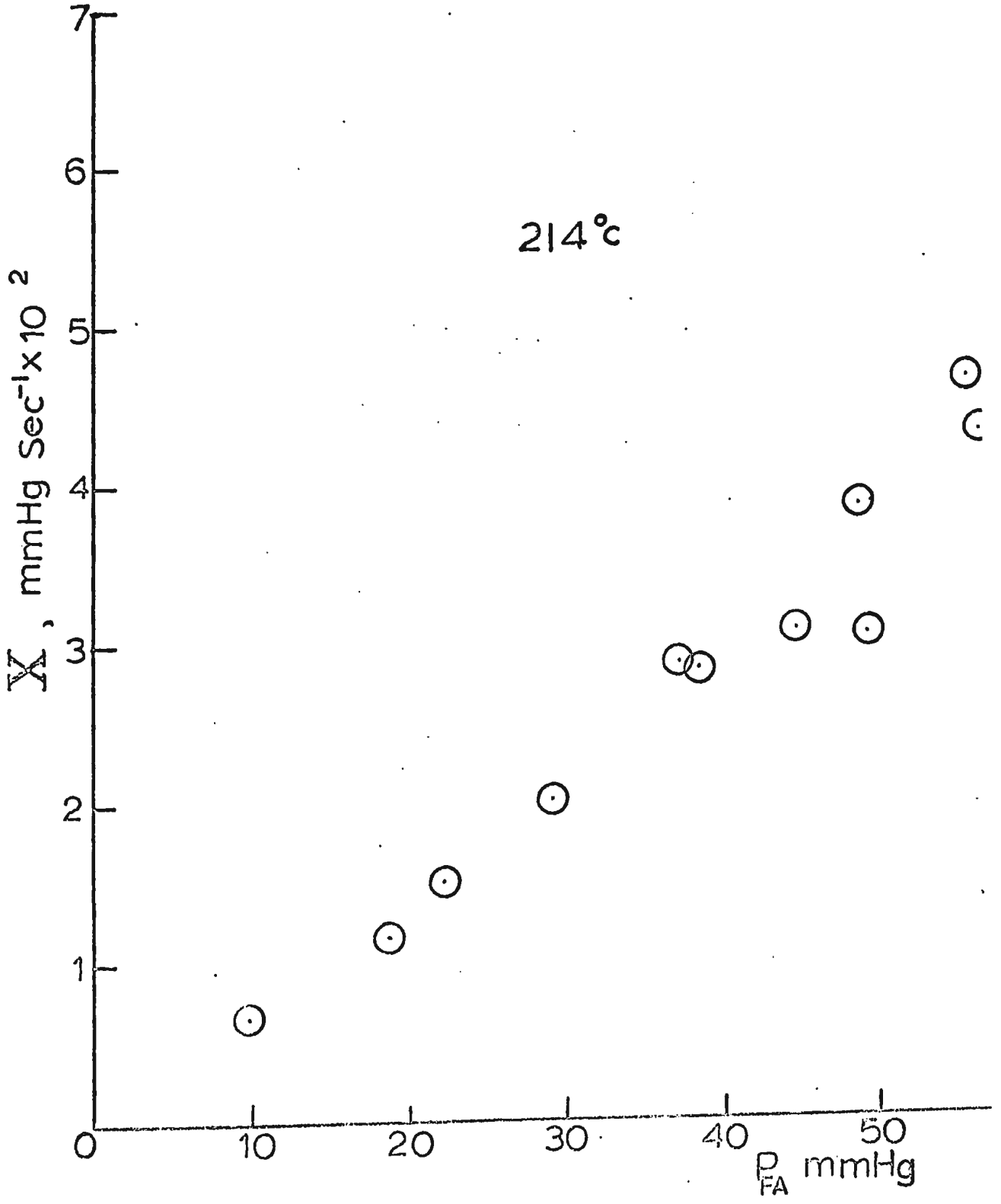
214°c
X, mmHg Sec⁻¹ x 10²
0
1
2
3
4
5
6
7
10
20
30
40
50
P_FA mmHg

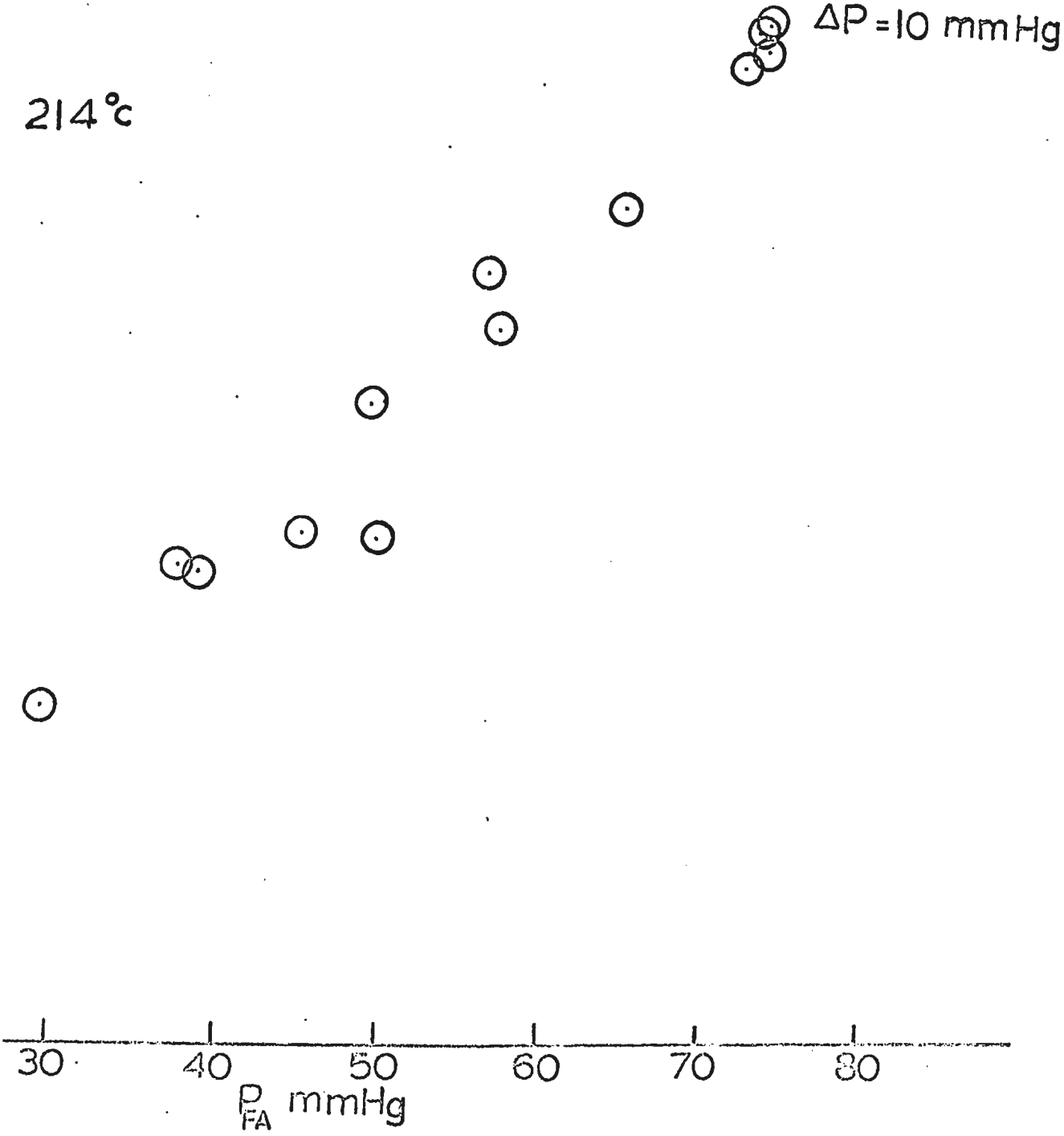
ΔP = 10 mmHg
214°c
30
40
50
60
70
80
P_{FA} mmHg

FIGURE 35

Autocatalytic contribution to the total rate as a function of P_{FA} at 214°C and ΔP = 14 mm Hg.

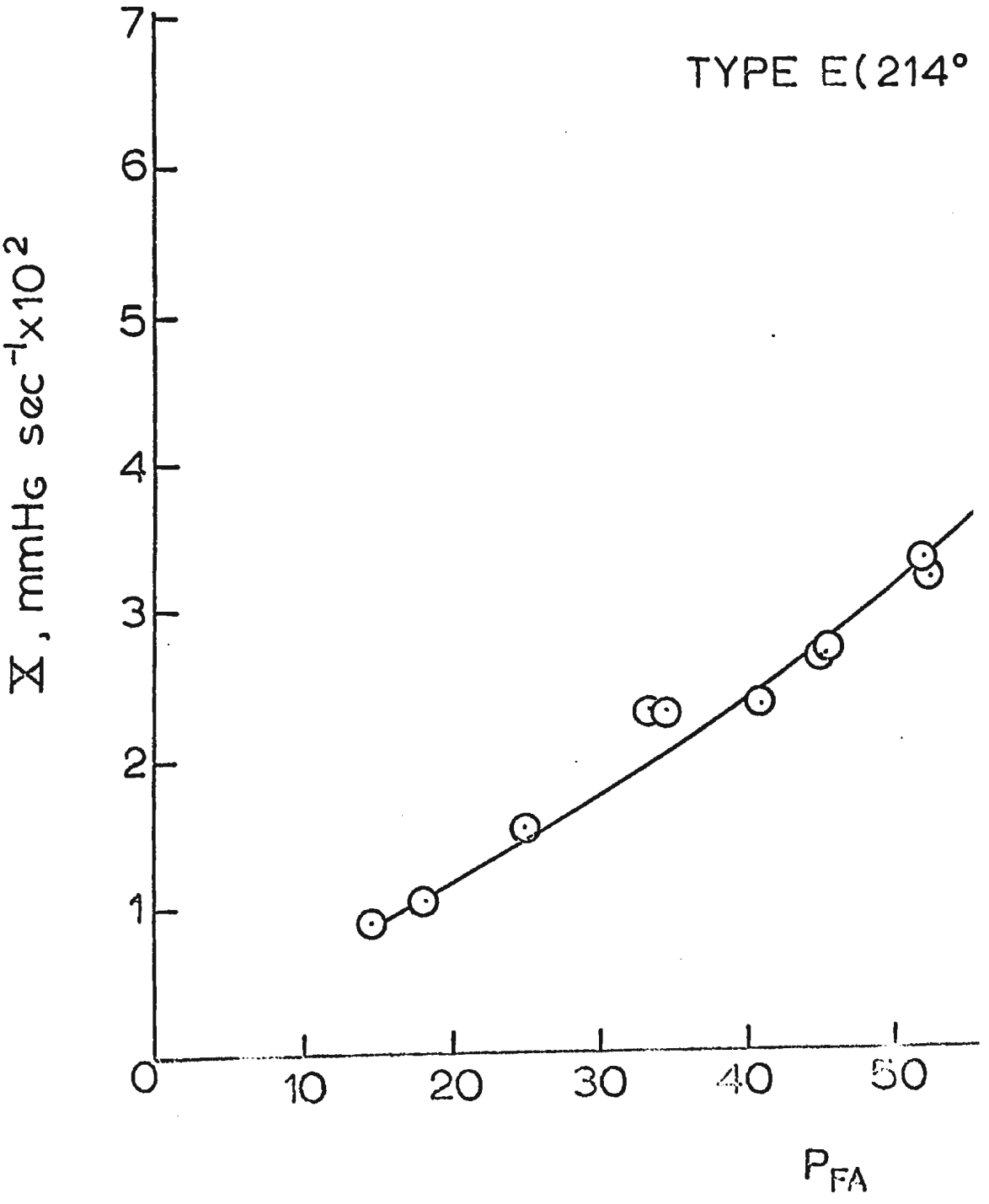
TYPE E(214°
$\dot{V}$, mmHg sec^{-1}x10^2
7
6
5
4
3
2
1
0
10
20
30
40
50
P_{FA}

TYPE E(214°)

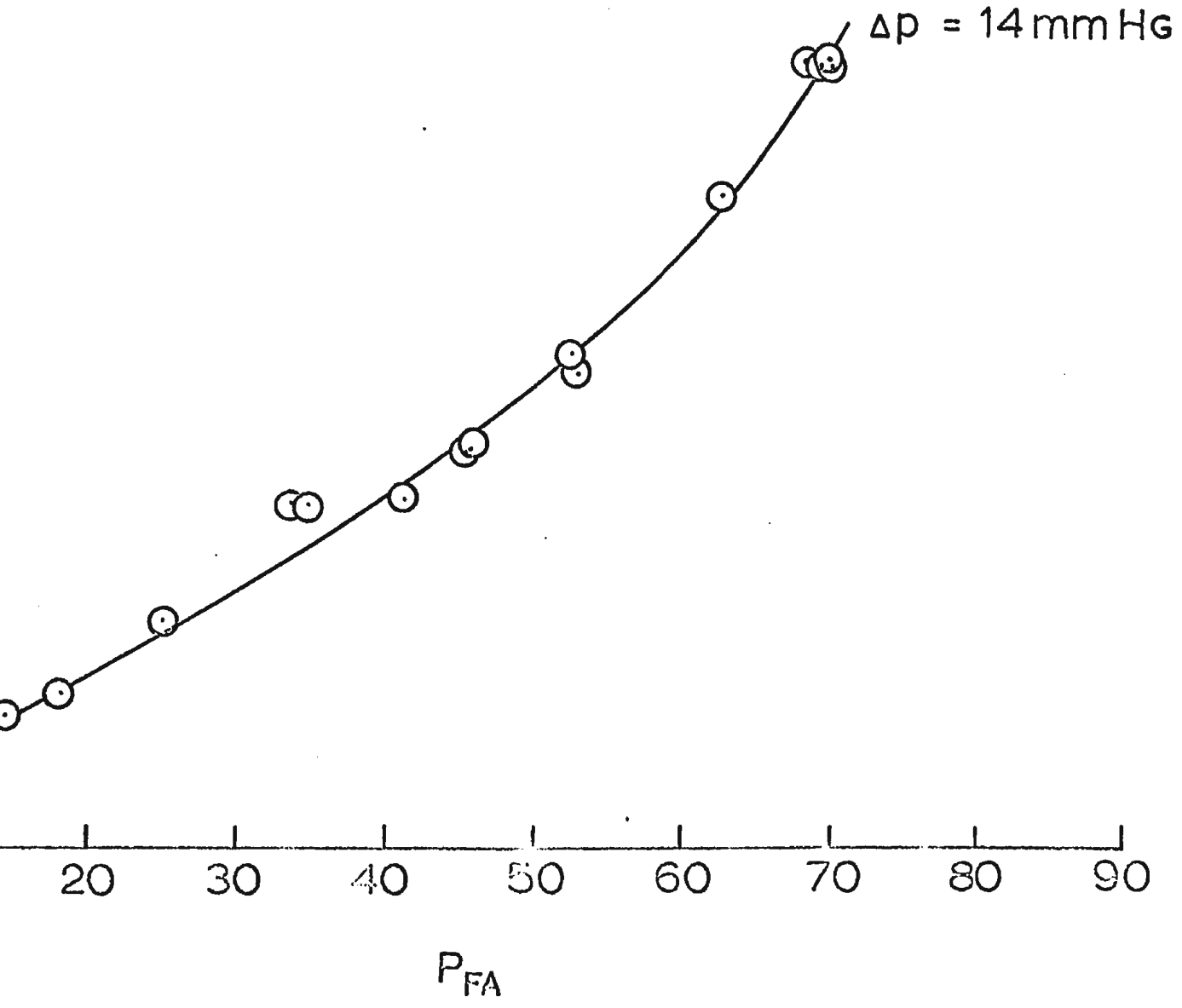

FIGURE 36

Autocatalytic contribution to the total rate as a function of P_{FA} at 214°C and ΔP = 14 mm Hg as a log-log plot.

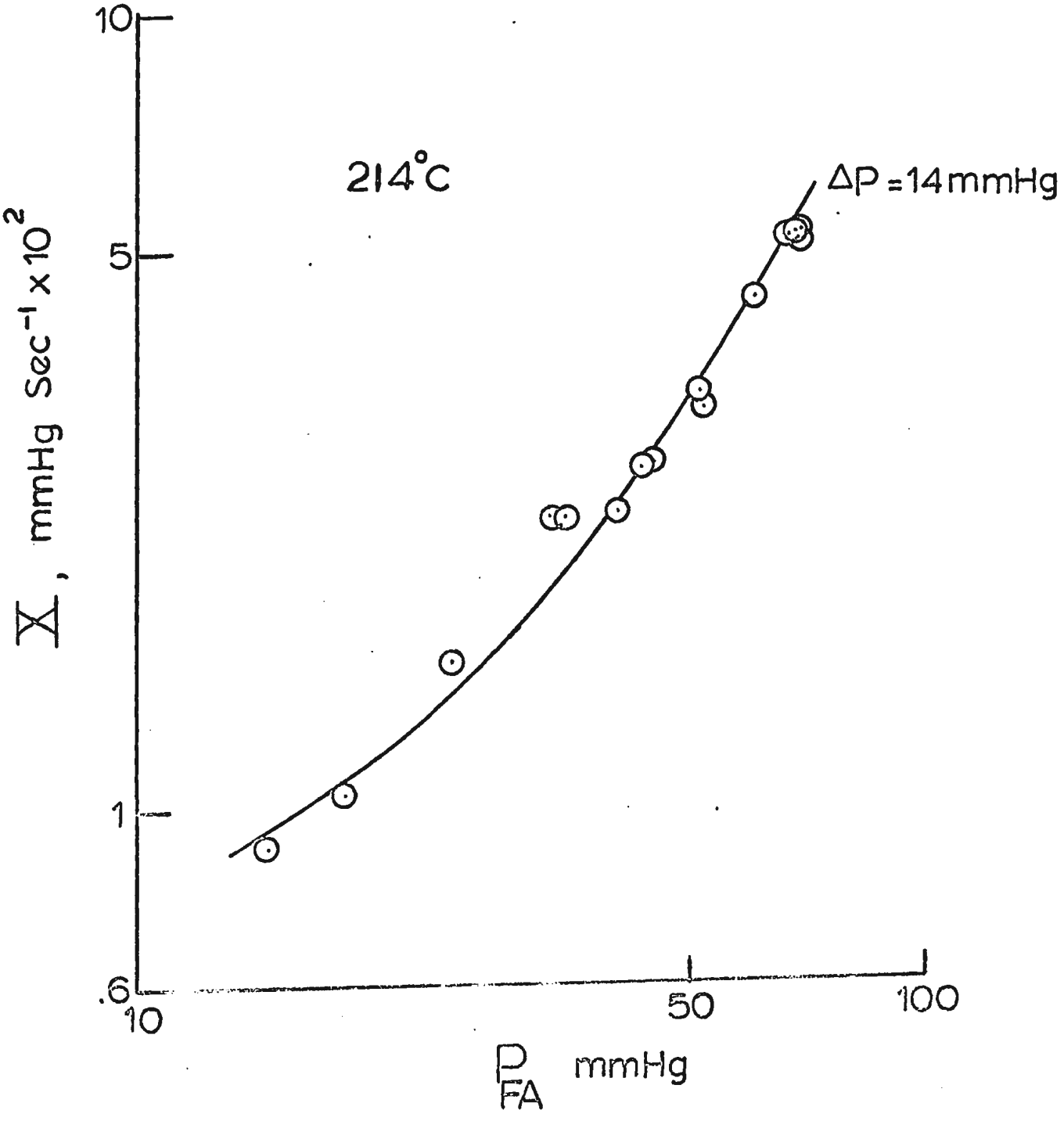
214°C
ΔP = 14 mmHg
10
5
1
.6
10
50
100
X, mmHg Sec⁻¹ x 10²
P FA mmHg

FIGURE 37

Comparison of $R_{calc.}$ and $R_{obsd.}$, $X_{calc.}$ and $X_{obsd.}$ as functions of pressure change in a reaction without NO added initially at 214°C (for run 86):

P_{FA} = 29.70 mm Hg

P_{NO_2} = 90.86 mm Hg

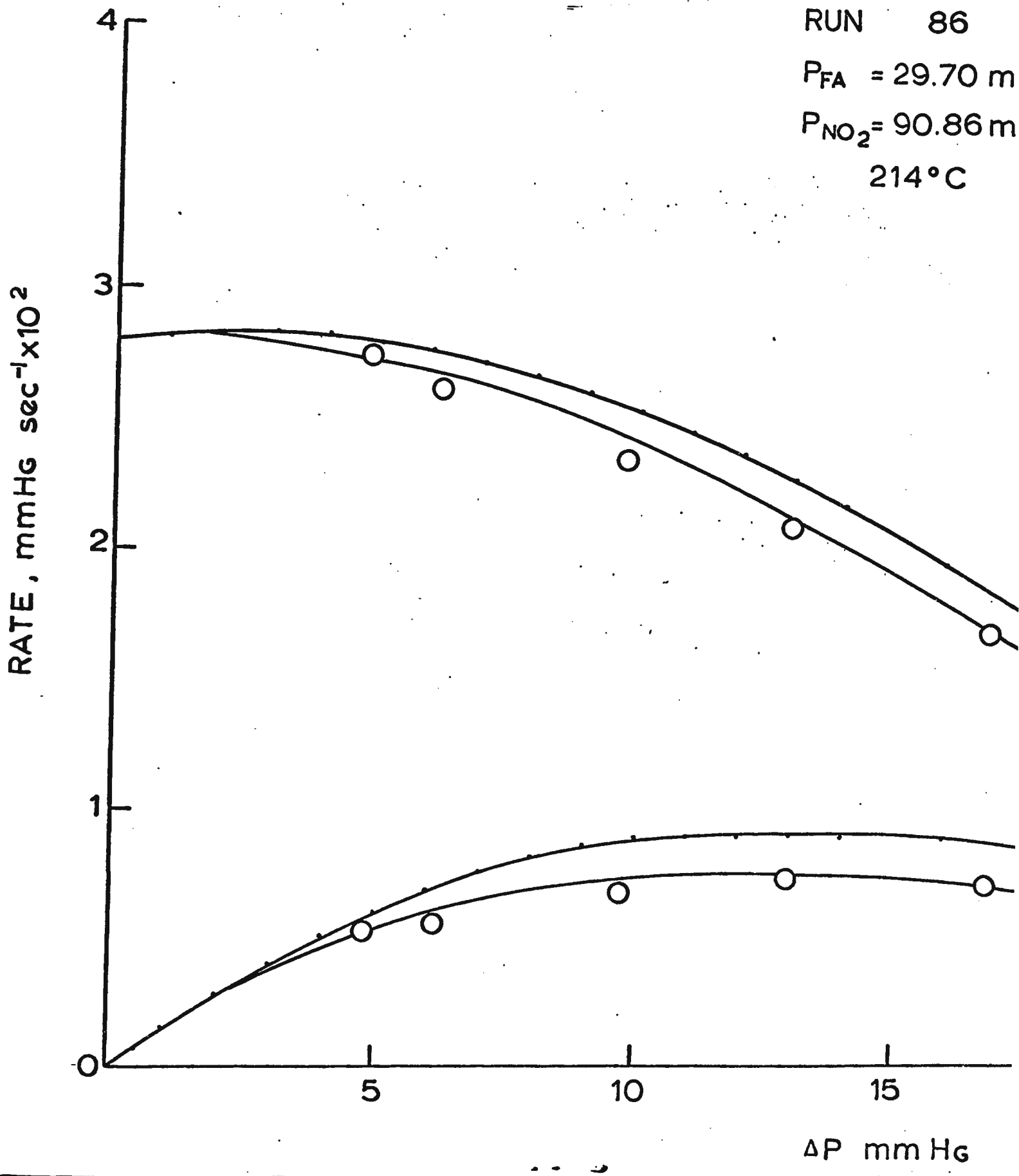
RUN 86
P_{FA} = 29.70 m
P_{NO_2} = 90.86 m
214°C
RATE, mmHg sec^{-1} x10^2
4
3
2
1
0
5
10
15
ΔP mm Hg

86

29.70 mmHg

90.86 mmHg

?14°C

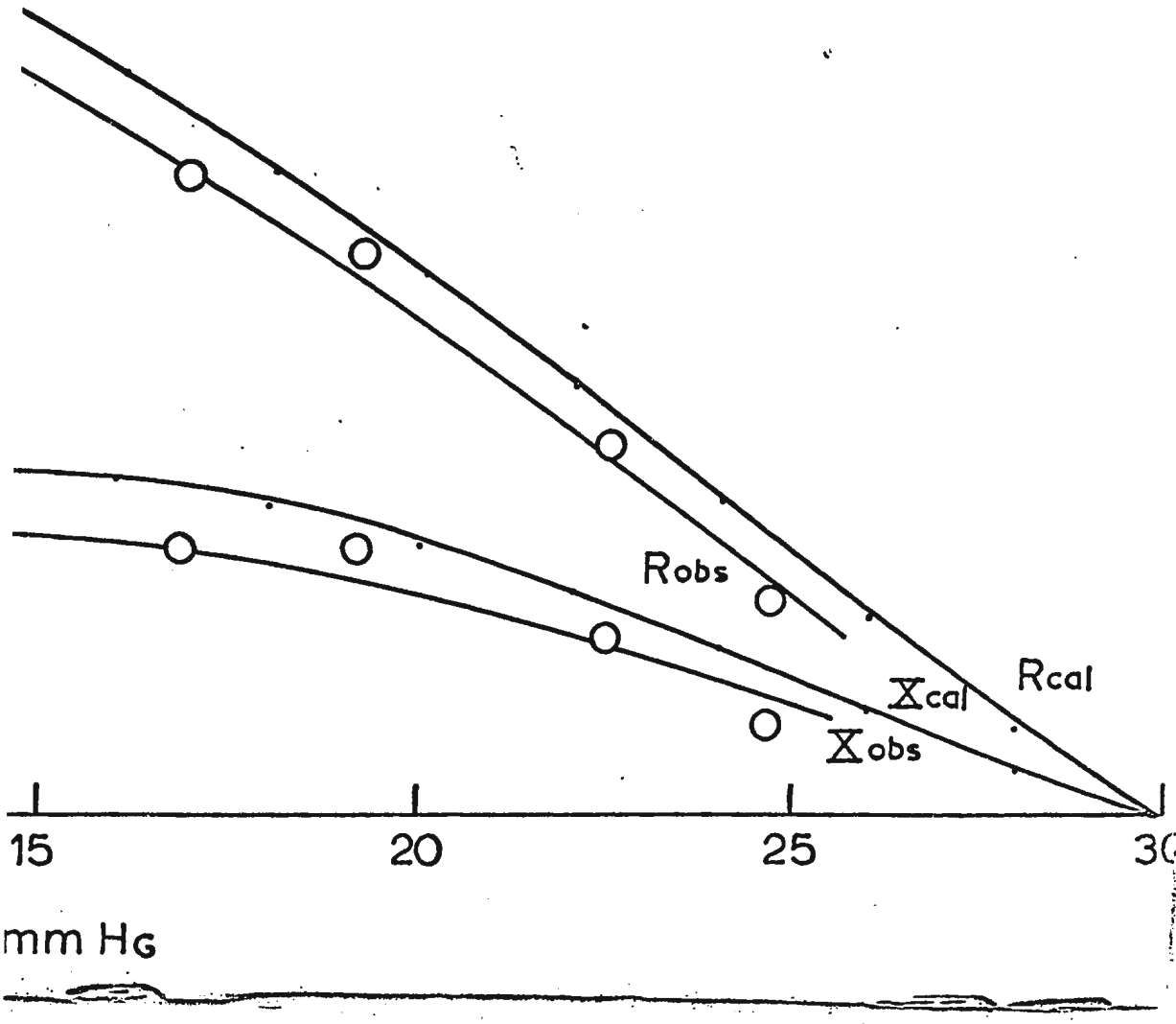

FIGURE 38

Comparison of $R_{calc.}$ and $R_{obsd.}$, $X_{calc.}$ and $X_{obsd.}$ as functions of pressure change in a reaction without NO added initially at 214°C (for run 130):

P_{FA} = 38.42 mm Hg

P_{NO_2} = 29.92 mm Hg

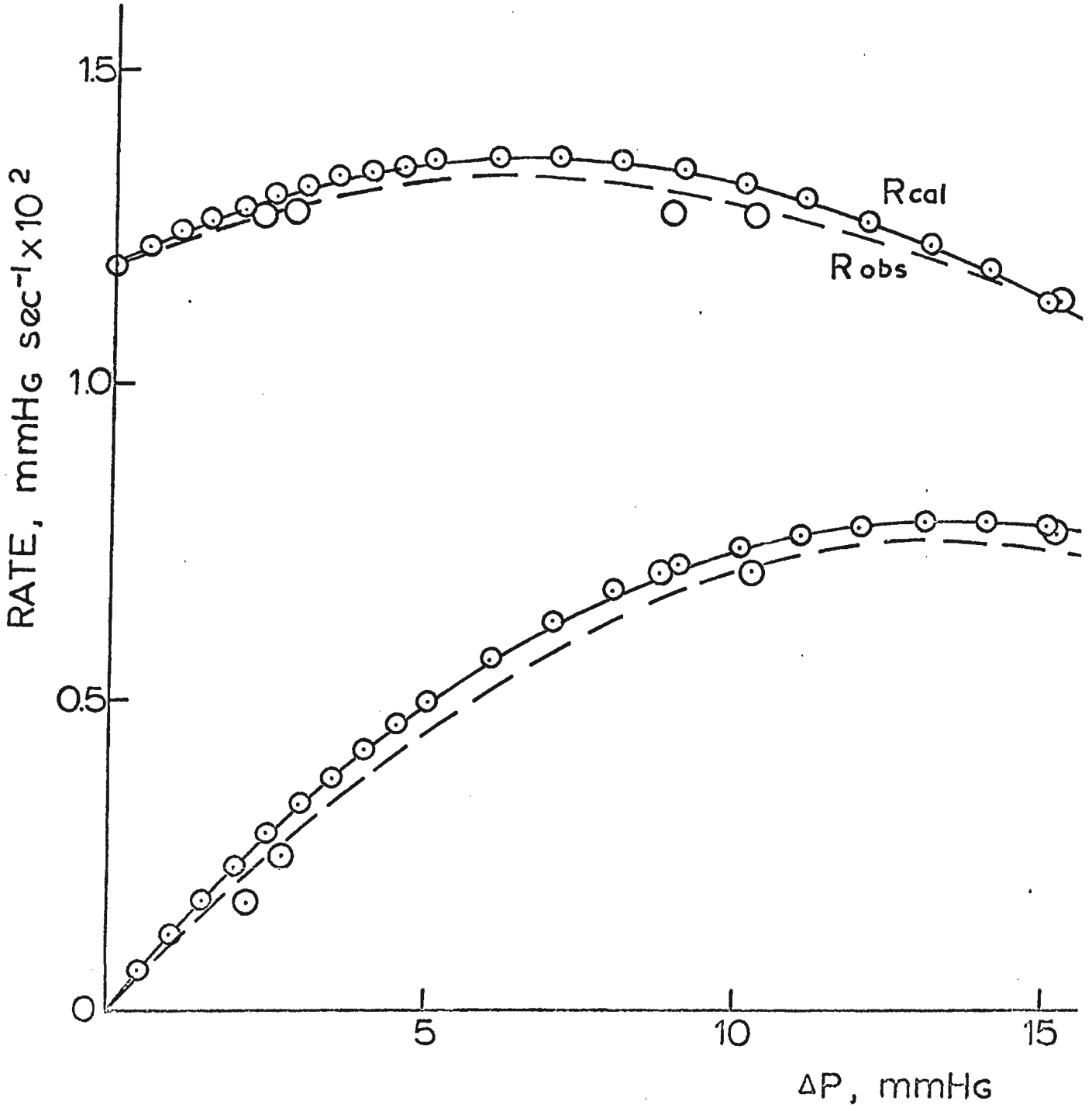
1.5
1.0
0.5
0
RATE, mmHg sec⁻¹ x 10²
Rcal
Robs
5
10
15
ΔP, mmHg

RUN # 130

P_{FA} = 38.42 mmHg

P_{NO_2} = 29.92 "

214 °C

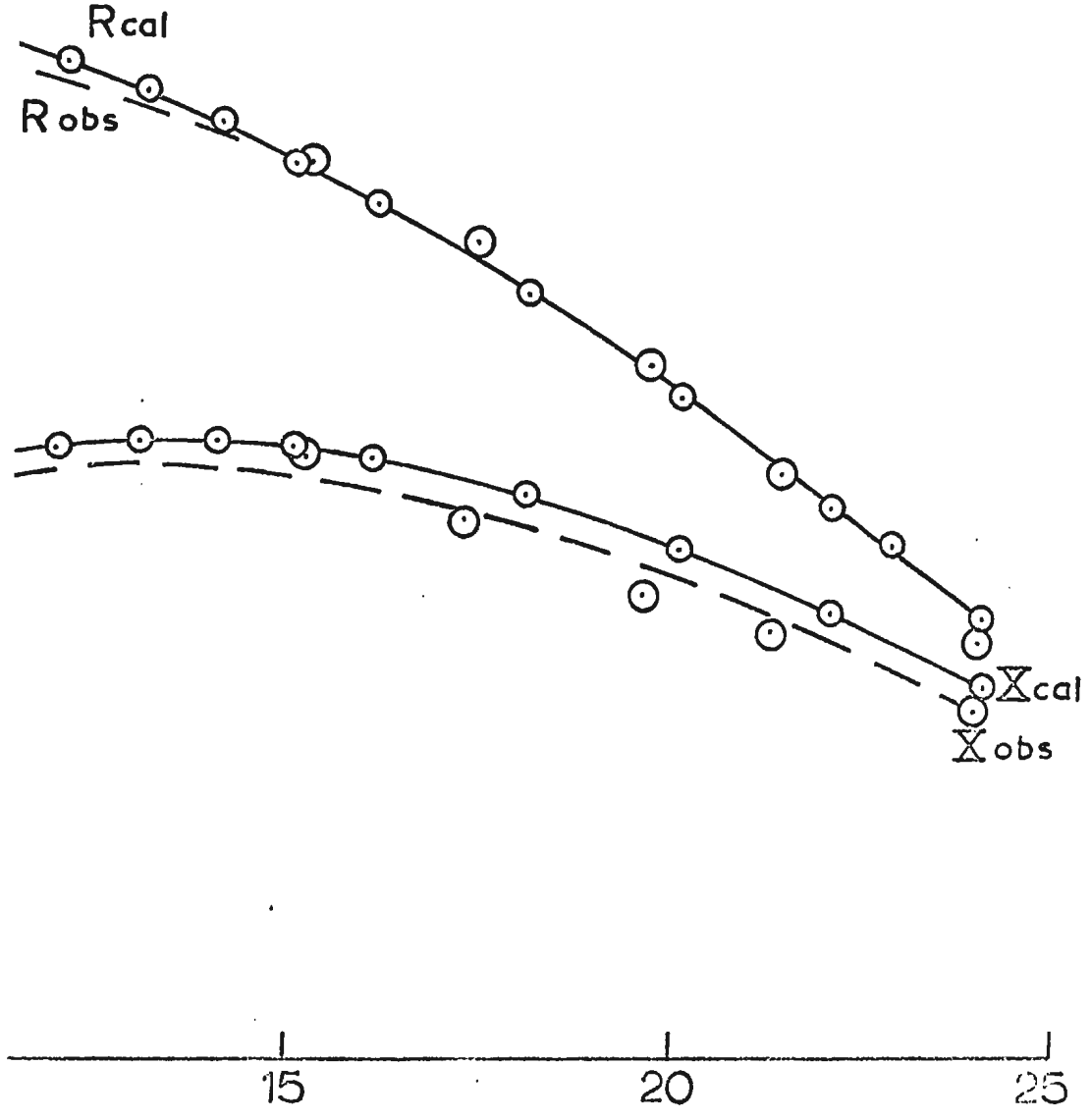

FIGURE 39

Comparison of $R_{calc.}$ and $R_{obsd.}$, $X_{calc.}$ and $X_{obsd.}$ as functions of pressure change in a reaction without NO added initially at 214°C (for run 117):

P_{FA} = 52.10 mm Hg

P_{NO_2} = 29.92 mm Hg

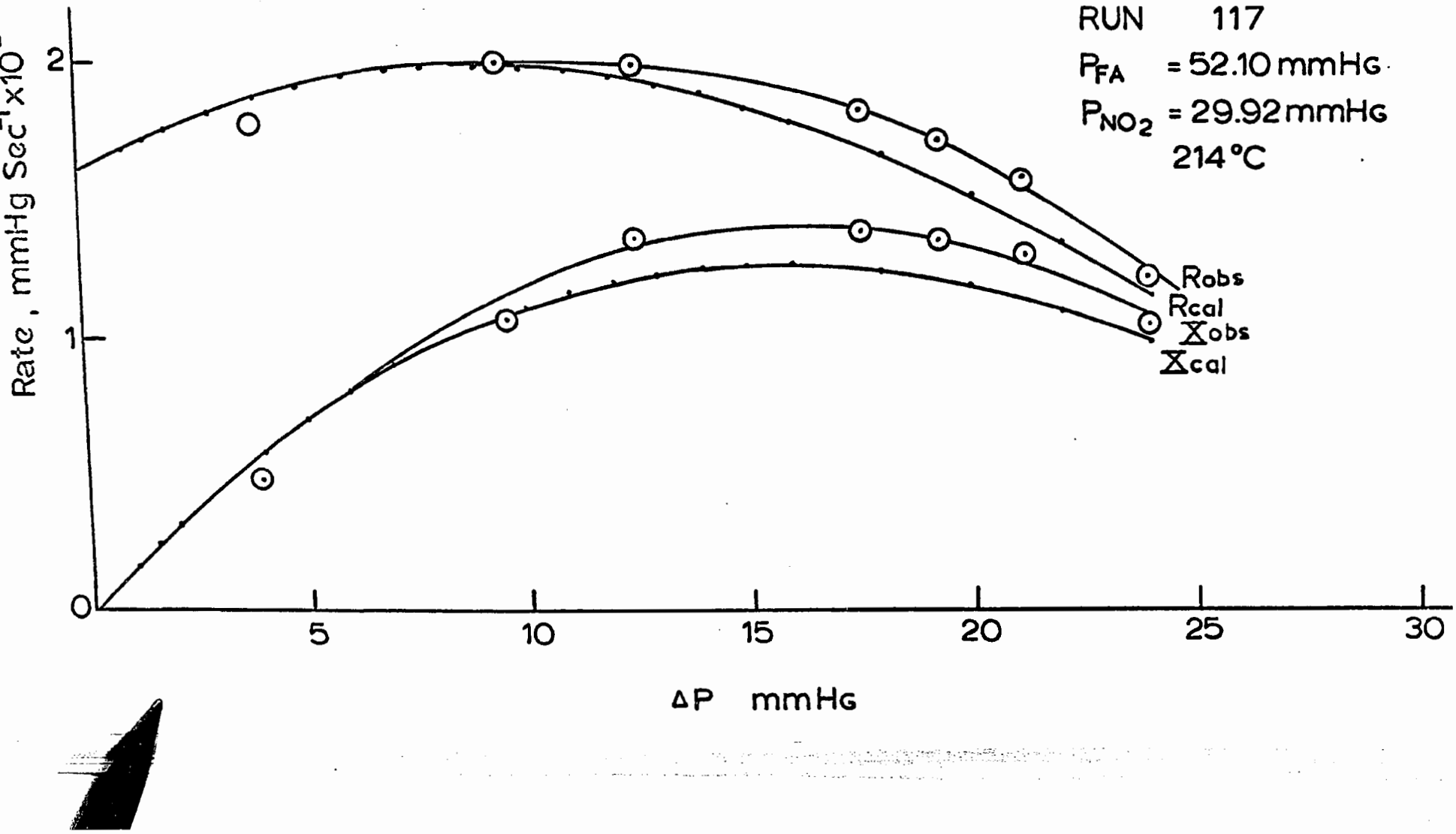
RUN 117
P_{FA} = 52.10 mmHg
P_{NO_2} = 29.92 mmHg
214 °C
Robs
Rcal
Xobs
Xcal
Rate, mmHg $Sec^{-1} \times 10^2$
0
1
2
5
10
15
20
25
30
ΔP mmHg

FIGURE 40

Comparison of $R_{calc.}$ and $R_{obsd.}$ as functions of pressure change (with high initial formic acid pressure.

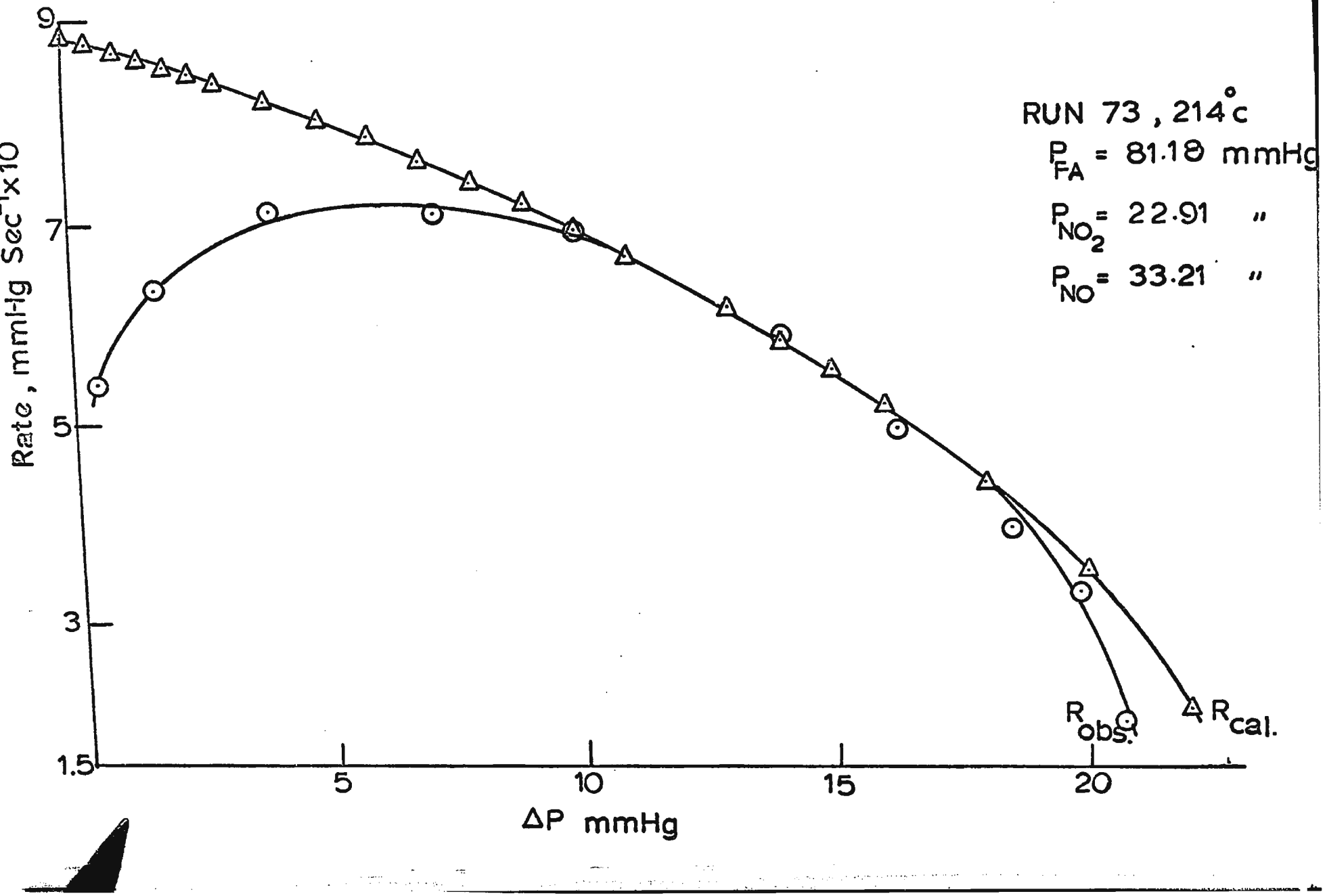
RUN 73 , 214°c
P_{FA} = 81.18 mmHg
P_{NO_2} = 22.91 "
P_{NO} = 33.21 "
Rate , mmHg $Sec^{-1} \times 10^2$
9
7
5
3
1.5
5
10
15
20
ΔP mmHg
$R_{obs.}$
$R_{cal.}$

FIGURE 41

Comparison of $R_{calc.}$ and $R_{obsd.}$ as functions of pressure change with moderate initial formic acid pressure.

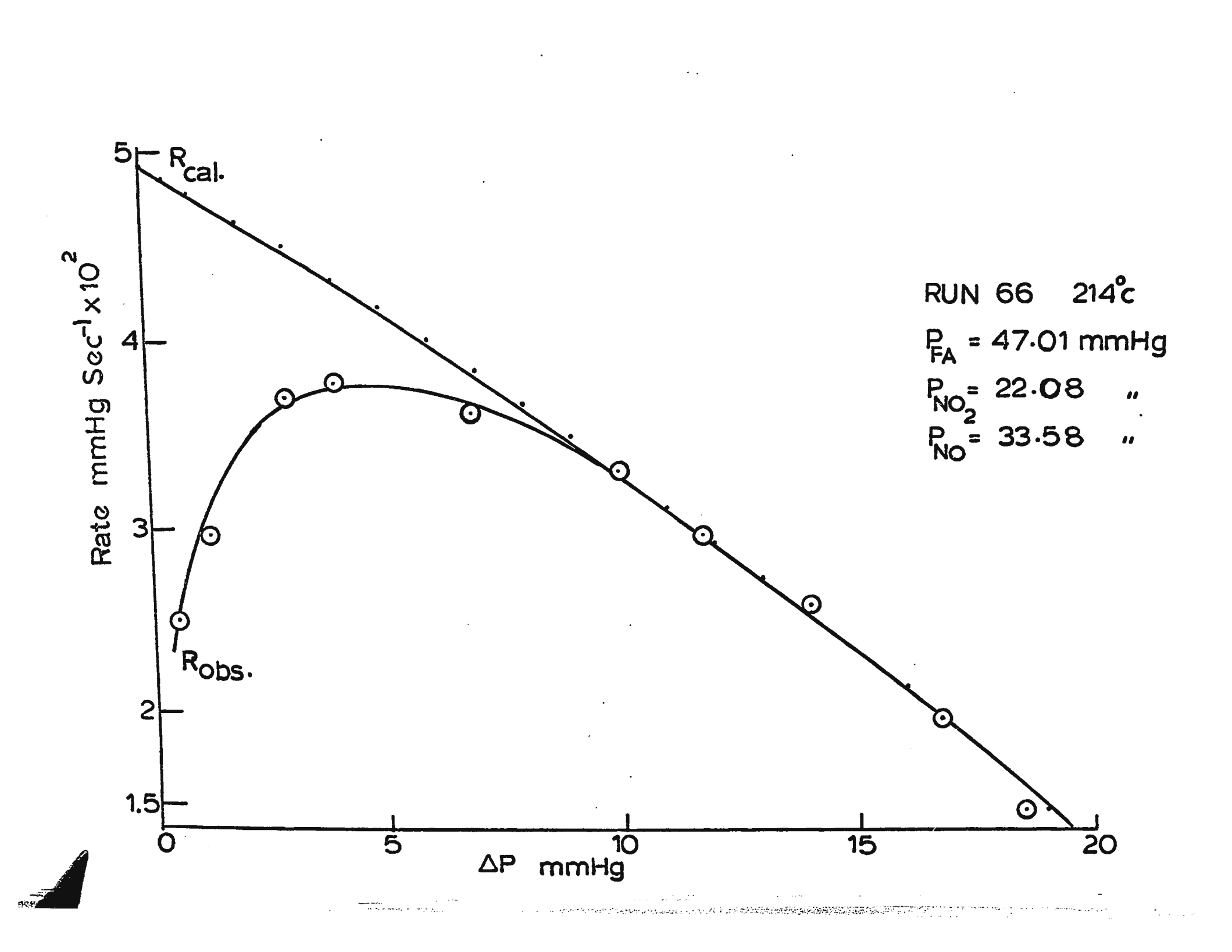
5
4
3
2
1.5
$R_{cal.}$
$R_{obs.}$
Rate mmHg $Sec^{-1} \times 10^2$
0
5
10
15
20
ΔP mmHg
RUN 66 214°c
P_{FA} = 47.01 mmHg
P_{NO_2} = 22.08 "
P_{NO} = 33.58 "

FIGURE 42

Comparison of $R_{calc.}$ and $R_{obsd.}$ as functions of pressure change with low initial formic acid pressure.

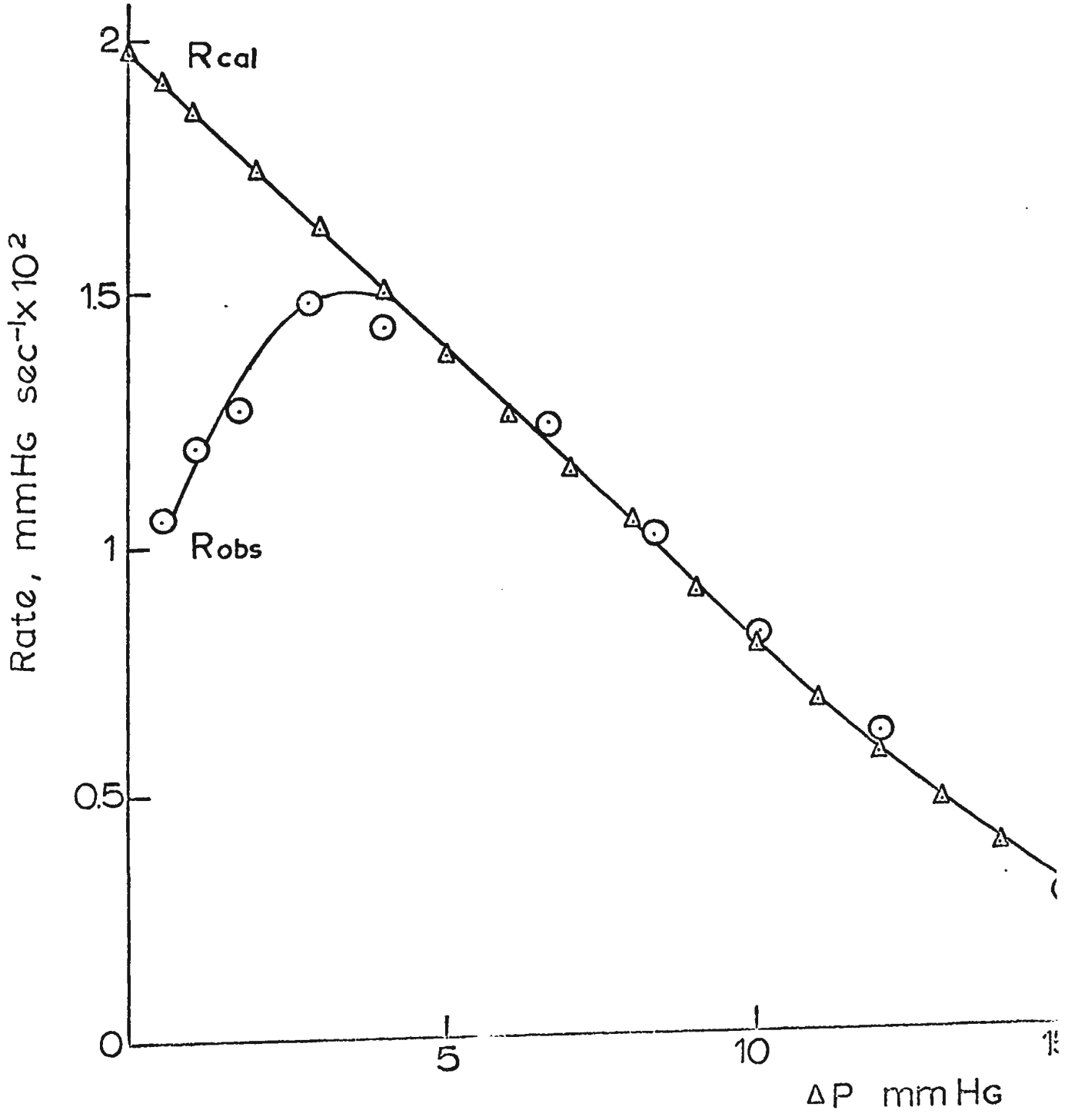
Rcal
Robs
Rate, mmHg sec⁻¹ x 10²
2
1.5
1
0.5
0
5
10
ΔP mm Hg

RUN # 91

P_{FA} = 19.93 mm Hg

P_{NO} = 23.04 "

P_{NO} = 33.17 "

214 °C

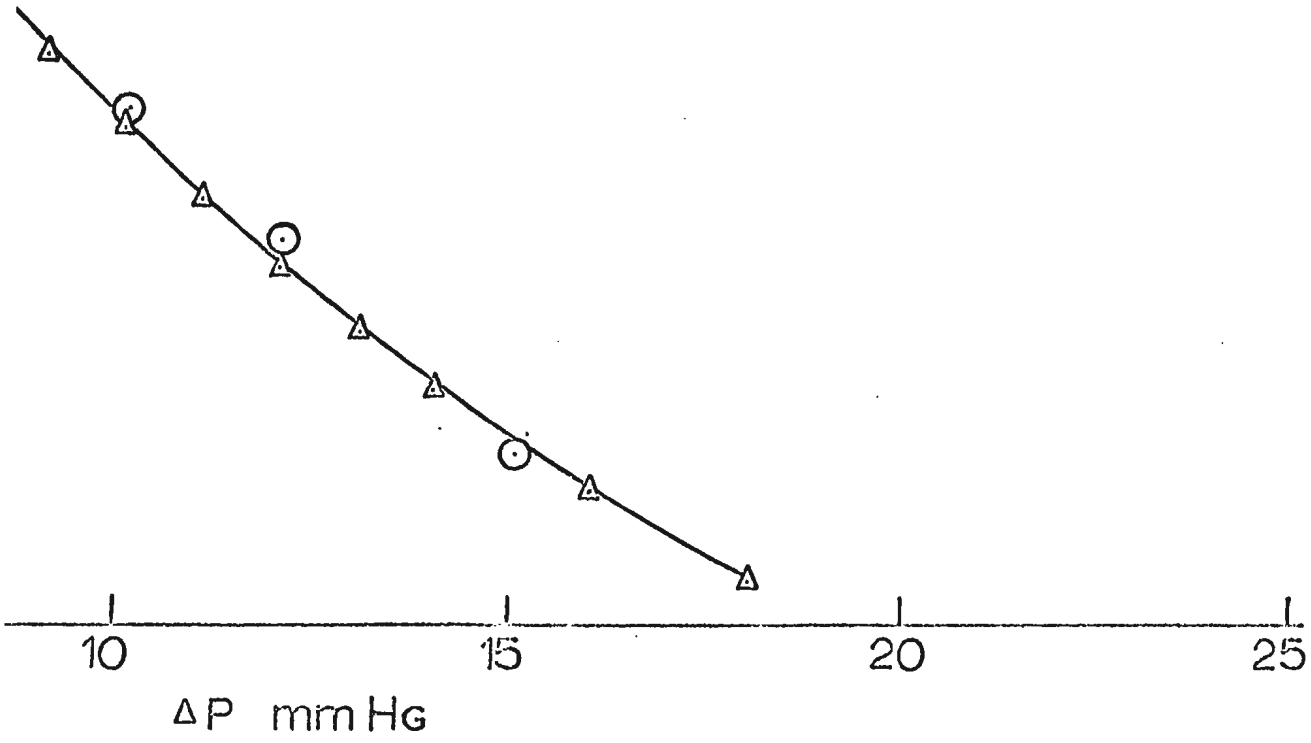

FIGURE 43

Comparison of $R_{calc.}$ and $R_{obsd.}$ as functions of pressure change with high initial NO_2 pressure.

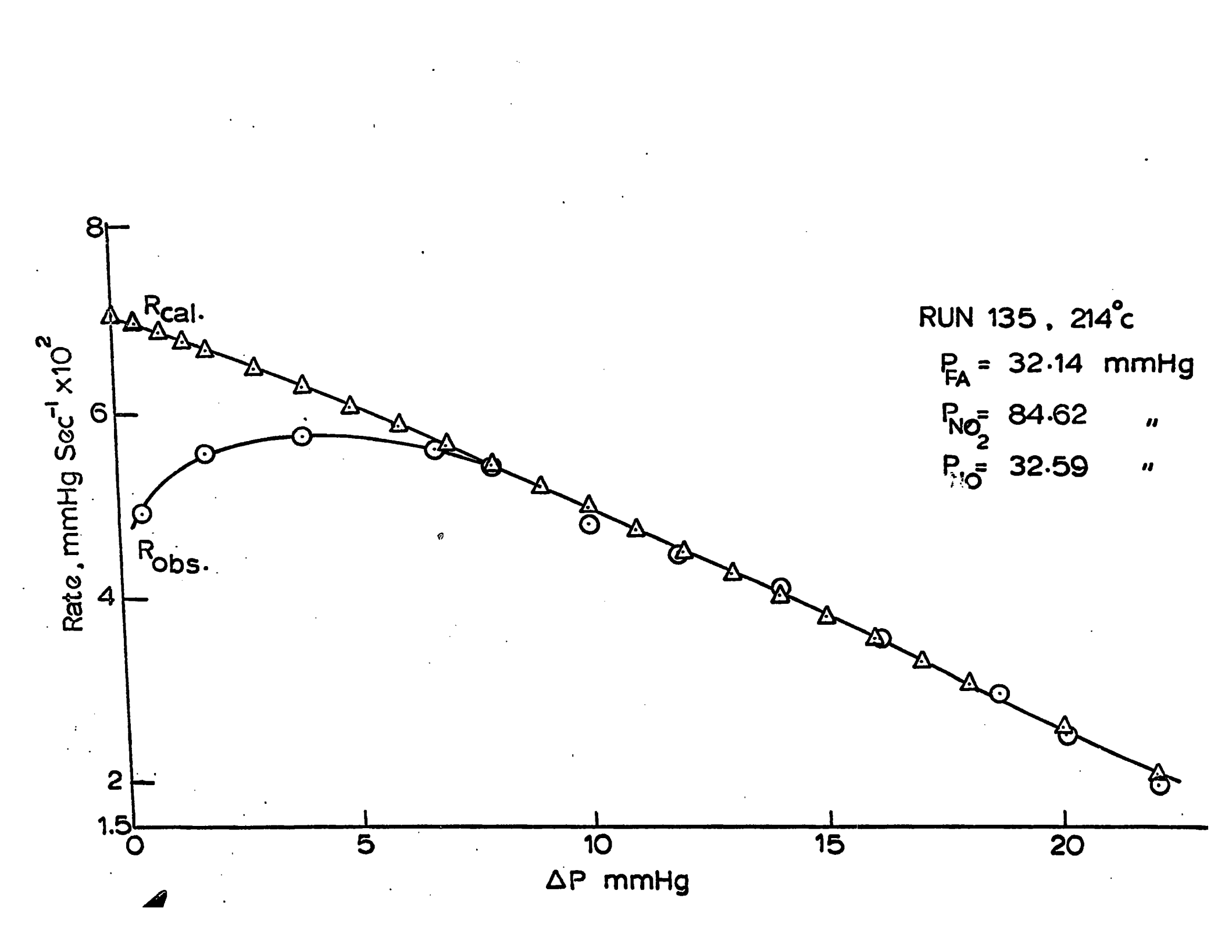
RUN 135 , 214°c
P_{FA} = 32.14 mmHg
P_{NO_2} = 84.62 "
P_{NO} = 32.59 "
$R_{cal.}$
$R_{obs.}$
Rate, mmHg Sec^{-1} x10^2
8
6
4
2
1.5
0
5
10
15
20
ΔP mmHg

FIGURE 44

Comparison of $R_{calc.}$ and $R_{obsd.}$ as functions of pressure change with moderate initial NO_2 pressure.

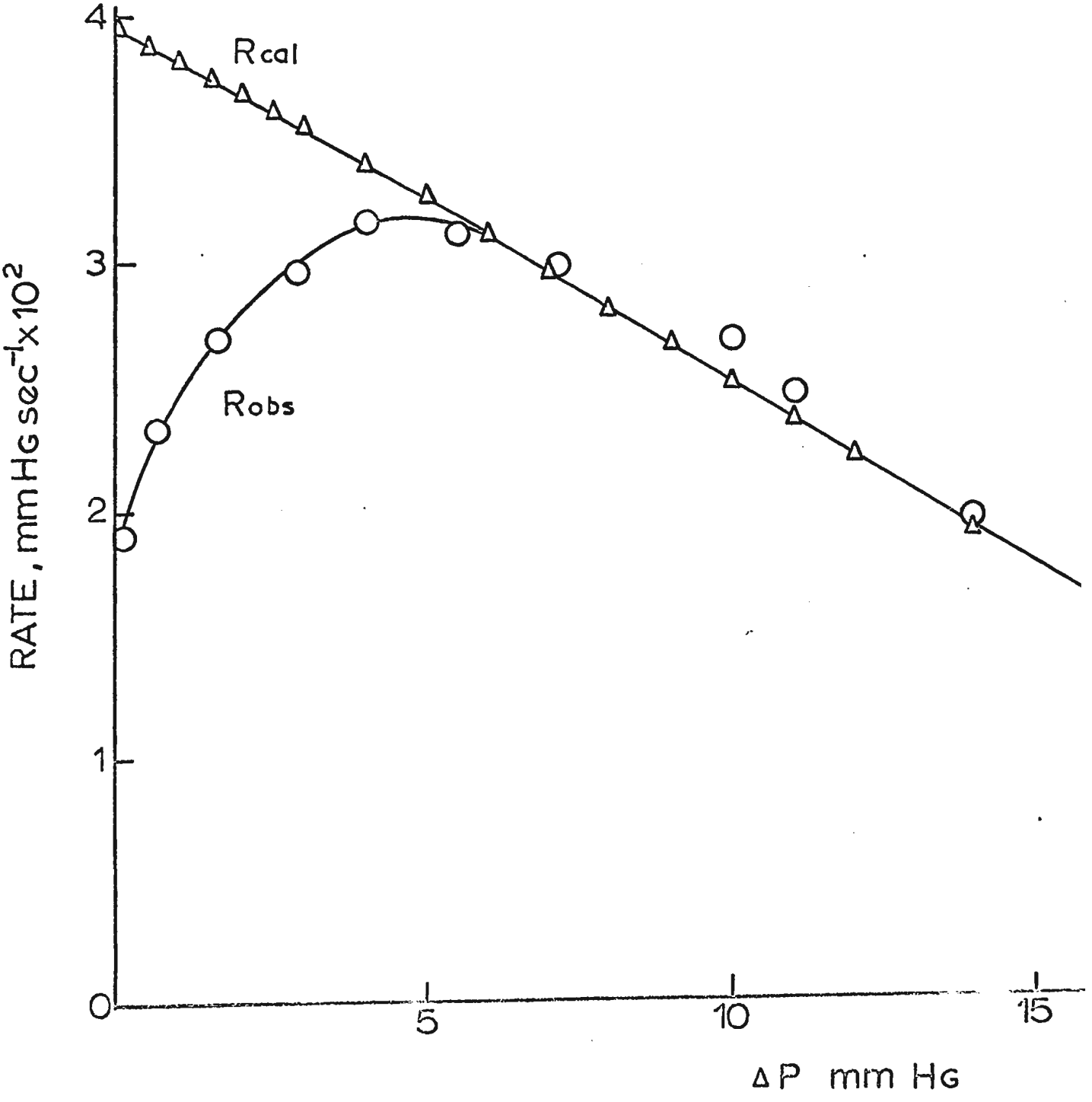
4
3
2
1
0
Rcal
Robs
RATE, mm Hg sec⁻¹ x 10²
5
10
15
ΔP mm Hg

RUN # 111

P_{FA} = 32.07 mm Hg

P_{NO_2} = 32.16 "

P_{NO} = 32.61 "

214°C

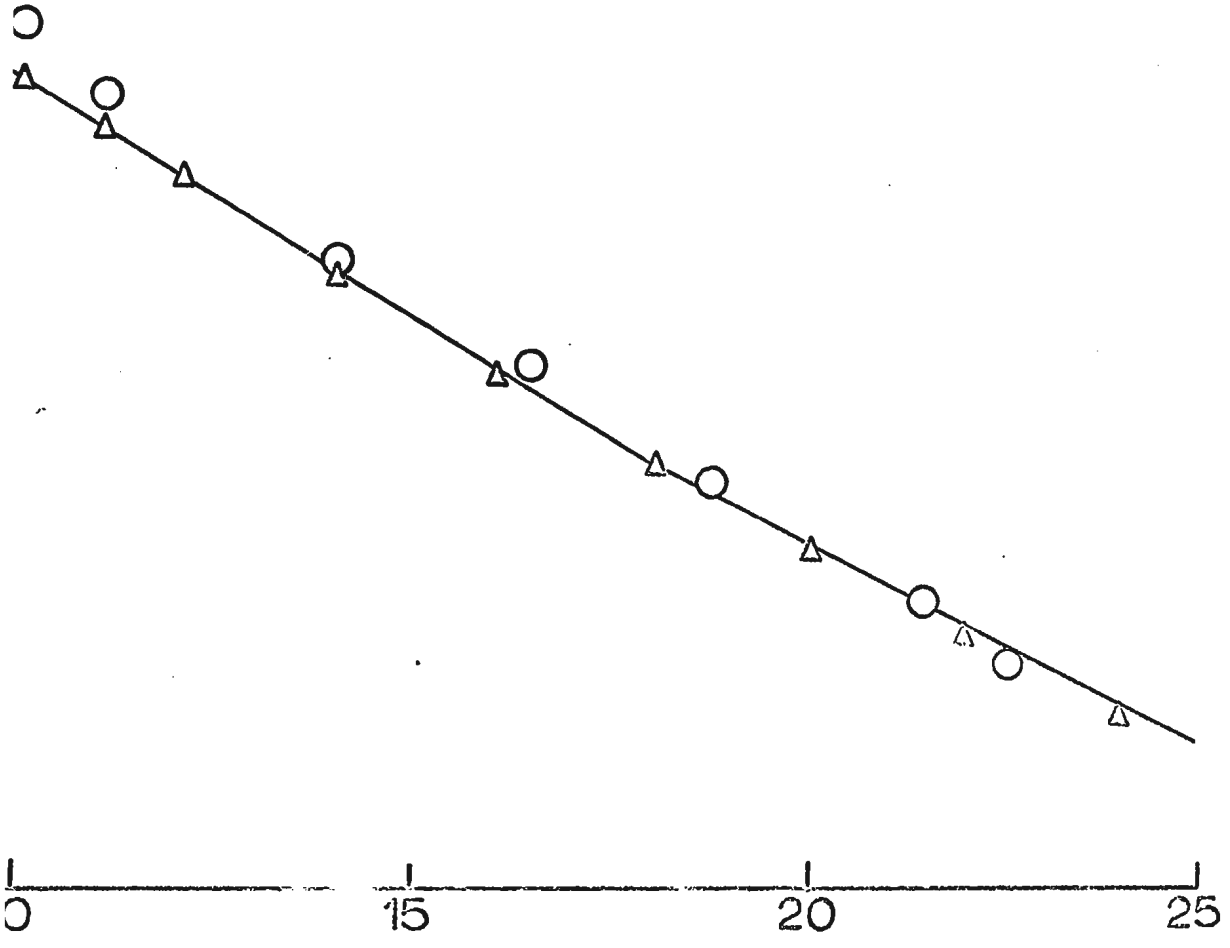

FIGURE 45

Comparison of $R_{calc.}$ and $R_{obsd.}$ as functions of pressure change with low initial NO_2 pressure.

FIGURE 46

Comparison of $R_{calc.}$ and $R_{obsd.}$ as functions of pressure change with high initial NO pressure.

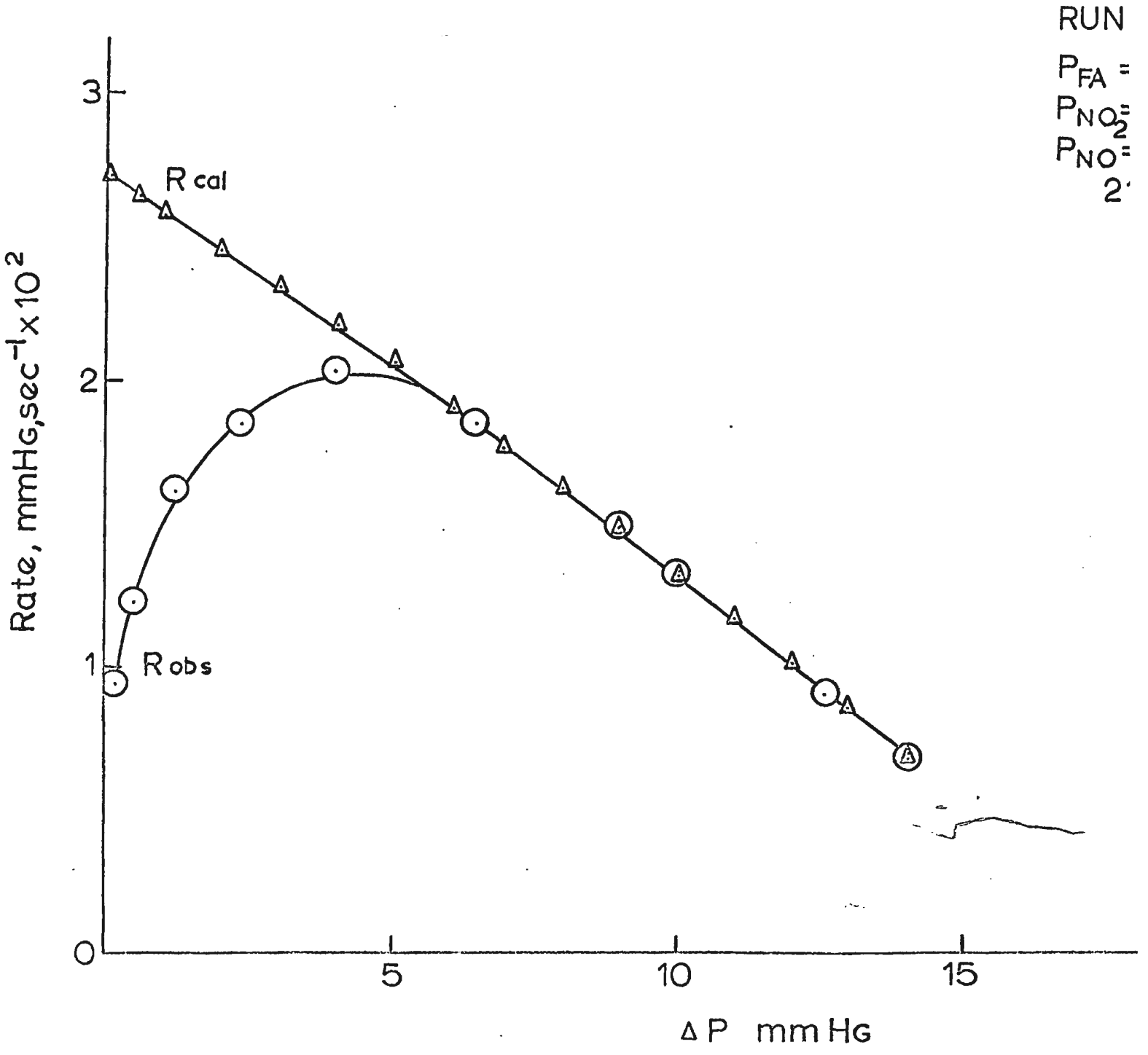
RUN
P_{FA} =
P_{NO_2} =
P_{NO} =
2·
R cal
R obs
Rate, mmHg, $sec^{-1} \times 10^2$
0
1
2
3
5
10
15
Δ P mm Hg

RUN # 112

P_{FA} = 32.10 mmH

P_{NO_2} = 15.99 "

P_{NO} = 32.67 "

214°C

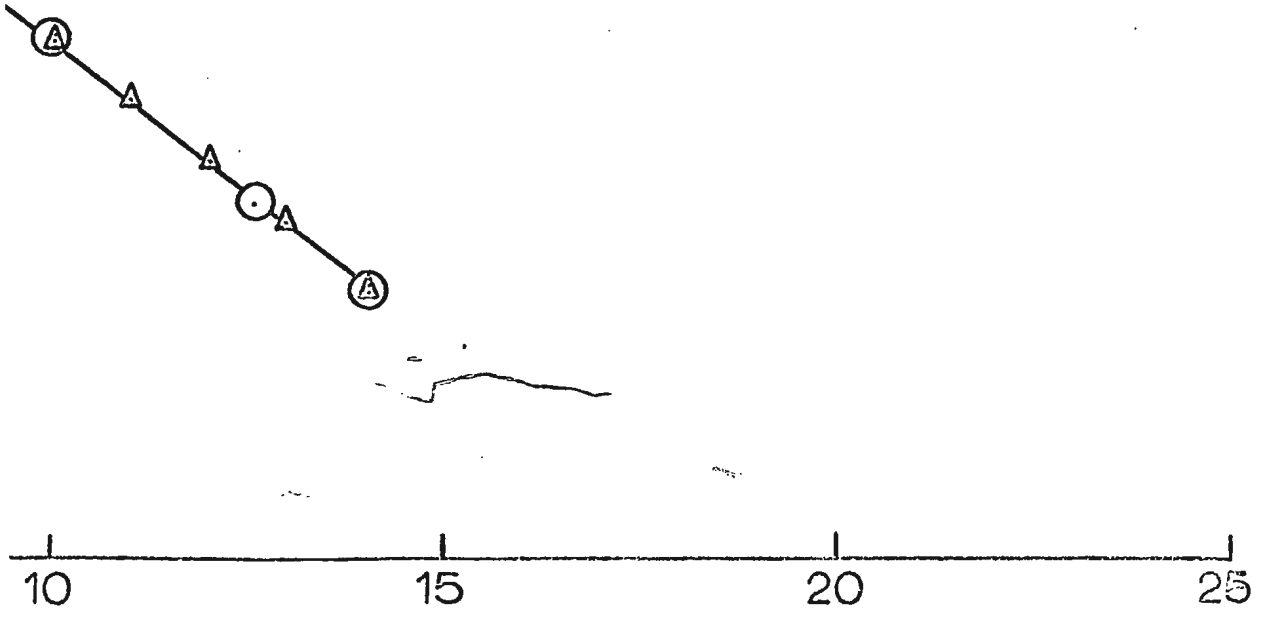

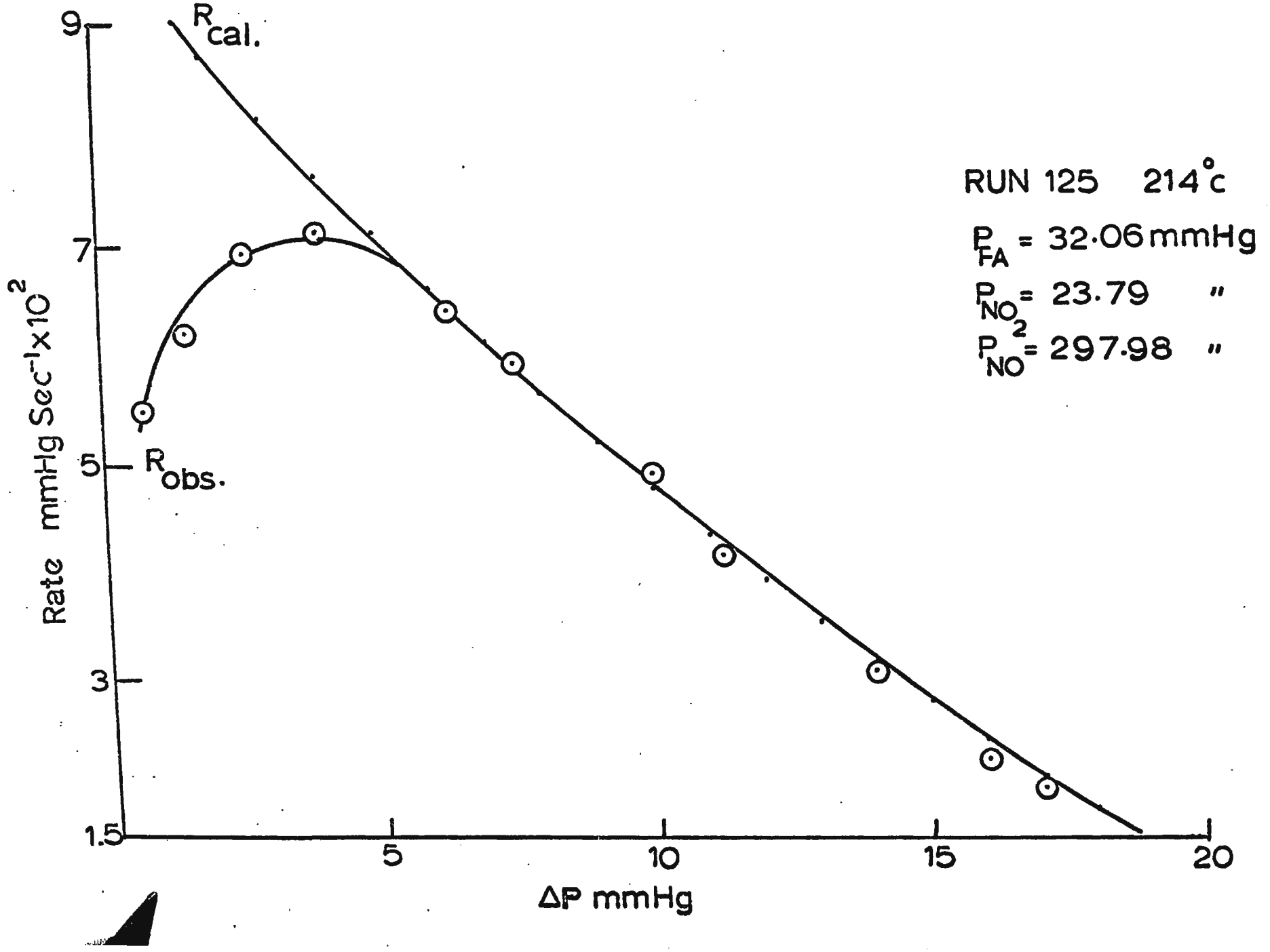
9
7
5
3
1.5
$R_{cal.}$
$R_{obs.}$
Rate mmHg $Sec^{-1} \times 10^2$
5
10
15
20
ΔP mmHg
RUN 125 214°c
P_{FA} = 32·06 mmHg
P_{NO_2} = 23.79 "
P_{NO} = 297.98 "

FIGURE 47

Comparison of $R_{calc.}$ and $R_{obsd.}$ as functions of pressure change with moderate initial NO pressure.

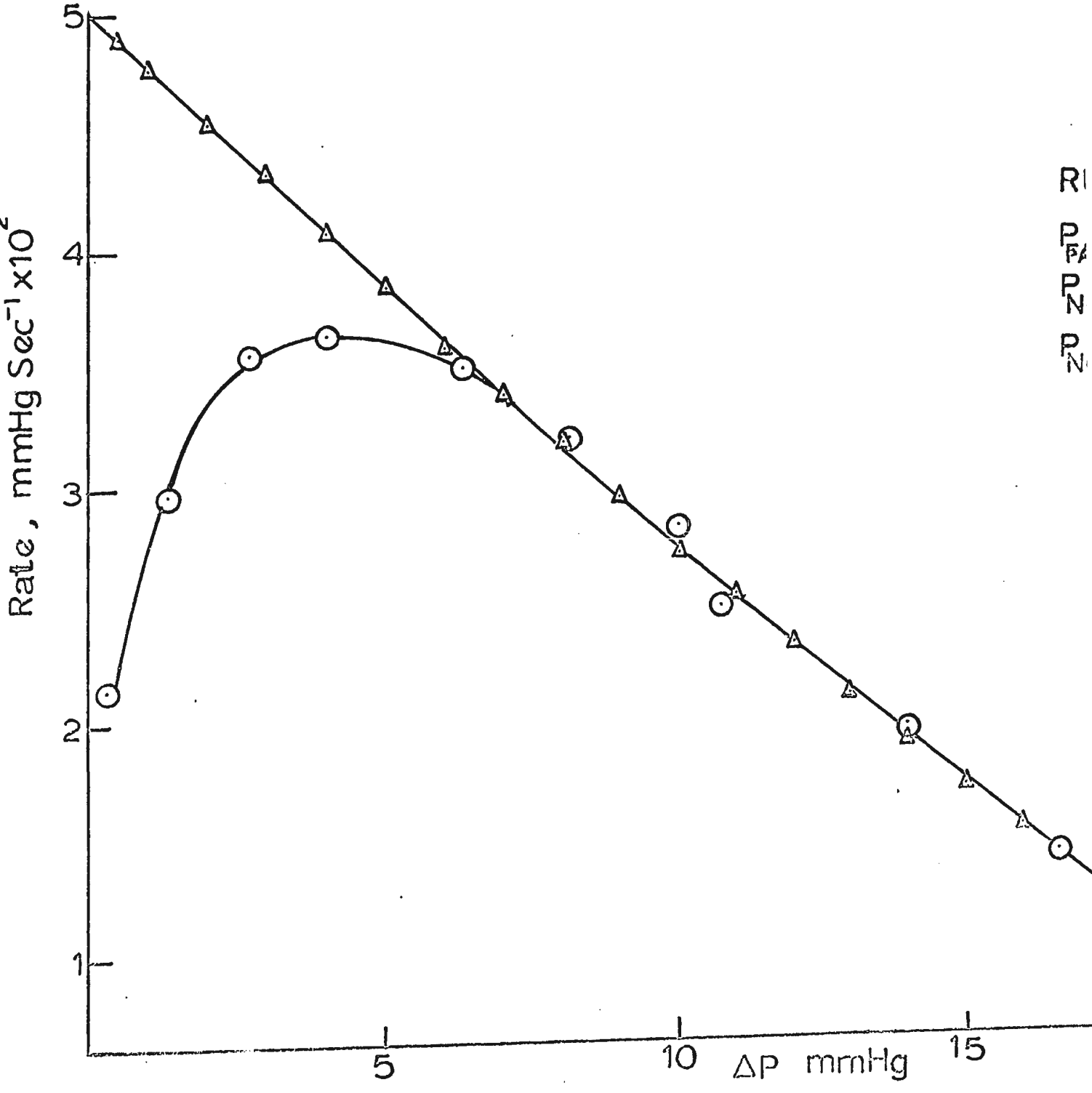
Rate, mmHg Sec^{-1} x10^2
5
4
3
2
1
5
10
15
ΔP mmHg

RUN # 106 214°c

P_{FA} = 32.18 mmHg

P_{NO_2} = 23.84 "

P_{NO} = 63.56 "

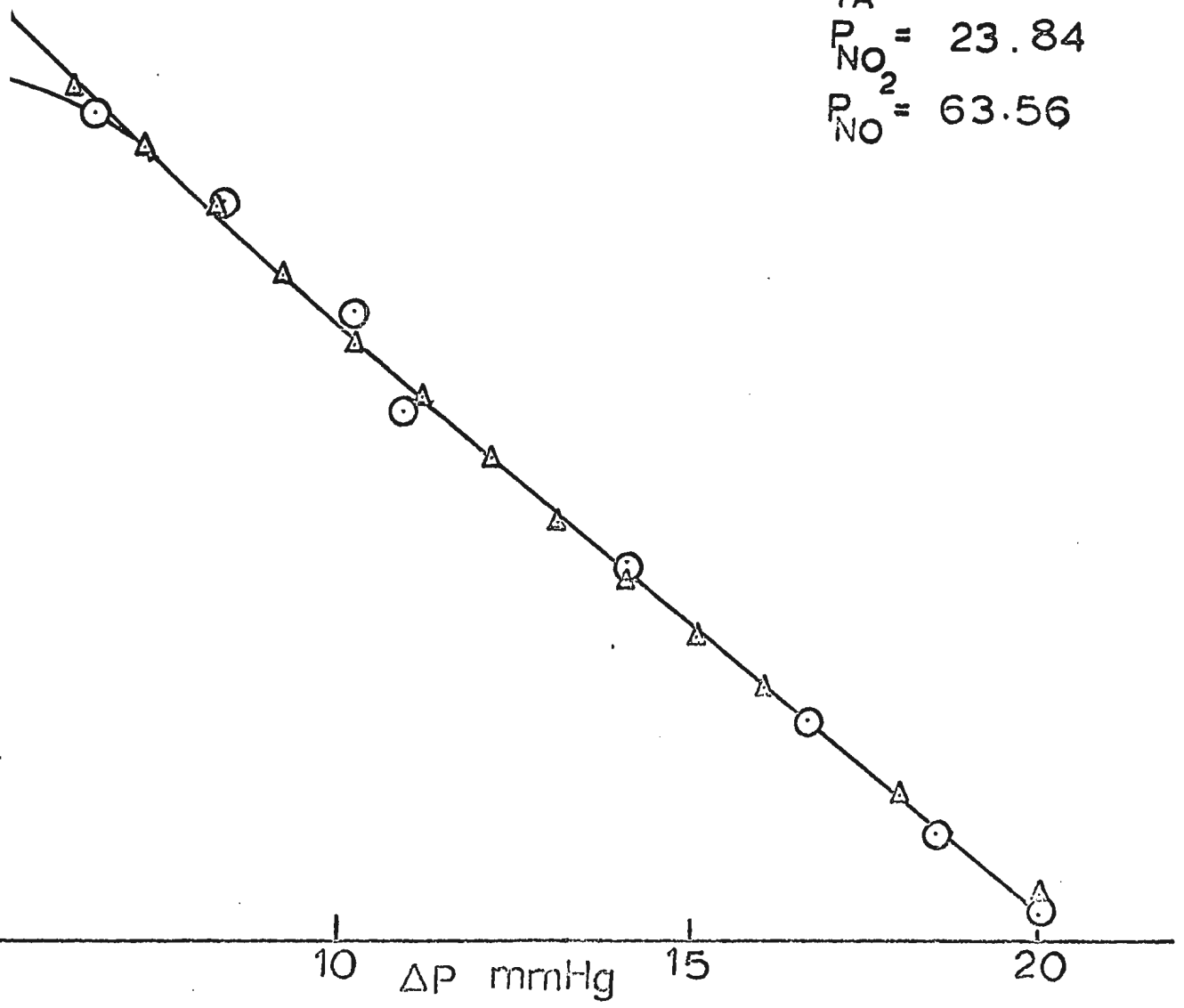

FIGURE 48

Comparison of $R_{calc.}$ and $R_{obsd.}$ as functions of pressure change with low initial NO pressure.

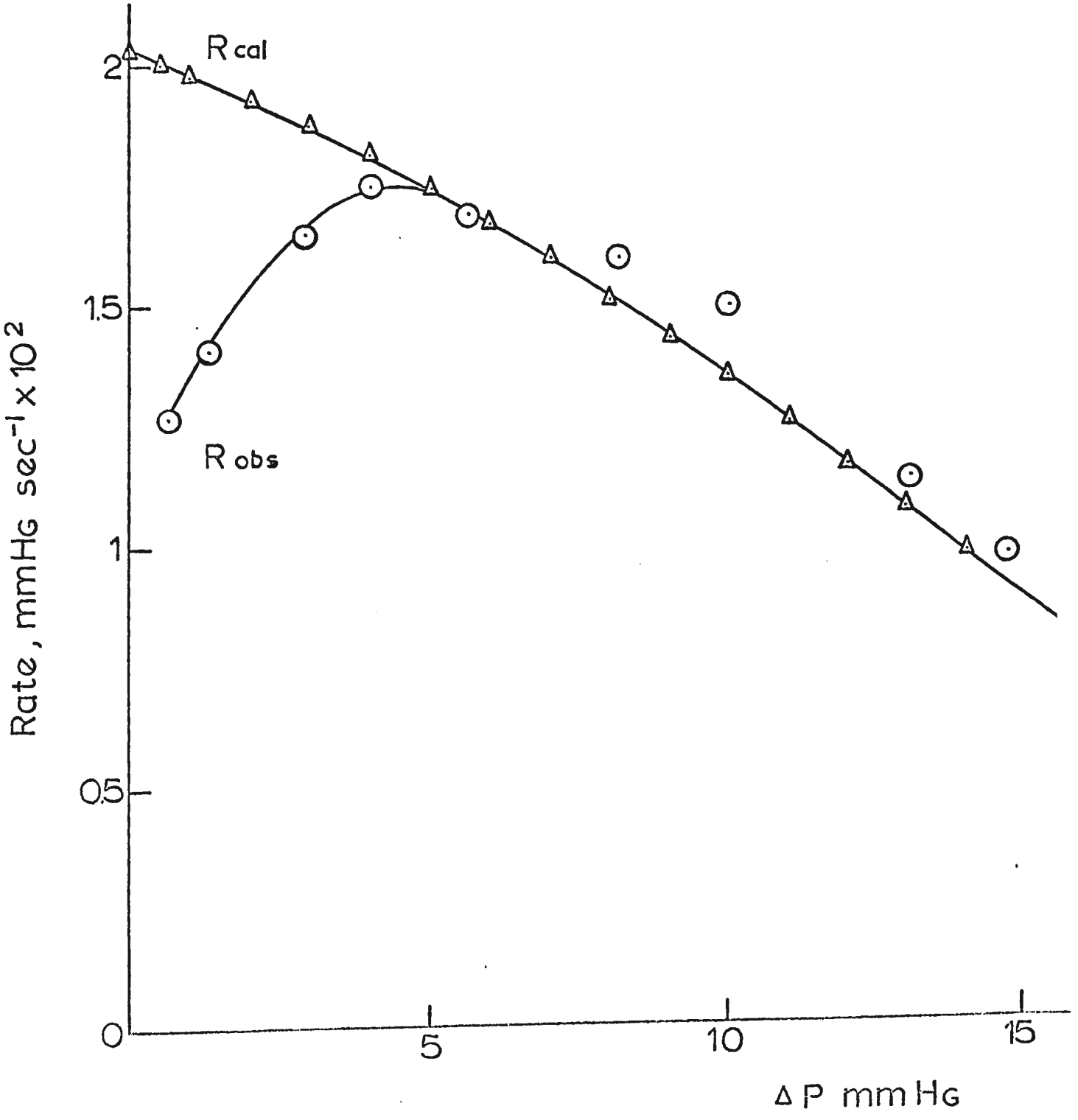
R cal
R obs
2
1.5
1
0.5
0
5
10
15
Rate, mmHg sec⁻¹ x 10²
ΔP mmHg

RUN #107

P_{FA} = 32.09 mmHg

P_{NO_2} = 22.81 "

P_{NO} = 14.77 "

214°C

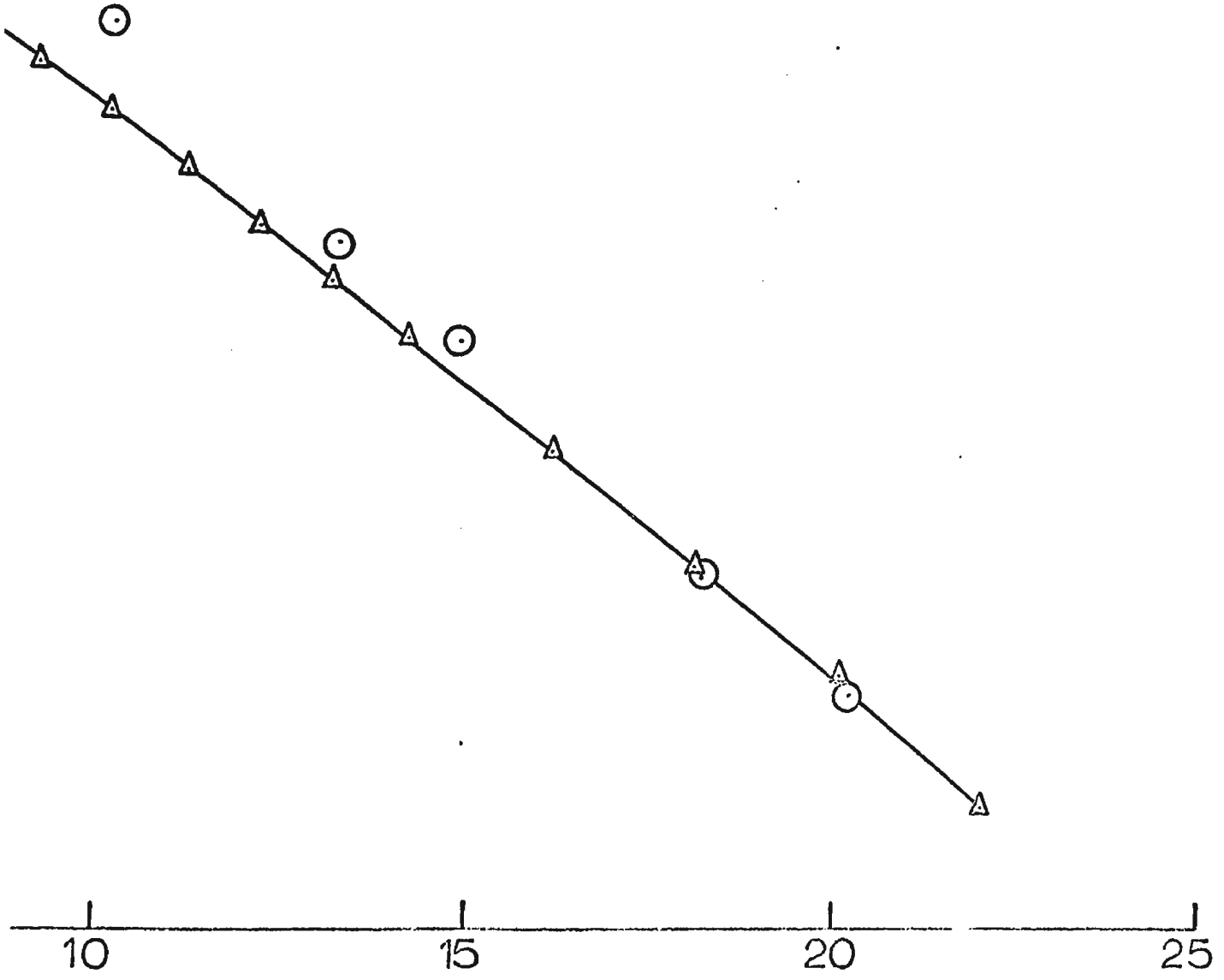

FIGURE 49

Comparison of $R_{calc.}$ and $R_{obsd.}$ as functions of pressure change with high initial NO pressure at 182°C.

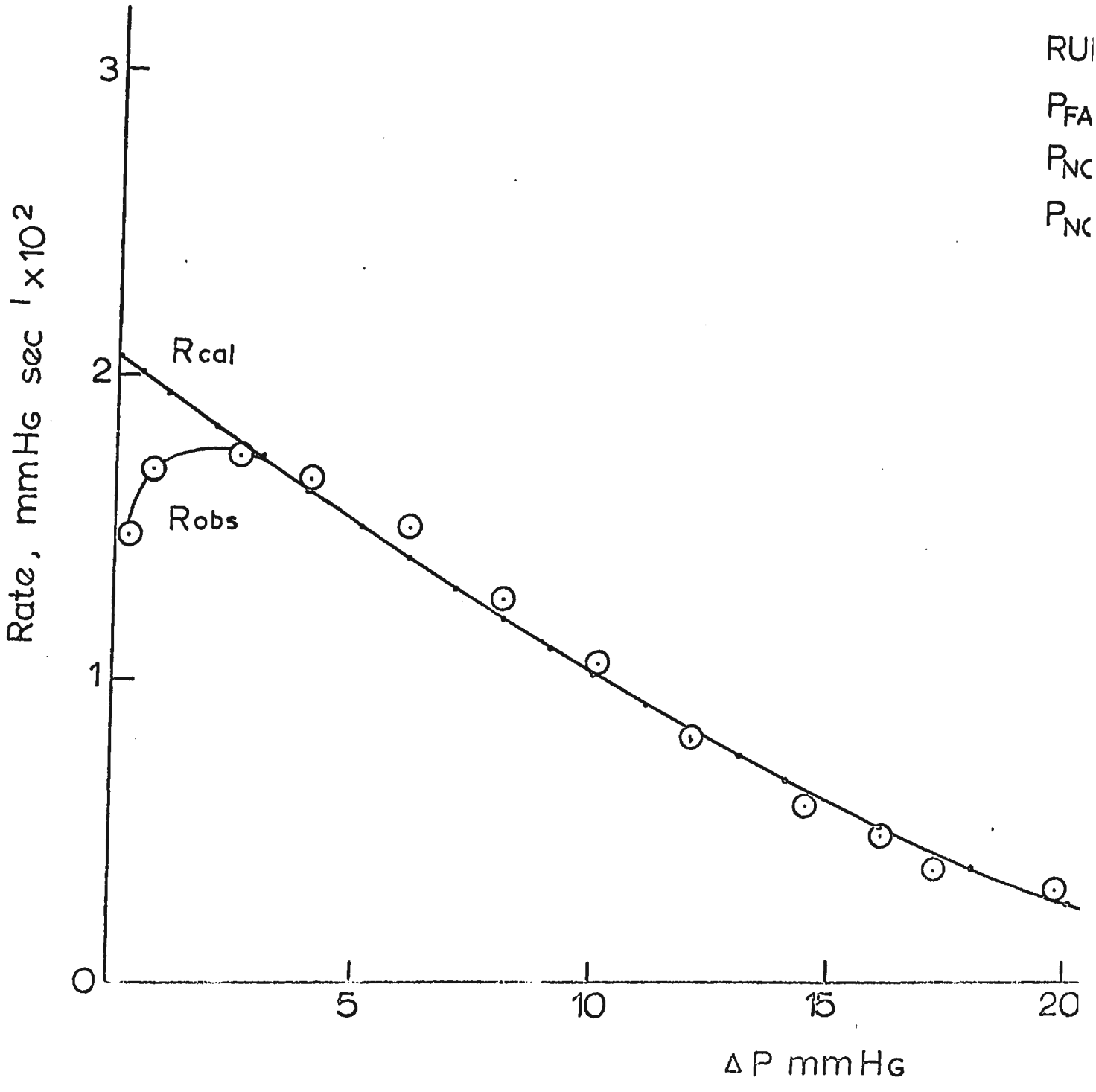

RU

P_{FA}

P_{NC}

P_{NC}

RUN # 40

P_{FA} = 29.02 mm Hg

P_{NO_2} = 28.15

P_{NO} = 88.29

182 °C

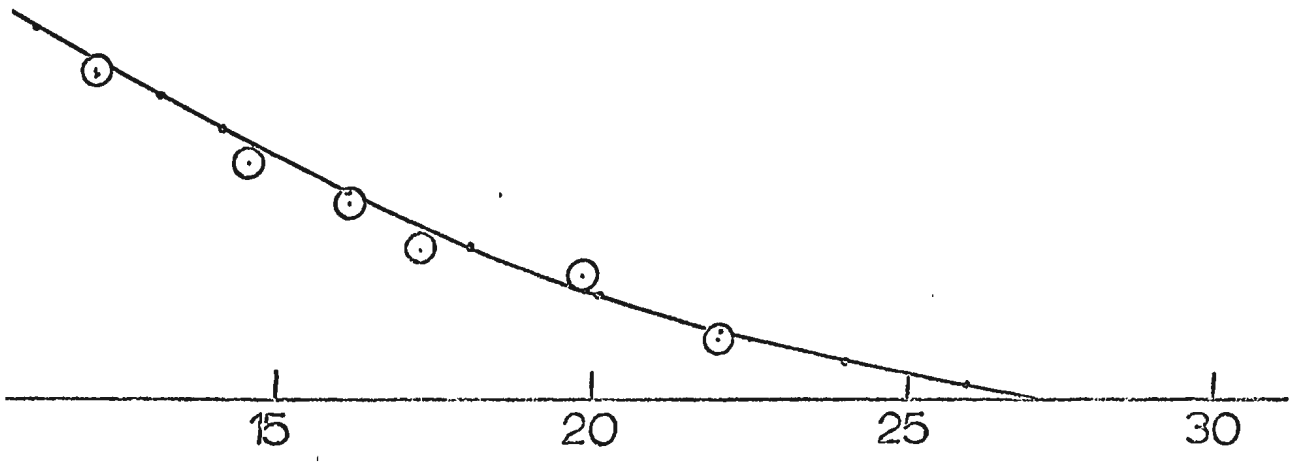

FIGURE 50

Comparison of $R_{calc.}$ and $R_{obsd.}$ as functions of pressure change with moderate initial pressures of HCOOH, NO, and NO_2 at 182°C.

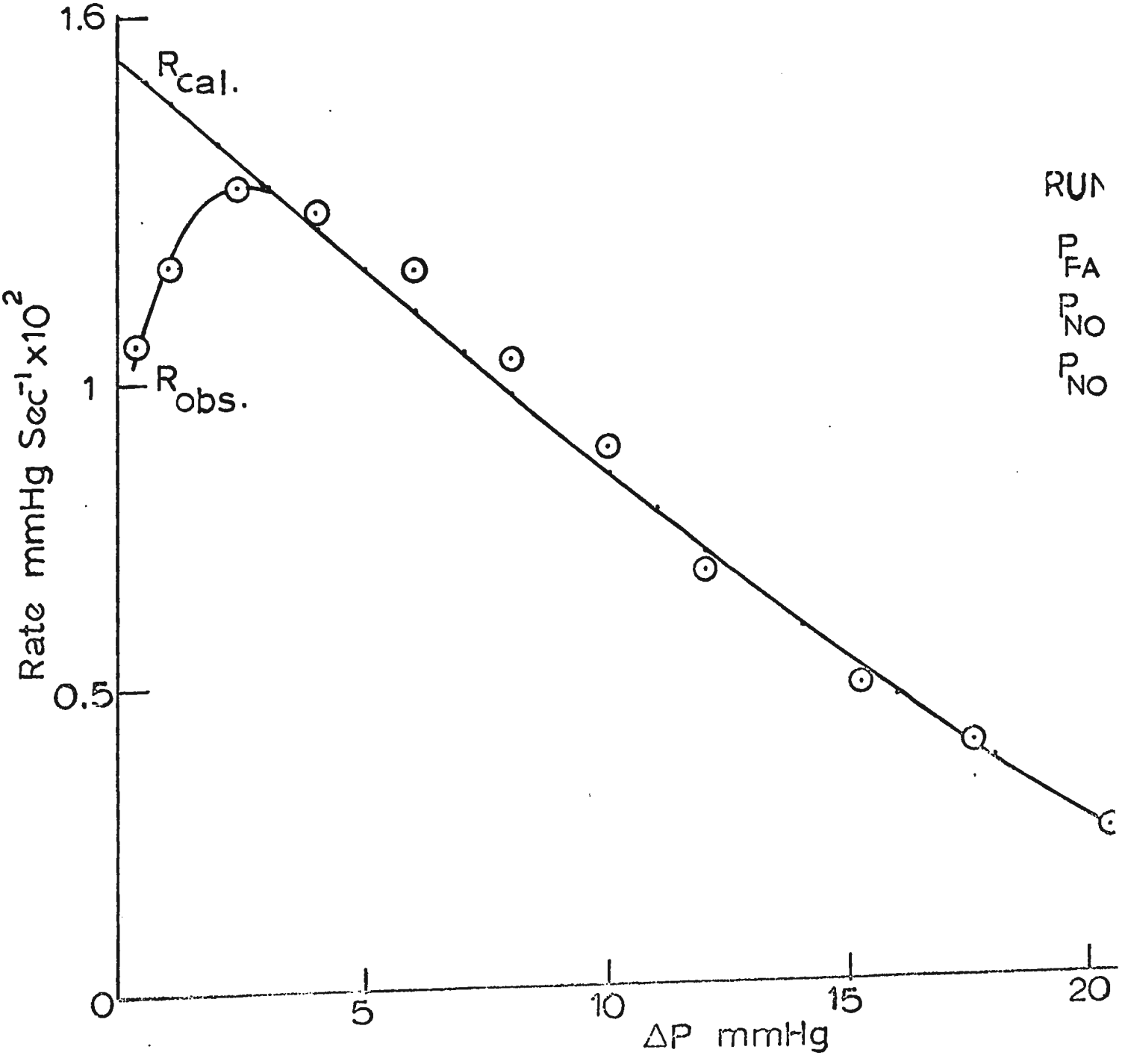
1.6
1
0.5
0
$R_{cal.}$
$R_{obs.}$
Rate mmHg $Sec^{-1} x10^2$
5
10
15
20
ΔP mmHg
RUN
P_{FA}
P_{NO}
P_{NO}

RUN 42 182°c

P_{FA} = 29.08 mmHg

P_{NO_2} = 30.83 "

P_{NO} = 39.49 "

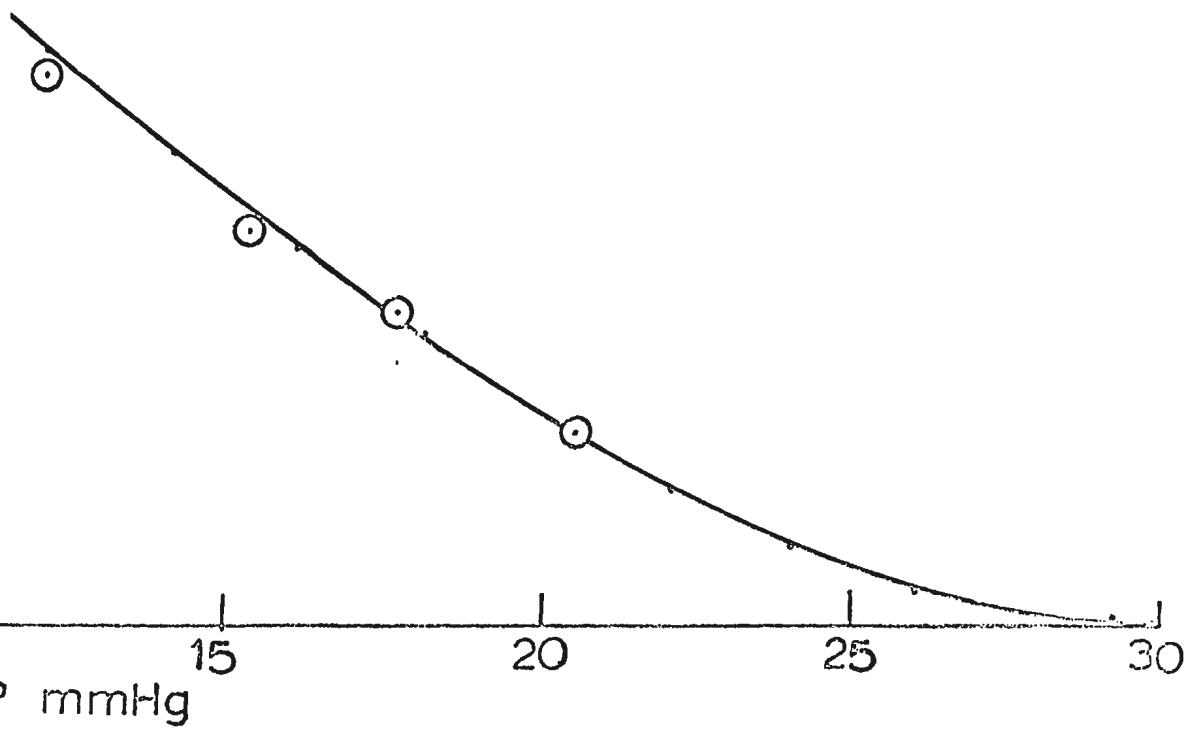

FIGURE 51

Comparison of $R_{calc.}$ and $R_{obsd.}$ as functions of pressure change with low initial NO pressure at 182°C.

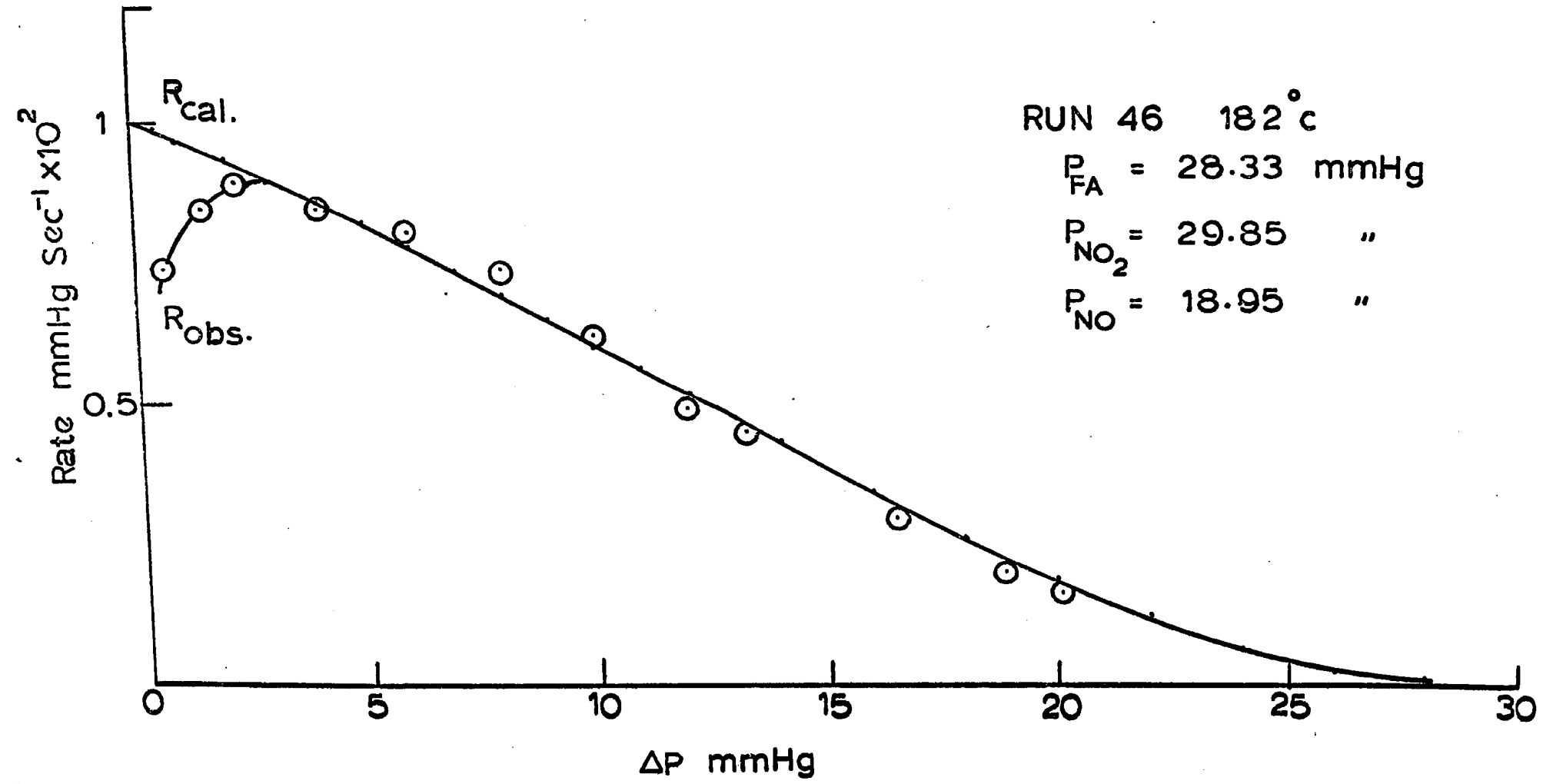
RUN 46 182°c
P_{FA} = 28.33 mmHg
P_{NO_2} = 29.85 "
P_{NO} = 18.95 "
$R_{cal.}$
$R_{obs.}$
Rate mmHg $Sec^{-1} \times 10^2$
1
0.5
0
5
10
15
20
25
30
ΔP mmHg

BIBLIOGRAPHY

1. F.H. Pollard and K.A. Holbrook. Trans. Faraday Soc., 53, 468 (1957).

2. B.G. Gowenlock and G. Porter. In Progress in Reaction Kinetics (Editor G. Porter), Vol. 3, Pergamon Press, Oxford, 1965, p 171.

3. D. Barton and P.E. Yankwich. J. Phys. Chem. 71, 3455 (1967).

4. A.S. Coolidge. J. Amer Chem. Soc., 50, 2166 (1928).

5. R.H. Pierson, A.N. Fletcher, and E.S. Clairgantz. J. Anal. Chem. 28, pp 1229 and 1234 (1956).

6. R.E. Nightingale, A.R. Downie, D.L. Rotenberg, B. Crawford Jr., and R.A. Ogg Jr. J. Phys. Chem., 58, 1047 (1954).

7. E.E. Hughes. J. Chem. Phys. 35, 1531 (1961).

8. J.G. Hooley. Can. J. Chem. 35, 1414 (1957).

9. Wm. F. Roeser and S.T. Longberger. Methods of Testing Thermocouples and Thermocouple Materials. N.B.S. Circular 590.

10. Handbook of Chemistry and Physics. The Chemical Rubber Co., 1964-65, pp E48 and E49.

11. V.N. Kondrat'ev. Chemical Kinetics of Gas Reactions. Pergamon Press, London, 1964, p 38.

12. F.H. Pollard, and R.M.H. Wyatt. Trans. Faraday Soc., 45, 760, (1949).

13. P.G. Blake and C.N. Hinshelwood. Proc. Roy. Soc. A255, 444-455, 1960.

14. S.W. Watson. M.Sc. Thesis, Michigan State University, 1967.

15. D. Barton and P.E. Yankwich, unpublished report.

16. J.H. Thomas. Trans. Faraday Soc., 49, 630 (1953).

17. P.G. Ashmore and B.P. Levitt. Trans. Faraday Soc., 53, 945 (1957).

18. Z.G. Szabo. Catalysis Reviews 2(2), 221-248 (1968).

19. P.G. Ashmore. Catalysis and Inhibition of Chemical Reactions, Butterworths, London, 1963. p 213.

APPENDIX I

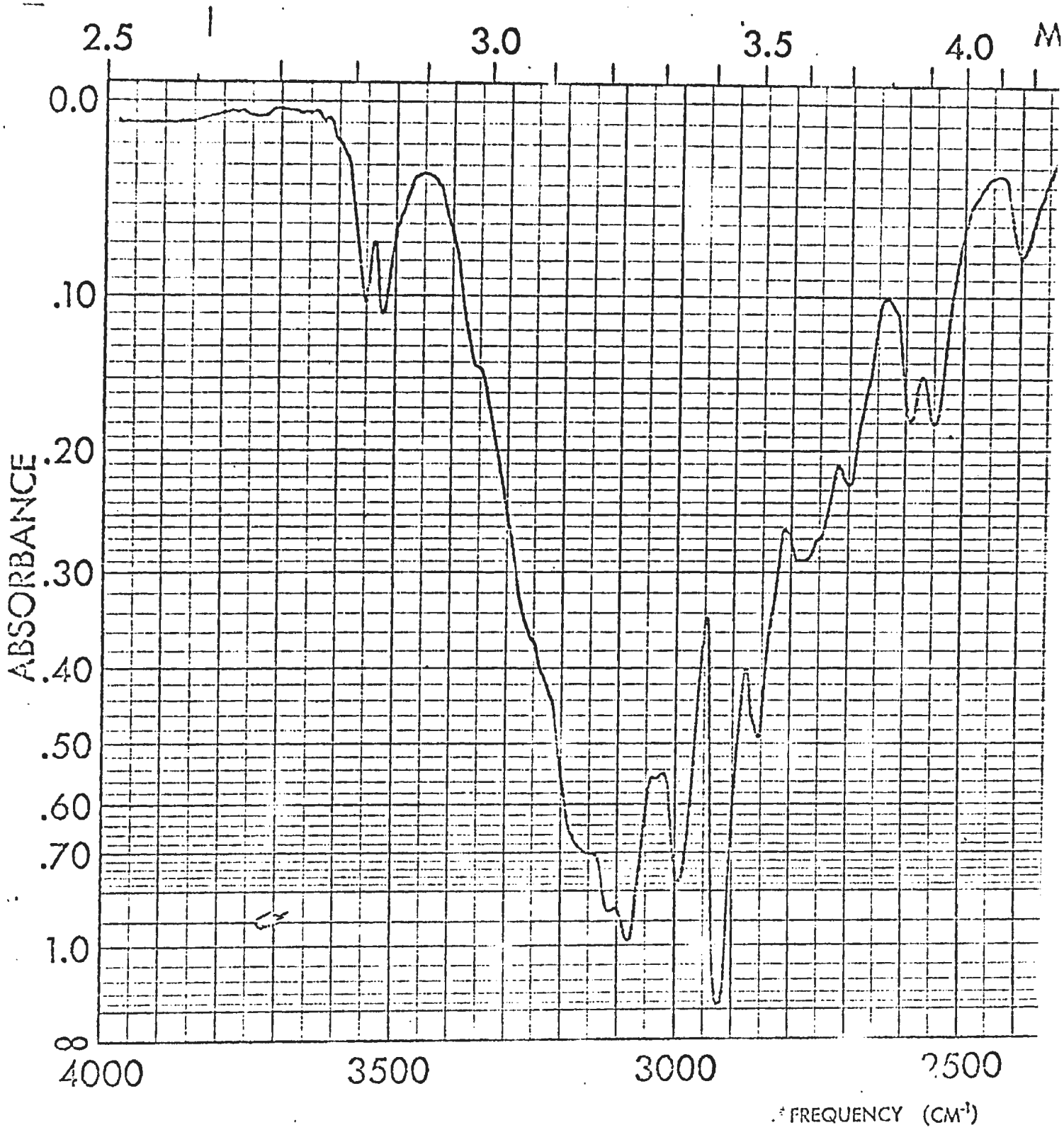

SAMPLE [illegible]	CURVE NO.
[illegible]	CONC.
ORIGIN	CELL PATH
SOLVENT	REFERENCE

PART NO. 237-1032 [illegible]©

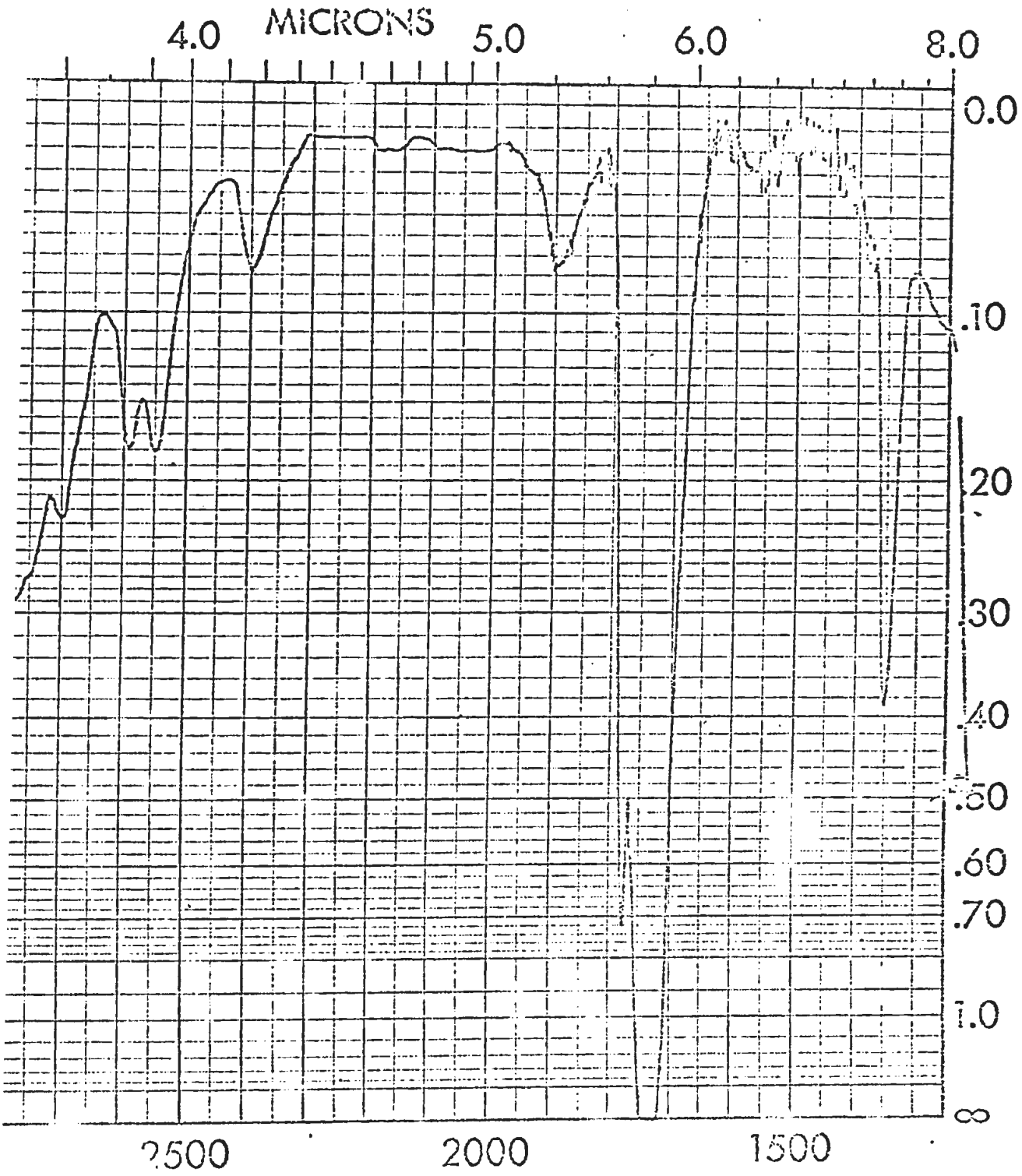

FREQUENCY (CM^{-1})

	SCAN SPEED	OPERATOR
	SLIT	DATE
	REMARKS	

PERKIN-ELMER

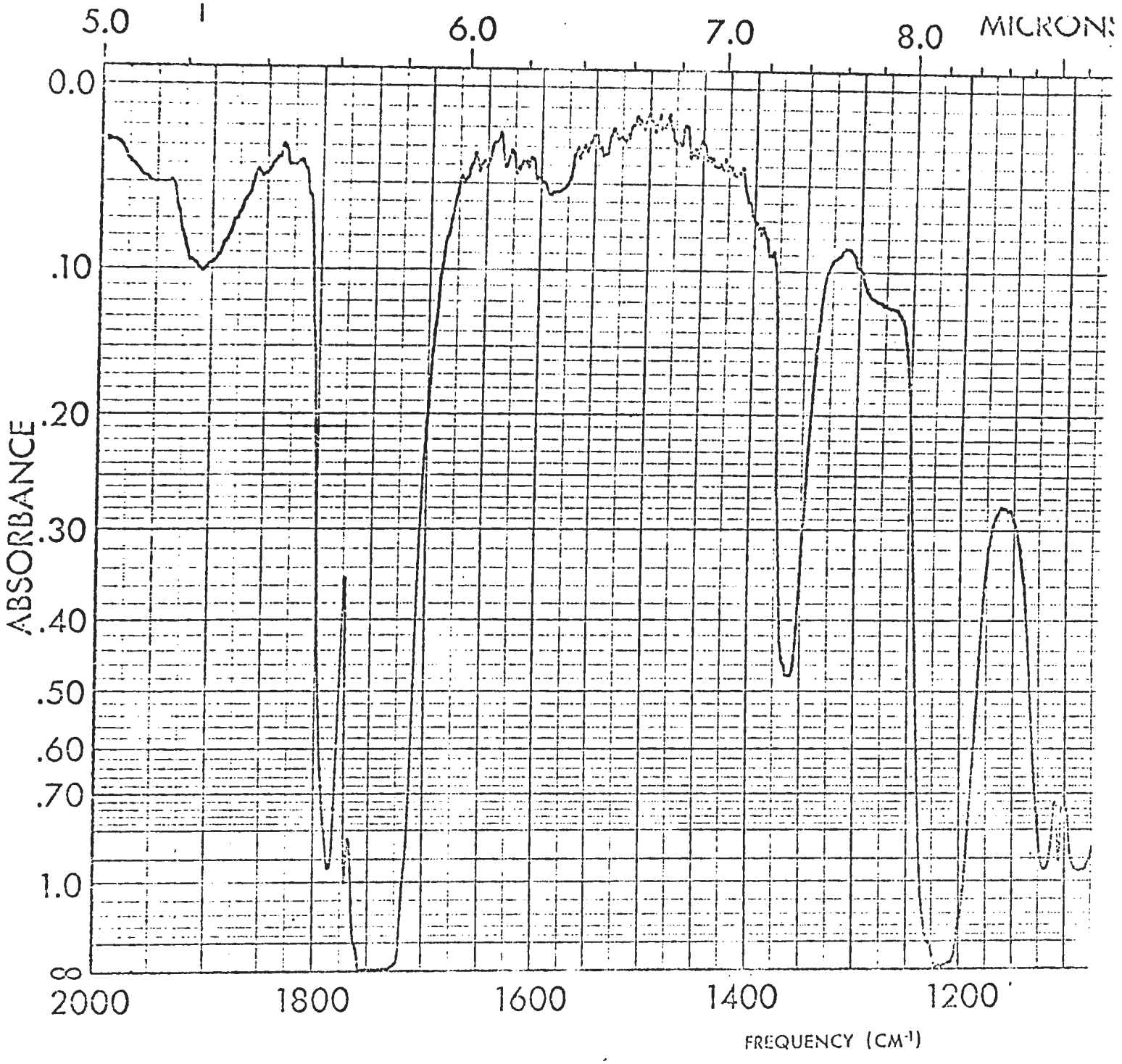

SAMPLE	CURVE NO.
	CONC.
ORIGIN	CELL PATH
SOLVENT	REFERENCE

PART NO. 237-1033 '74 ®

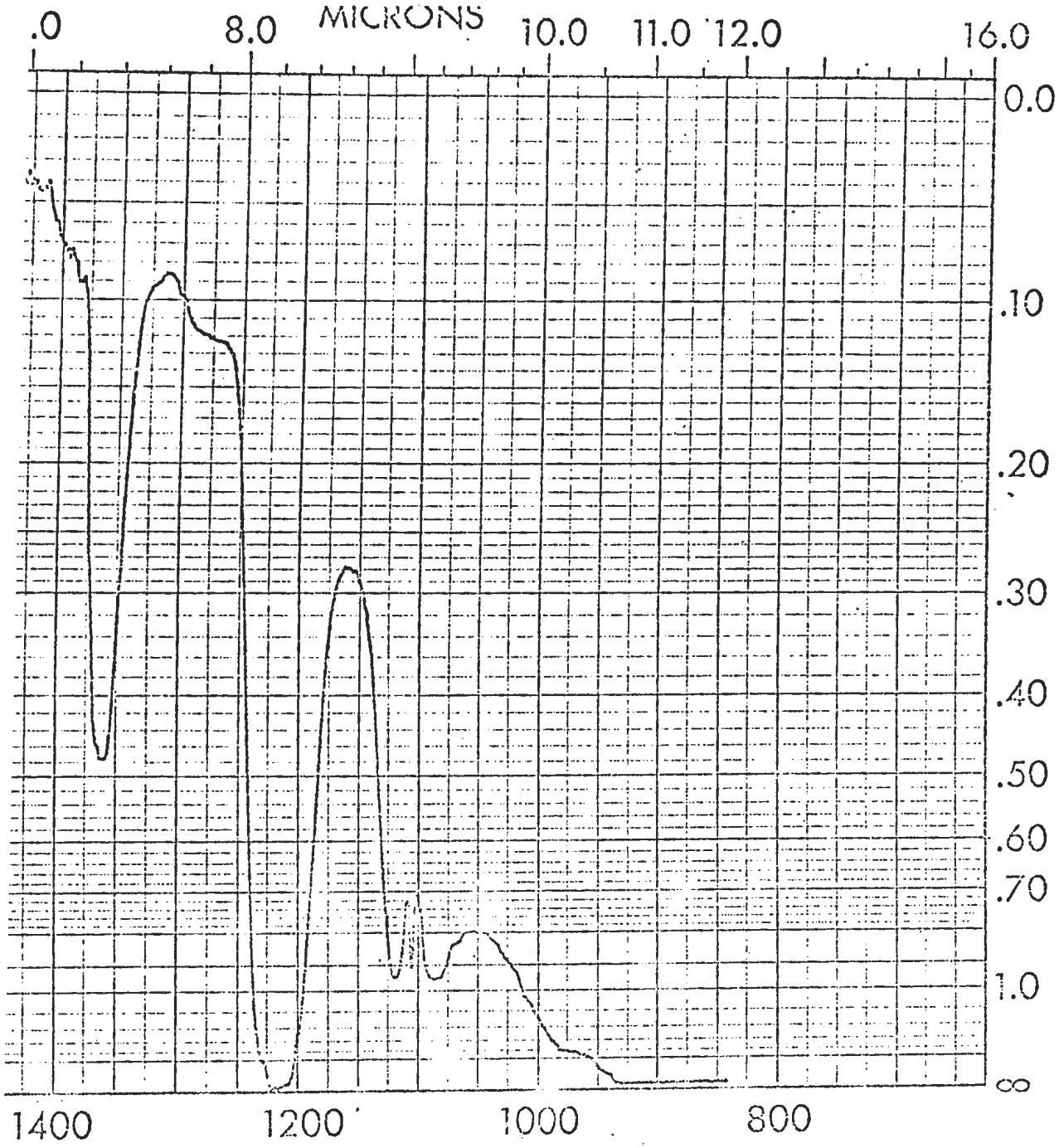

	SCAN SPEED	OPERATOR
	SLIT	DATE
	REMARKS	

PERKIN-ELMER

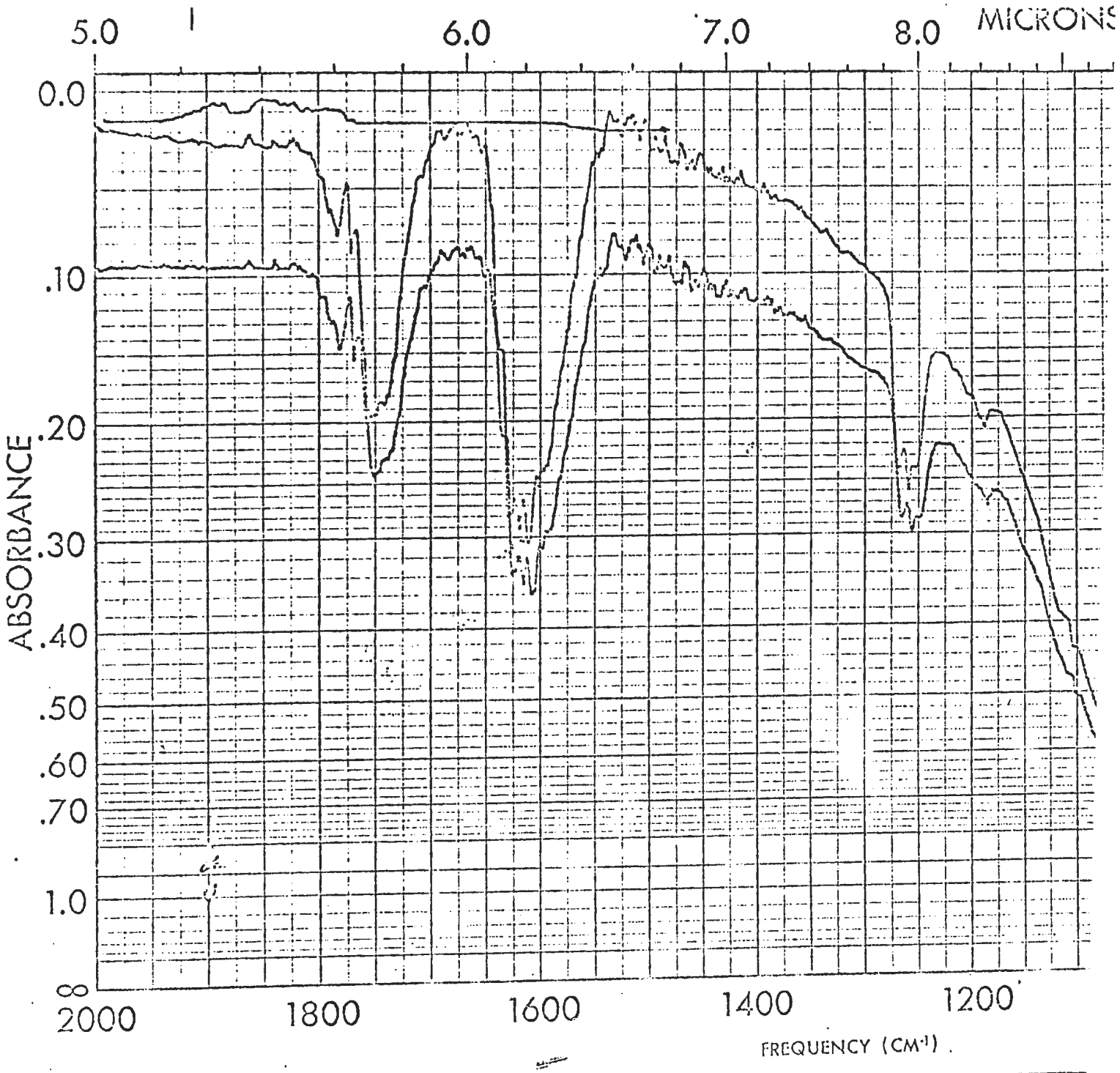

SAMPLE	CURVE NO.
ORIGIN	CONC.
SOLVENT	CELL PATH
	REFERENCE

PART NO. 237-1033

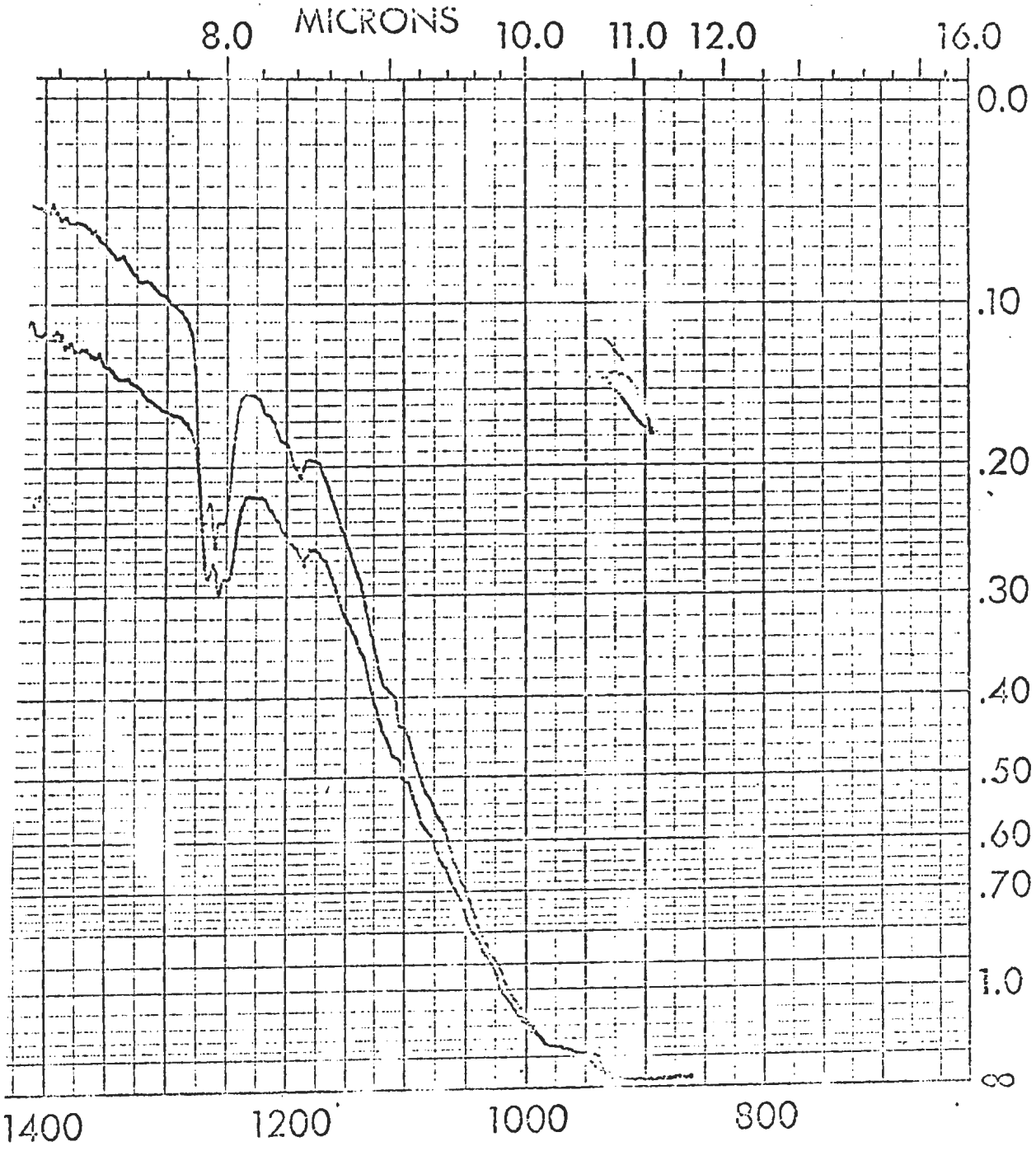

SCAN SPEED

OPERATOR

SLIT

DATE

REMARKS

PERKIN-ELMER

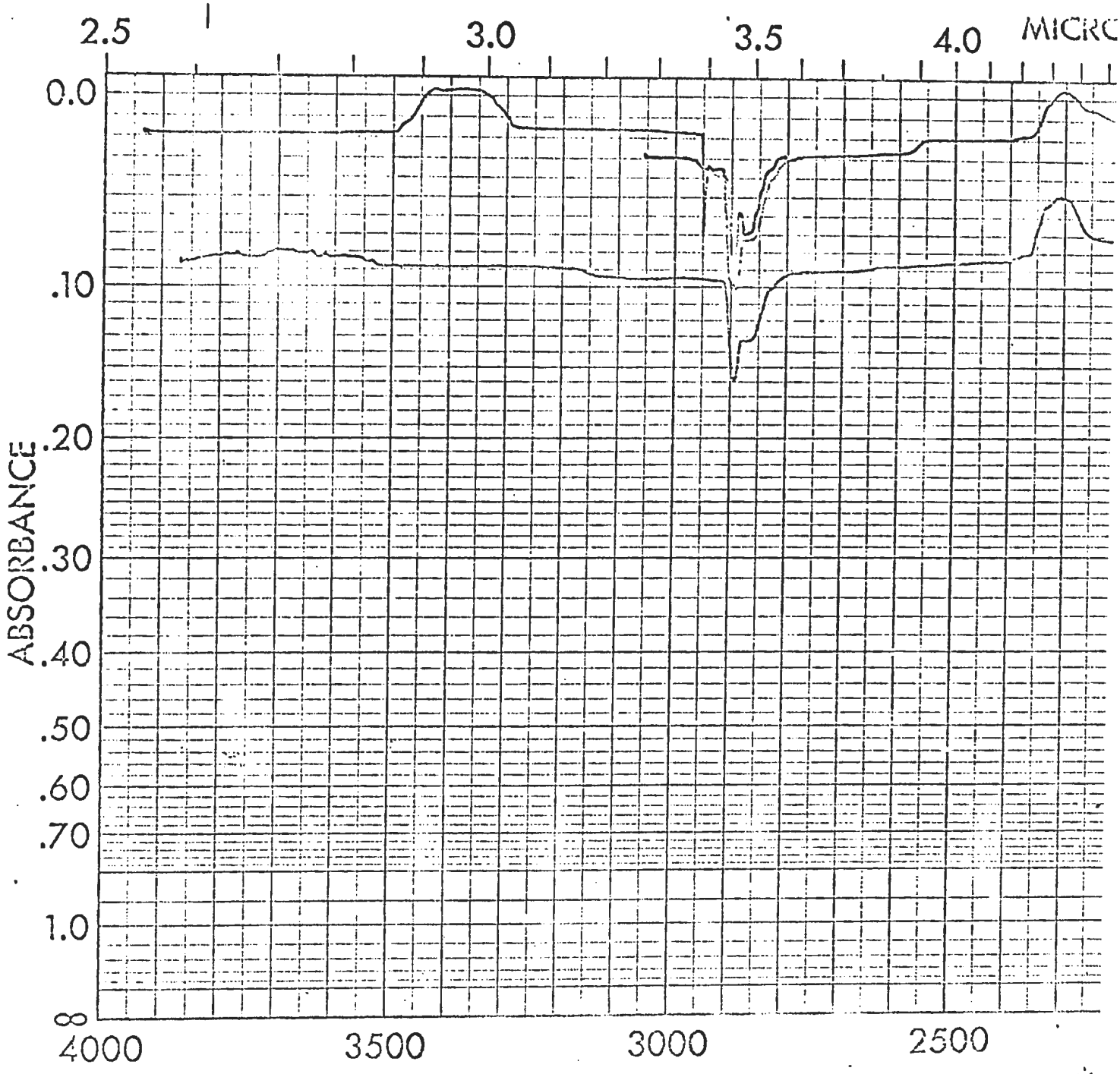

SAMPLE	CURVE NO.
ORIGIN	CONC.
SOLVENT	CELL, PATH
	REFERENCE

PART NO. 237-1032

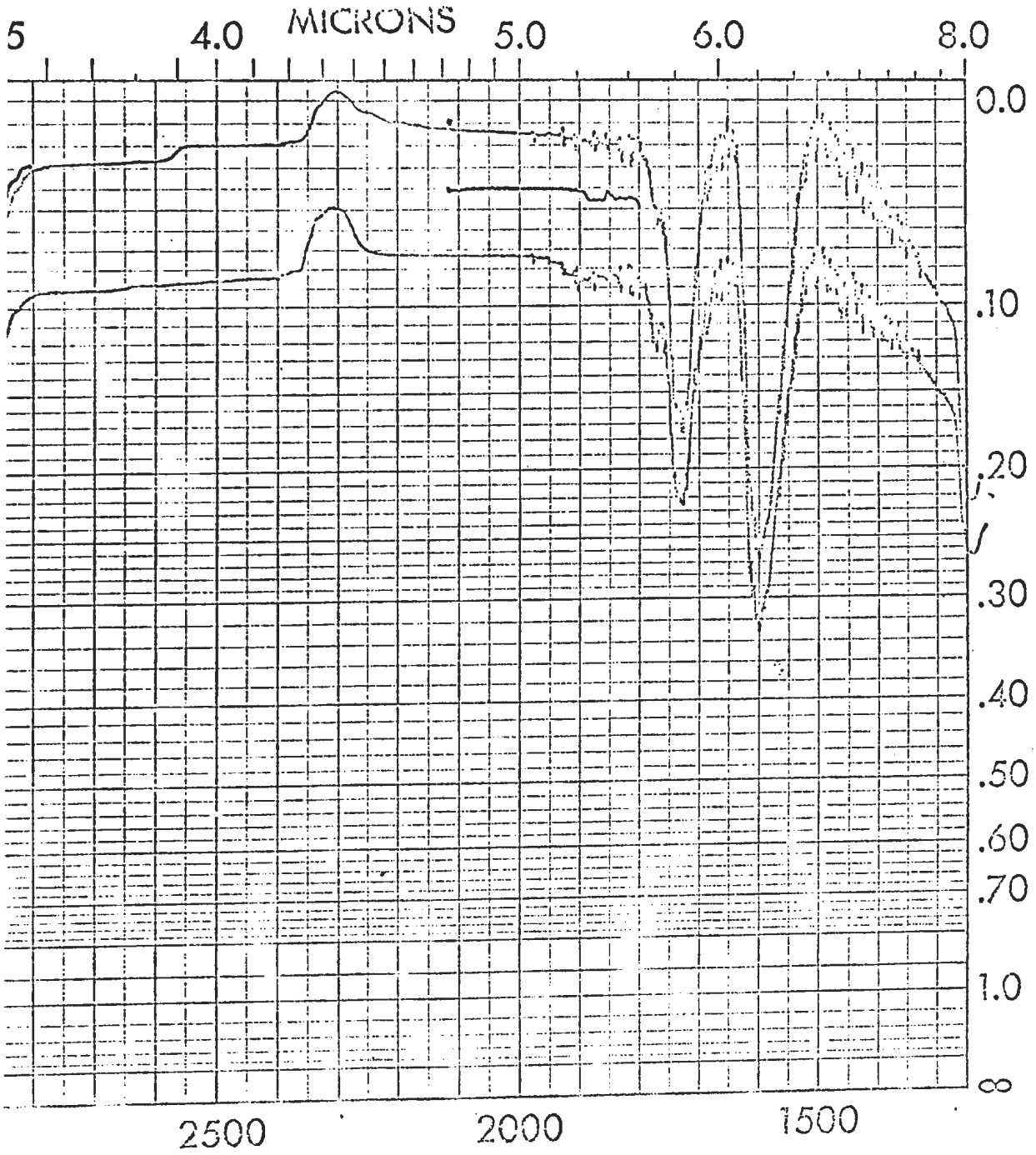

SCAN SPEED

SLIT

OPERATOR

DATE

REMARKS

PERKIN-ELMER

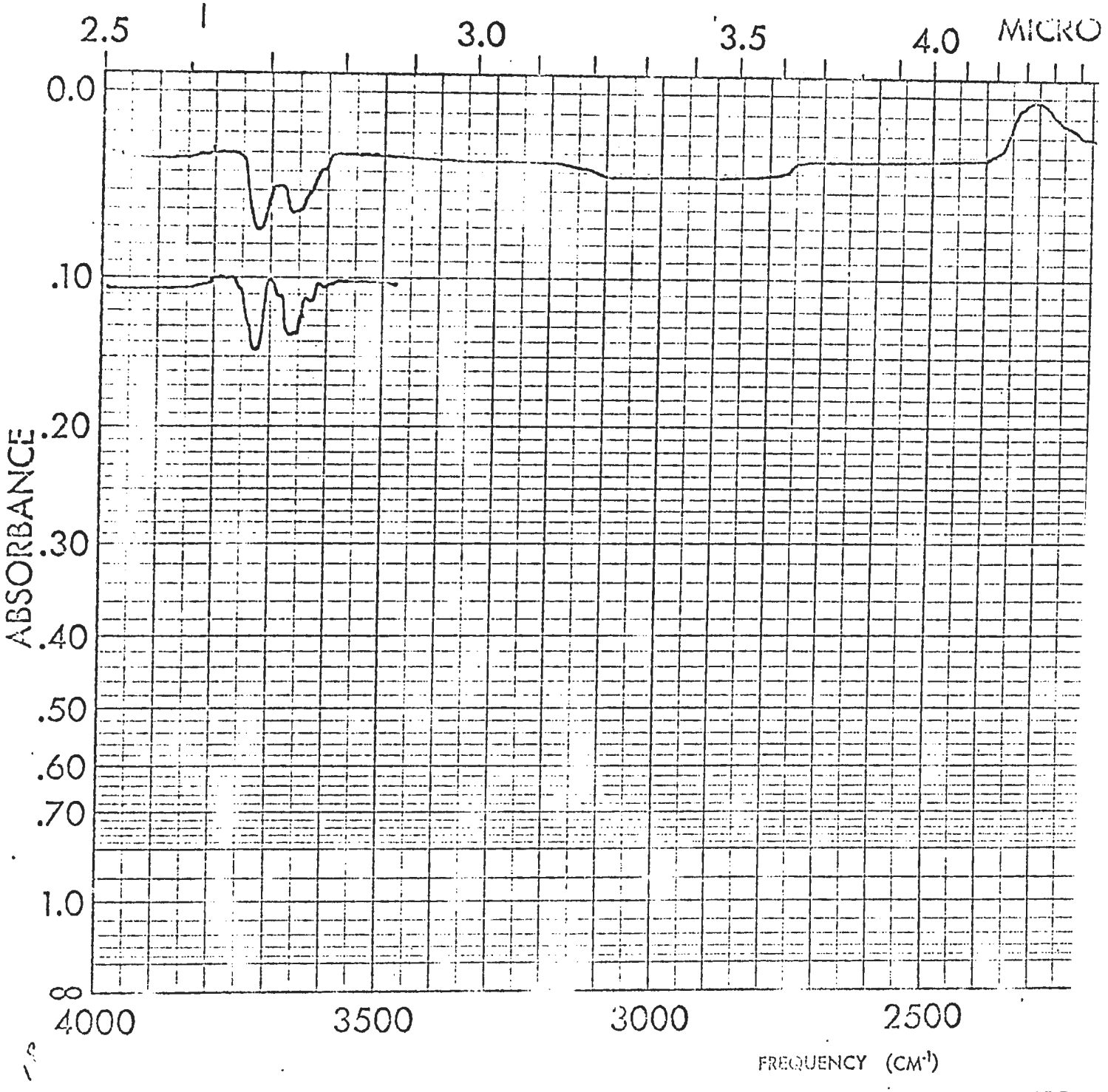

SAMPLE	CURVE NO.
	CONC.
ORIGIN	CELL PATH
SOLVENT	REFERENCE

PART NO. 237-1032 ©

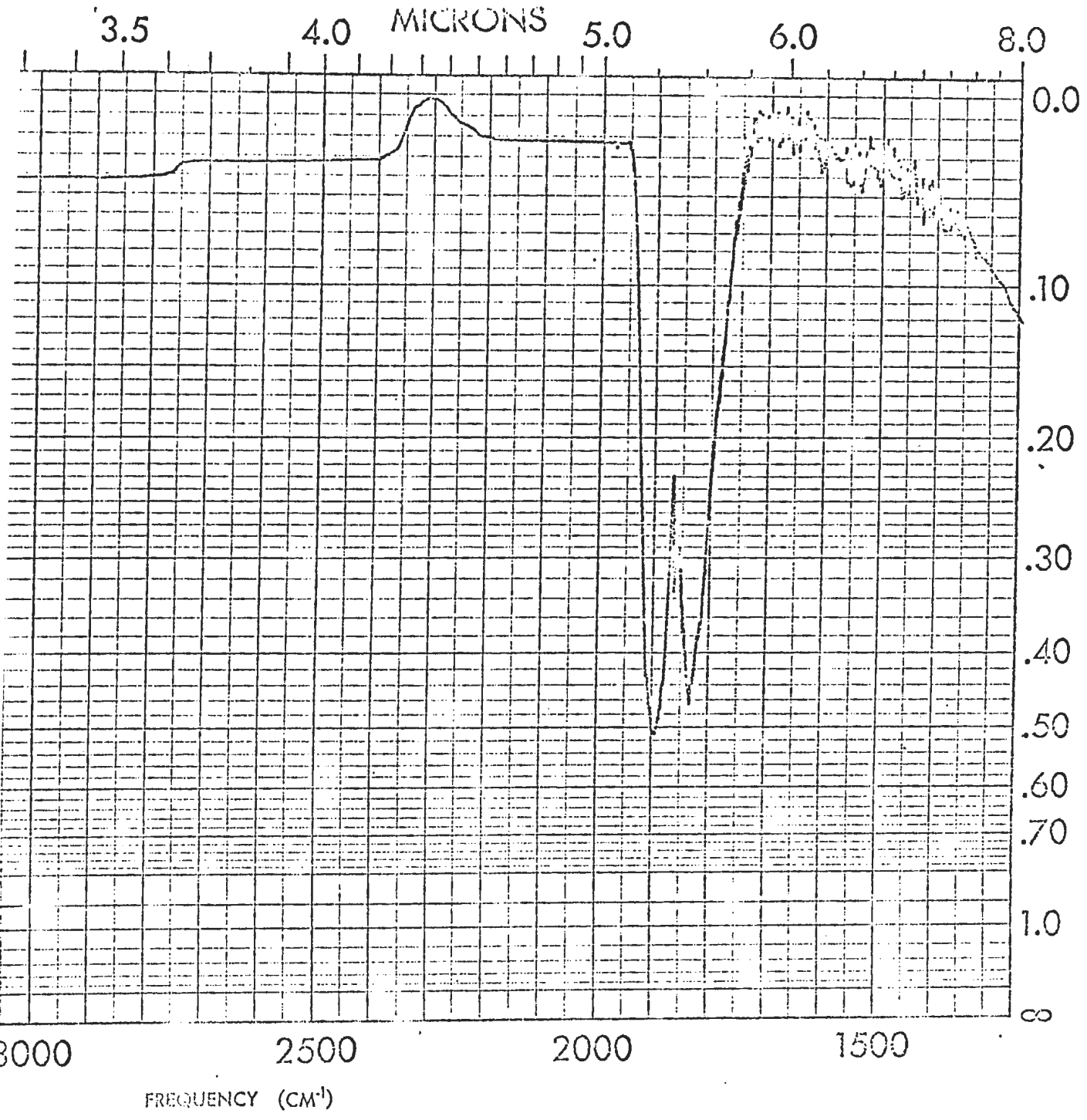

CURVE NO.	SCAN SPEED	OPERATOR
CONC.	SLIT	DATE
CELL PATH	REMARKS	
REFERENCE		

PERKIN-ELMER

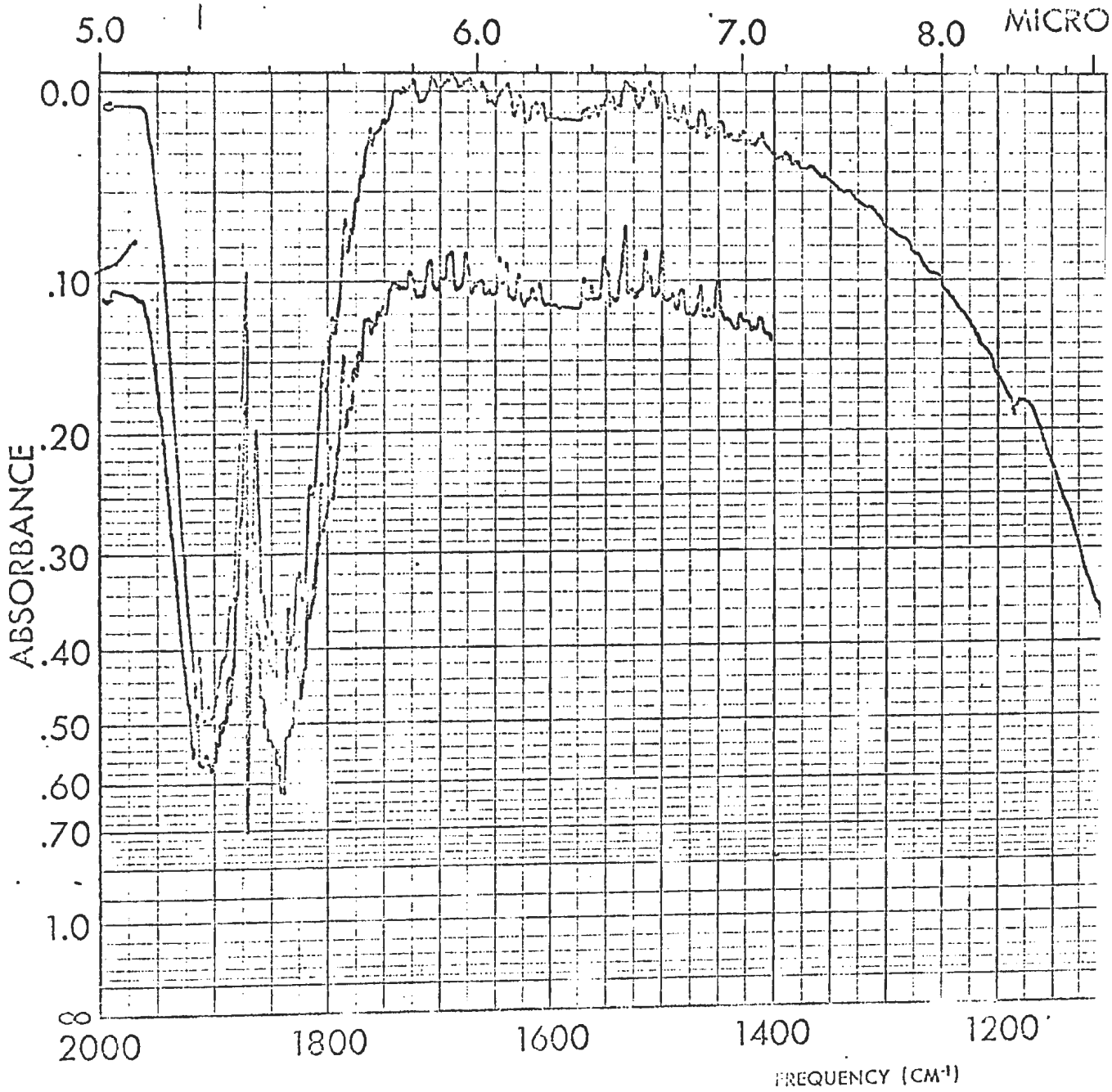

SAMPLE	CURVE NO.
ORIGIN	CONC.
SOLVENT	CELL PATH
	REFERENCE

PART NO. 237-1033

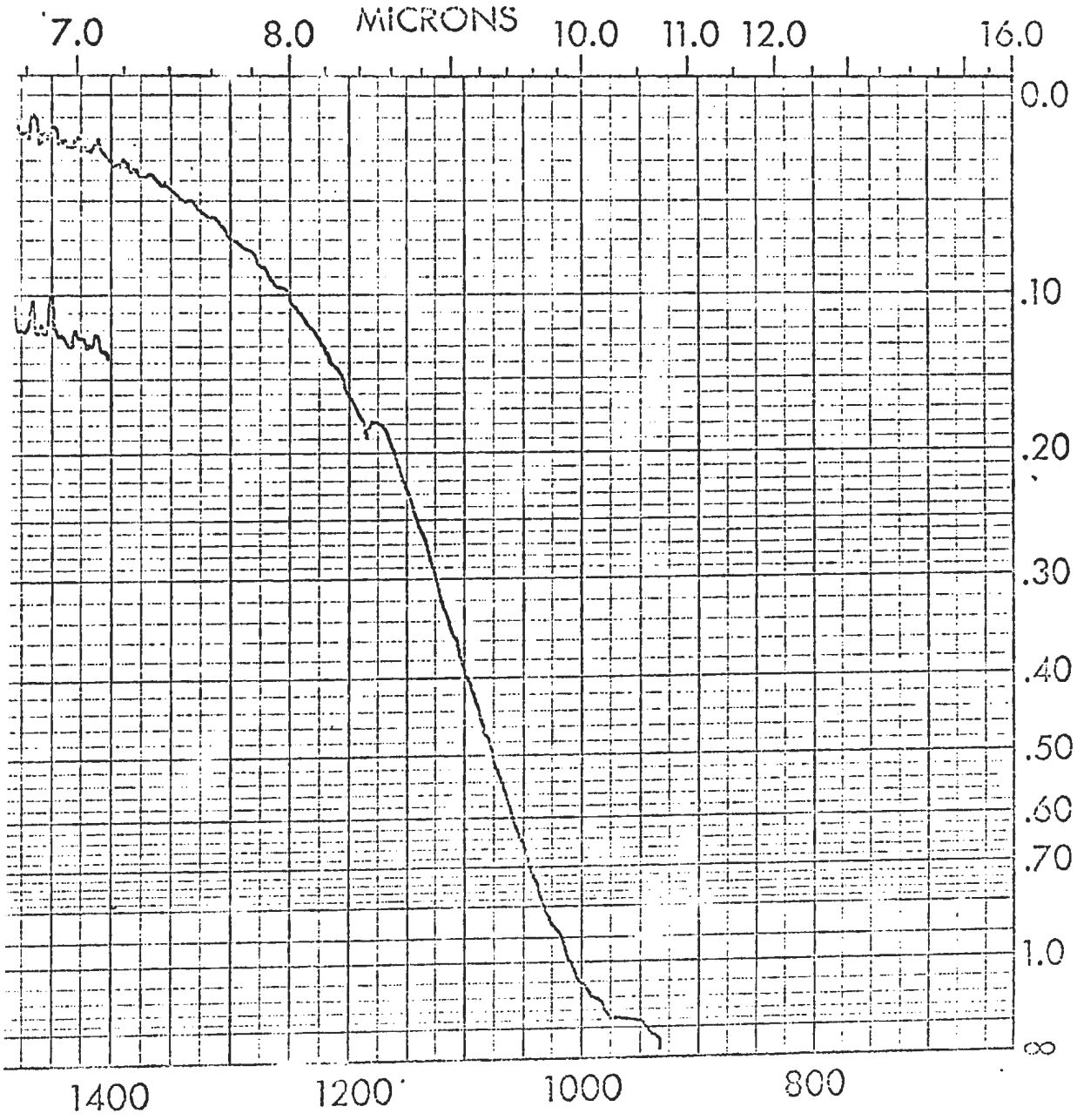

'E NO. _____

C. _____

PATH _____

RENCE _____

SCAN SPEED _____ OPERATOR _____

SLIT _____ DATE _____

REMARKS _____

PERKIN-ELMER

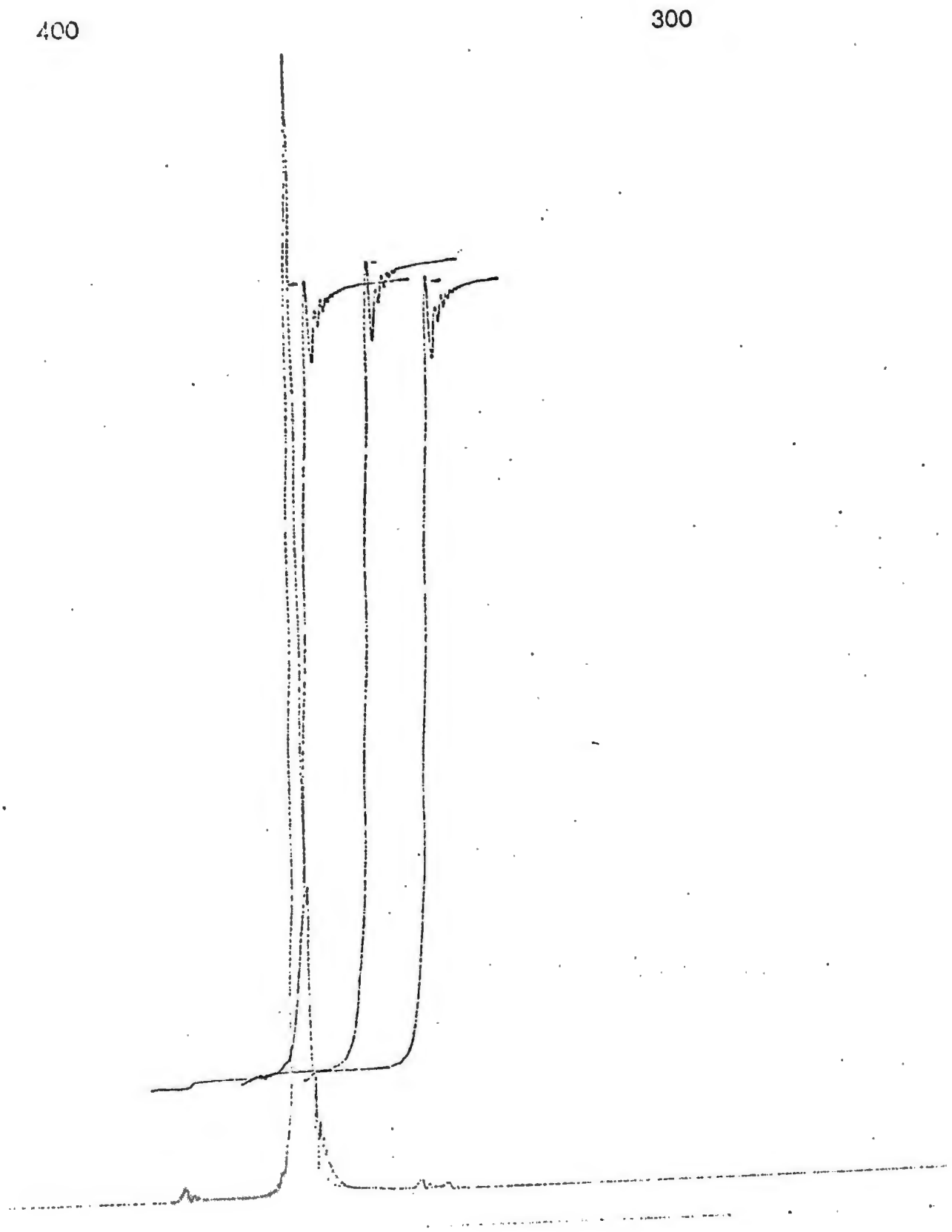
400
300